1 OF 2

1

BMI/ONWI-523
Distribution Category UC-70

BMI/ONWI--523

DE84 010105

Characterization of Cement-Based Ancient Building Materials in Support of Repository Seal Materials Studies

Technical Report

December 1983

D. M. Roy
C. A. Langton
of
Materials Research Laboratory
The Pennsylvania State University

prepared for

Office of Nuclear Waste Isolation
Battelle Memorial Institute
505 King Avenue
Columbus, OH 43201-2693

The content of this report was effective as of May 1983. This report was prepared by Materials Research Laboratory, The Pennsylvania State University, under Subcontract E512-04200 with Battelle Project Management Division, Office of Nuclear Waste Isolation under Contract Nos. DE-AC06-76RLO1830 and DE-AC02-83CH10140 with the U.S. Department of Energy.

ACKNOWLEDGMENTS

The authors would like to express appreciation for the financial support of a National Geographic grant for travel for the sample collection field work, which took place under the initiative of the late T. A. Wertime, Smithsonian Associate. The participation of Joan Mishara, Conservation Scientist, Smithsonian Institution, and T. Wertime in the field work, and the planning support of the Smithsonian Institution is gratefully acknowledged. Contributions by personnel at the Materials Research Laboratory were also much appreciated, especially the following: R. Prave, C. Tanner, and L. Wakeley.

RECEIVED BY TIC FEB 13 1984

DOE Form RA-426
(10/80)

U.S. DEPARTMENT OF ENERGY

OMB NO. 038-R0190

DOE AND MAJOR CONTRACTOR RECOMMENDATIONS FOR
ANNOUNCEMENT AND DISTRIBUTION OF DOCUMENTS

See Instructions on Reverse Side

1. DOE Report No. BMI/ONWI-523	2. Contract No. DE-AC02-83CH10140	3. Subject Category No. UC-70

4. Title Characterization of Cement-Based Ancient Building Materials in Support of Repository Seal Materials Studies

5. Type of Document ("x" one)
☒ a. Scientific and technical report
☐ b. Conference paper: Title of conference ____________
____________ Date of conference ____________
Exact location of conference ____________ Sponsoring organization ____________
☐ c. Other (specify planning, educational, impact, market, social, economic, thesis, translations, journal article manuscript, etc.)

6. Copies Transmitted ("x" one or more)
☒ a. Copies being transmitted for standard distribution by DOE–TIC.
☐ b. Copies being transmitted for special distribution per attached complete address list.
☐ c. Two completely legible, reproducible copies being transmitted to DOE–TIC. (Classified documents, see instructions)
☐ d. Twenty-seven copies being transmitted to DOE–TIC for TIC processing and NTIS sales.

7. Recommended Distribution ("x" one)
☒ a. Normal handling (after patent clearance): no restraints on distribution except as may be required by the security classification.
Make available only ☐ b. To U.S. Government agencies and their contractors. ☐ c. within DOE and to DOE contractors.
☐ d. within DOE. ☐ e. to those listed in item 13 below.
☐ f. Other (Specify)

8. Recommended Announcement ("x" one)
☒ a. Normal procedure may be followed. ☐ b. Recommend the following announcement limitations:

9. Reason for Restrictions Recommended in 7 or 8 above.
☐ a. Preliminary information. ☐ b. Prepared primarily for internal use. ☐ c. Other (Explain)

10. Patent, Copyright and Proprietary Information
Does this information product disclose any new equipment, process or material? ☒ No ☐ Yes If so, identify page nos. ____________
Has an invention disclosure been submitted to DOE covering any aspect of this information product? ☒ No ☐ Yes
If so, identify the DOE (or other) disclosure number and to whom the disclosure was submitted.
Are there any patent-related objections to the release of this information product? ☒ No ☐ Yes If so, state these objections.
Does this information product contain copyrighted material? ☒ No ☐ Yes
If so, identify the page number ____________ and attach the license or other authority for the government to reproduce.
Does this information product contain proprietary information? ☒ No ☐ Yes If so, identify the page numbers ____________.
("x" one ☒ a. DOE patent clearance has been granted by responsible DOE patent group.
☐ b. Document has been sent to responsible DOE patent group for clearance.

11. National Security Information (For classified document only; "x" one)
Document ☐ a. does ☒ b. does not contain national security information

12. Copy Reproduction and Distribution
Total number of copies reproduced 1,075 Number of copies distributed outside originating organization 1,005

13. Additional Information or Remarks (Continue on separate sheet, if necessary)

14. Submitted by (Name and Position) (Please print or type)
Alfonza Smith, Reports Distribution Supv

Organization
Battelle Project Management Division

Signature Alfonza Smith	Date February 8, 1984

ABSTRACT

Ancient mortars and plasters collected from Greek and Cypriot structures dating to ~5500 BC have been investigated because of their remarkable durability. The characteristics and performance of these and other ancient cementitious materials have been considered in the light of providing information on longevity of concrete materials for sealing nuclear waste geological repositories. The matrices of these composite materials have been characterized and classified into four categories: 1) gypsum cements; 2) hydraulic hydrated lime and hydrated-lime cements; 3) hydraulic aluminous and ferruginous hydrated-lime cements (± siliceous components); and 4) pozzolana/hydrated-lime cements. Most of the materials investigated, including linings of ore-washing basins and cisterns used to hold water, are in categories 2) and 3). The aggregates used included carbonates, sandstones, shales, schists, volcanic and pyroclastic rocks, and ore minerals, many of which represent host rock types of stratigraphic components of a salt repository.

Numerous methods were used to characterize the materials chemically, mineralogically, and microstructurally and to elucidate aspects of both the technology that produced them and their response to the environmental exposure throughout their centuries of existence. Their remarkable properties are the result of a combination of chemical (mineralogical) and microstructural factors. Durability was found to be affected by matrix mineralogy, particle size and porosity, and aggregate type, grading, and proportioning, as well as method of placement and exposure conditions. Similar factors govern the potential for durability of modern portland cement-containing materials, which are candidates for repository sealing.

TABLE OF CONTENTS

Page

TABLE OF CONTENTS (Continued)

TABLE OF CONTENTS (Continued)

LIST OF FIGURES

LIST OF FIGURES (Continued)

LIST OF FIGURES (Continued)

EXECUTIVE SUMMARY

Cementitious materials, because of their engineering properties combined with the potential for long-term geochemical stability, are expected to be used as major sealing materials for shafts, tunnels, drifts, and boreholes in underground repositories for isolating nuclear waste. The oldest man-made materials resembling modern repository sealing materials (portland cements) are the ancient cementitious materials used in the Mediterranean regions. Studies were made of some of these ancient materials for purposes of providing information on the potential longevity of concretes, mortars, and grouts where used for sealing nuclear waste geologic repositories.

The present study has characterized durable ancient mortars and plasters from sites in Greece dating back to Hellenistic age (∿350 to 400 BC); and in Cyprus dating back to 5800 to 1600 BC. Samples were collected from structures used for impounding water, such as cisterns and ore-washing basins. Despite centuries of use and exposure, such materials have endured - often better than the natural stone or brick found in the same structures. The results of the current studies provide direct information on the response of various cementitious materials to exposure to the atmosphere, saturated and unsaturated soils, and to dissolved species in solutions, under warm climatic conditions, and encompassing much longer time periods than those reported previously.

The matrices of the cementitious materials have been characterized and classified into four categories: 1) gypsum cements; 2) hydraulic hydrated lime and hydrated-lime cements; 3) hydraulic aluminous and ferruginous hydrated-lime cements (± siliceous components); and 4) pozzolana/hydrated-lime cements. Most of the materials investigated in the current study fit within categories 2) and 3). The aggregates used included carbonates, sandstones, and shales, which are also common rock types occurring in potential salt repository sites. The results of the current characterization and microstructural studies have been integrated with previous knowledge (especially from Roy and Langton, 1982) and used to consider the long-term durability of this type of material.

Detailed analyses of the chemical, mineralogical, microstructural, and macroscopic characteristics of the ancient mortars and plasters suggest that the remarkable durability of these materials is the result of a combination of both chemical and microstructural factors. Comparisons with modern cementitious materials properties lead to the conclusion that the durability of ancient

materials, like that of modern construction materials, is affected by initial composition and design, and by quality control of the starting materials and of the manufacturing and construction processes.

From this study it is additionally evident that while most of the binding phases in hydrated calcium silicate cements (ancient and modern) have amorphous or subcrystalline structure, these phases, for all practical considerations, are kinetically inert under their exposure conditions and do not change form for at least 3,000 years in a variety of environments, including burial in saturated and unsaturated soils and exposure to the atmosphere. Therefore, deleterious recrystallization of the majority of the matrix components of modern portland cement-based materials of similar composition may not be expected to reduce their durability under analogous conditions.

Formulations currently under investigation for salt repository sealing are being conceived carefully and designed under controlled laboratory conditions, aimed at optimizing the chemistry, mineralogy, and the physical properties which affect durability (permeability, porosity, compressive strength, diffusivity, etc.). Environmental compatibility of the matrix-aggregate-wall rock assemblages is being evaluated under potential exposure conditions.

Studies of this nature provide insight into durability of man-made cementitious materials spanning time periods compatible with repository sealing requirements.

1 INTRODUCTION

1.1 ORIGIN AND IMPORTANCE OF STUDY

The desire to isolate high-level and transuranic wastes from the biosphere for relatively long periods of time has necessitated detailed reviews of the present status of scientific and technological knowledge pertinent to the National Waste Terminal Storage program. Successful isolation of radioactive waste in mined repositories and/or deep boreholes appears to be the near-term option, and prediction of longevity for such repository systems is necessary for periods of thousands of years. Therefore, a credible systems approach to radioactive waste management, particularly risk assessment, must contain input from several fields including geology, geochemistry, geophysics, and nuclear, construction, and materials engineering.

A thousand years is generally accepted as a sufficient amount of time to permit decay of fission products that represent the most hazardous fraction in the waste material. Beyond a thousand years and during the time in which actinides and a few long-lived fission products remain toxic, the ability to predict repository behavior, and therefore, the assurance of successful isolation, diminishes.

Since most current repository designs incorporate the use of portland cement-based materials as components in multiple-barrier waste package systems, longevity predictions for these materials are critical. The need for extraordinarily long-term durability and phase stability of borehole-plugging and shaft-sealing systems places unique requirements on materials such as cement, mortar, and concrete and it is difficult to determine the ultimate design suitability on the basis of operating experience, experimentation, or prototype testing. For these reasons, researchers are currently placing increased emphasis on the extrapolation of longevity data for engineered materials from natural analogs.

In this study, an attempt was made to develop a chemical and physical explanation for the observed durability of selected ancient cement-containing materials. This line of investigation should serve as a means of obtaining support data to aid in the assessment of durability, longevity, and thermodynamic stability of portland cement-containing materials proposed for borehole and shaft sealing. Ultimately, these data are intended to aid in the performance and risk assessment of multiple-barrier systems for radionuclide containment.

1.2 STATEMENT OF THE PROBLEM

To date, most research related to repository sealing has been associated with segments of industry such as mining and chemical waste disposal and storage. Here, the overall requirements for longevity and performance are not as stringent as those for nuclear waste isolation. Assuming that portland cement-based materials will be important for such sealing efforts, it is timely to review the potential for long-term durability and stability of these materials (Roy et al, 1979). However, historically, cement chemistry-engineering has been primarily concerned with bulk properties of the cements themselves and has provided little information on the long-term behavior of cement-containing materials and provides an independent source of data for the prediction of longevity of modern cements used in borehole plugging and shaft sealing. This line of investigation arises from the fact that certain cement-containing ancient structures (up to 2,000 years old and older) are still functioning today and thereby provide historical documentation of the extended durability of these materials. These materials have survived environmental conditions which, in many respects, are more severe than those anticipated for borehole-plugging materials.

The objectives of this study were as follows:

1. Conduct a literature review dealing with the chemistry of ancient building materials.
2. Obtain representative samples of a variety of ancient calcium silicate-containing building materials.
3. Establish procedures for characterization of these samples.
4. Characterize samples.
5. Determine and evaluate the interaction between these ancient materials and the environments in which they exist.
6. Provide information regarding the potential for long-term durability of portland cement.
7. Provide information regarding the phase stabilities of the hydrated calcium silicate components of portland cement.

8. Provide a foundation for preliminary experimental and theoretical work concerning the longevity, durability, and thermodynamic stability of portland cement-containing materials, and a basis for future diagnosis.

This study was also intended to complement and expand on data reported by Roy and Langton (1982).

1.3 BACKGROUND INFORMATION

1.3.1 Information From the Literature

A brief review of the literature on the history of building materials and construction techniques has been presented by Roy and Langton (1982). These authors have also summarized the results of a comprehensive literature survey of the following topics: chemical studies of ancient mortars and concretes, matrix-aggregate reactions in ancient mortars and concretes, and engineering studies of ancient concretes. In addition to the work previously reviewed, the history of cementing materials from antiquity to the middle of the 19th century is comprehensively discussed by Znaczko-Janworski (1958). In his publication, Znaczko-Janworski describes the historical development of gypsiferous and calcareous cementing materials in Eastern and Western Europe as well as in the USSR.

1.3.2 Definition of Terms

The terminology proposed by Roy and Langton (1982), which was based on age of structures or on the age of the cementitious materials used in these structures, has proved useful for describing the wide range of samples analyzed in this study. Terminology based on function and composition of archaeological specimens (Roy and Langton, 1982) has also proved necessary for consistent characterization in both field and laboratory analyses.

As a result of the present study, two additional terms were found to be useful in describing the construction of masonry walls. The following nomenclature is currently used through the modern construction industry and was found to be suitable for describing archaeological structures:

Ashlar Masonry - Masonry which incorporates hewn or squared stones with or without the use of mortar.

Rubble Masonry - Masonry which incorporates stones in their natural form, that is, uncut fieldstones with or without the use of mortar.*

In addition, as a result of the present study, it became necessary to better define the term plaster. This need arose because of the common application of plasters on floors in the pre-Roman era. Since many of these plasters were multimodal with respect to their aggregate distributions, they initially appeared to be concretes. However, upon more detailed examinations, these plasters were similar or identical to those used for walls in the same structures. Therefore, in addition to the previous definition, plasters were defined as those layered materials which were emplaced onto surfaces with trowels or trowel-like tools as opposed to concretes which were poured between rigid forms.

1.4 SAMPLE AND SITE LOCATION INFORMATION

The cementitious samples chosen for study were selected using four major criteria: 1) they were very old (generally BC) and hence very durable; 2) they had not been intensively characterized previously (some were relatively new excavations); 3) many of the structures were used to hold water, suggesting low permeability; and 4) the sites were well documented and reasonably well dated.

1.4.1 Greece

A total of 19 samples were collected by C. Langton in Greece: 18 from four different areas within the Lavrion mining district, Hellenistic in age (∿350 to 400 BC) (Conophagos, 1980), and one sample of Roman age (50 BC to 200 AD) from an ancient aqueduct about 50 kilometers north of Athens. (Five additional samples from the Agora excavation in Athens were requested from the Director of the Agora Museum, Greece; however, they were not received until after analyses on the other samples were completed.) A tabulation of the sample sites and excavation locations in Greece is presented in Appendix A, Table A-1. The four site locations in the Lavrion mining district are shown in Figure A-1,

---

*This is not to be confused with the term rubble concrete as defined by Roy and Langton (1982).

and planview maps of excavations showing individual sample locations at these sites are schematically illustrated in Figures A-2 to A-4.

1.4.2 Cyprus

A total of 20 samples were collected by C. Langton from seven different excavation sites in The Republic of Cyprus (Figure A-5). A tabulation of the location information for both the sites and samples, in addition to excavation references, is presented in Appendix A, Table A-2. Figures A-6 to A-10 are generalized excavation plans for these various sites on which sample locations have been approximately located. In all cases, sample locations were photographically documented. The recently uncovered Amathus and Northwestern Kourion excavations were documented only photographically.

1.5 FIELD DESCRIPTIONS OF SAMPLES AND SITE LOCATIONS

Field descriptions of the hand specimens and site descriptions are presented in Appendix A, Tables A-3 and A-4 for Greece and the The Republic of Cyprus, respectively. Where possible, site locations were noted on excavation grids. However, it was often necessary to make sketch maps of the various field areas. All site and sample locations were photographically documented and this information stored in the Materials Research Laboratory/Office of Nuclear Waste Isolation archives at The Pennsylvania State University.

1.6 TECHNICAL APPROACH

1.6.1 General

The total samples analyzed in this study were the 19 hand-specimens collected by C. Langton from Greece and the 20 samples from The Republic of Cyprus. J. Mishara, from the Smithsonian Institution, Washington, DC, and the late T. Wertime, Smithsonian associate, also participated in the collection and documentation of other samples collected from Greece and Cyprus. In all of these cases, hand specimens and sample locations were photographically documented, and samples were catalogued in accordance with a numerical system which also took into account the site location.

Intensive study of these specimens combined analytical and interpretive methods in a multimethod analysis: (1) macroscopic and microscopic analyses; (2) thermal analyses; (3) chemical analyses of selected fractions; and (4) structural (phase identification) studies.

Two methods were used for separating the matrix from the bulk sample:

Method A

1. Remove coarse-aggregate fraction from bulk specimen
2. Separate matrix fraction from fine-aggregate fraction by light crushing and sieving (-325 mesh)

Method B

1. Remove coarse-aggregate fraction from bulk specimen
2. Crush remaining sample to ∿0.5 cm
3. Ultrasonify in distilled water (5 to 10 minutes at ∿20,000 Hz)
4. Decant liquid and retain coarser fraction
5. Settle suspended matrix fraction (∿20 to 1 μm)
6. Concentrate <1 μm matrix fraction retained in suspension by evaporation of liquid.

Identification of the crystalline phases making up the matrix fractions of the materials analyzed in this study was accomplished first by X-ray diffraction (XRD) analyses, and complemented with data from differential thermal analysis (DTA) and thermogravimetric analysis (TGA), scanning electron microscopy (SEM) including energy-dispersive X-ray (EDX) analysis, and microprobe analyses, with some information gained from thin sections. The XRD, DTA, and TGA techniques are bulk analysis tools and are sensitive to phases present in amounts greater than about 2 to 5 weight percent depending on the specific characteristics of the sample. Precision of thermal analysis (DTA and TGA) results is dependent on crystal size, degree of crystallinity, heating rates, and the composition of the atmosphere in which the experiments are conducted (Courtault, 1979; Ramachandran, 1969; Mackenzie, 1970). Petrographic microscope techniques resulted in a maximum magnification of about

1,000X which was insufficient for the resolution or identification of extremely small particles. However, it was adequate for easy detection of gypsum and calcite crystals greater than about 0.001 mm in size.

To isolate and identify amorphous phases and also phases constituting a small percentage of the total matrix, several additional types of analyses were used in addition to X-ray and thermal techniques. SEM was a useful technique for determining the presence of phases which occurred in minor quantities and also for isolating calcium silicate and/or aluminate gel particles. Detection was accomplished primarily on the basis of morphologic characteristics of these matrix particles, and supplemented by EDX analysis. Ultrasonic separation of the -1 μm size fraction in hydraulic cement-containing building materials produced concentrated samples of amorphous phases which were relatively easy to analyze by the previously described techniques.

Other methods for detecting the presence and degree of polymerization of calcium silicate and/or aluminosilicate gel particles utilize chemical dissolution methods combined with chromatographic analyses.

1.6.2 Macroscopic Analysis

Macroscopic analyses of all samples studied were carried out by hand-specimen examination with the aid of a 14X hand lens and also a 40X binocular microscope. Emphasis was placed on describing a variety of parameters for the matrix (binder) material, aggregates, and miscellaneous properties in each sample. The principal parameters are:

Binder	Aggregates	Miscellaneous
1. degree of coherency	1. type (rock/mineral/ ceramic/other)	1. sample size
2. color	2. size	2. charcoal
3. mottling	3. mineralogy	3. secondary mineral
4. relative porosity	4. angularity	4. vug fillings
5. degree of carbonation	5. color	5. other
6. relative amount	6. relative amount	

1.6.3 Petrographic Analysis

Petrographic analyses were carried out using a Reichert polarizing microscope to determine the mineralogy and homogeneity of the matrix material, nature of the aggregates, nature of the matrix/aggregate interfacial regions, and microtexture of the composite sample. The matrix phases were studied using an oil-immersion, 100X, objective lens which resulted in a total magnification of about 1,000X. However, most observations were made over the magnification range of 45 to 720X.

Thin sections were prepared for each of the ancient samples studied. Modifications of standard thin section preparation techniques for ancient cement-based materials have been discussed by Roy and Langton (1982). Specific sample parameters of interest in the thin section analyses included those listed for macroscopic analysis in Section 2.

1.6.4 SEM Analysis

SEM imagery, combined with qualitative elemental analysis as determined by characteristic EDX analysis, proved to be very useful techniques for studying the microstructure of the bulk samples and the morphology of individual particles. The advantages of using SEM techniques included: large depth of focus, sample preparation simplicity, high resolution, and qualitative elemental analysis of crystalline and noncrystalline phases exposed on fractured surfaces. The maximum working magnification using a secondary electron signal was between 10,000 and 20,000X or higher, depending on the individual sample. However, the practical maximum magnification in the lower stage which was coupled with the EDX capabilities was about 3,000X.

An ISI-DS-130 SEM unit was equipped to analyze signals generated by secondary electrons, back-scattered electrons, and X-rays characteristic of individual elements with atomic numbers greater than neon (although sodium is not very sensitive). Morphologic and chemical data were correlated with XRD powder pattern data for final phase identification. Several examples of data obtained from SEM imagery are discussed.

1.6.5 XRD Analysis

XRD analyses were conducted on the matrix (binder) fractions of all samples discussed herein and also on selected aggregates. Separation of the matrix and aggregate fractions was performed according to the procedure (method B) described by Roy and Langton (1982) or by ultrasonic disaggregation (method B) as follows: All samples analyzed by XRD techniques consisted of particles less than 45 μm in size. Each sample was mounted on a standard, pre-cleaned microscope slide by dispersing the XRD powder in a collodion solution or packed in an aluminum sample holder when it was important to ensure random orientation. X-ray data were obtained with a Philips automated powder diffractometer (APD-3600/01) by using copper radiation, standard settings at 45 kV and 30 mA, and a θ-compensating slit which eliminated the necessity of slit changes. A Data General Nova/4A computer was used to collect, store, and process data. Software programs were run from a fixed-firm disk, whereas XRD powder patterns were stored on a removable-firm disk. All ancient cement data were stored on a special reserved disk in a library directory called ANCCEMENT. Peak searches were conducted using a second derivative algorithm employing background fitting, peak smoothing, and α_2 stripping capabilities. Data manipulation was done on a Tektronix CRT 4012 using an interactive mode with the PLOT program. Comparisons were made with the XRD powder patterns using the COMPARE routine.

1.6.6 Thermal Analyses - DTA and TGA

DTA were performed using a Harrop DTA 716 coupled with a Harrop TA700 programmer, controller, and recorder unit. This instrument was calibrated using the transition temperature of quartz and the melting temperature of indium. The standardization procedure was carried out using a standard sample size of 80 mg of material which was packed and tamped into a quartz sample holder. Corundum, α-Al_2O_3, was used as the reference material for measuring the temperature differential between the sample and a standard inert phase. A heating rate of 10 C/min was used, and the temperature differential was recorded in millivolts over the temperature range 26 to 1000 C. Platinum thermocouples were used. All analyses were conducted under atmospheric conditions in accordance with the procedure described (method B).

TGA were performed using a Harrop TGA 716 coupled with a Harrop TA700 programmer, controller, and recorder unit. Thermocouples were standardized using the dehydration temperatures of copper sulfate pentahydrate, and weight calibration for the balance portion of the instrument was performed using Cahn calibrating weights. All analyses were conducted under atmospheric conditions at a heating rate of 10 C/min over the temperature interval 26 to 1000 C. Between 20 and 35 mg of crushed (-200 mesh) material was used for each of these analyses.

1.6.7 Quantitative Chemical Analyses

Approximately 500 mg of separated matrix material was required for each total analysis. Chemical analyses of the oxide components were conducted primarily by plasma emission spectrometry. Silica was determined gravimetrically, and calcium oxide was determined according to a wet chemical procedure based on getting the calcium into solution and then precipitating it as calcium oxalate by means of a solution of ammonium oxalate, according to the reaction $Ca^{++} + C_2O_4^{=} \rightarrow CaC_2O_4$. The calcium oxalate was then ignited to form calcium oxide and the latter compound was weighed.

Total sulfur analyses were conducted using a rapid analysis technique which employed a Leco Sulfur Analyzer. The samples were placed in the sample chamber of this instrument, where they were heated and reacted with oxygen. Sulfur dioxide was formed, then titrated to determine the amount of sulfur present. Sulfate and sulfide were not distinguished by this analysis. The analyses are reported as weight percent sulfur trioxide.

Determination of adsorbed water ($H_2O_{110\ C}$), water incorporated in the crystal structure ($H_2O_{total} - H_2O_{110\ C}$), and carbonate (reported as CO_2) were made by weight losses observed in the TGA. This procedure was described in the section on thermal analyses.

1.6.8 Chemical Structure Determination

The trimethylsilylation (TMS) technique is a chemical method of studying silicate structure, particularly those of poorly crystalline or noncrystalline silicates, including cement-related compounds and their hydration products. The structure, or rather the degree of condensation of the silicate groups in the original phase, can be estimated by gas-liquid chromatographic measurements of trimethylsilyl derivatives (T-derivatives). These derivatives are formed by the reaction between trimethylsilyl and silanol groups, the latter produced by acid dissolution of the original silicate compounds. The procedure used in this study was adapted from that of Tamas et al (1976) and Uchikawa and Furata (1980), and has been described by Roy and Langton (1982).

1.6.9 Other Methods of Investigation

1.6.9.1 Microprobe Analysis

Microprobe analyses of selected samples were carried out to obtain quantitative chemical data for unidentified matrix and aggregate phases and matrix/aggregate interfacial regions. Analyses were conducted using an ETEC-Autoprobe equipped with three variable spectrometers and a KEVEX energy analyzer. Samples were analyzed for aluminum, carbon, iron, potassium, magnesium, manganese, sodium, sulfur, and silicon, and Bench Albee Correction Routine was used to compute oxide percentages.

Compositional data resulting in oxide components totalling between 35 and 65 weight percent were typical for the samples analyzed. Even after the approximate weight percentages of H_2O and CO_2 (determined by TGA) had been taken into account, the resulting totals were well below acceptable values. Applications of these data are therefore limited, and caution must be used in interpreting the results.

1.6.9.2 Determination of Organic Constituents

Ancient building materials from Greece and The Republic of Cyprus were collected from structures which served as containers or carriers for water, such as cisterns, pipes, ore-washing basins, dams, or aqueducts. Therefore, chemical analyses were conducted on selected samples to determine if organic compounds, such as oils, resins, or waxes, were incorporated into these materials to act as water-proofing agents. Two methods of analysis were used. The first involved crushing the sample and then leaching it in hexane for 48 hours in a soxhlet. This solution was filtered, concentrated, and then analyzed by liquid chromatography.

The second method used for detecting the presence of organic compounds incorporated into ancient building materials involved dissolution of 50 to 100 grams of sample in a 50 percent HCl solution at 60 C for 24 hours. This was followed by dissolution of the remaining solid material in a 1:1 mixture with 50 percent HCl and 50 percent HF at 60 C for 24 hours. This solution was diluted and filtered. Residue remaining on the filter paper was again treated with a 50 percent HCl solution for 12 hours. Since the organic polymers anticipated to be present (naturally occurring compounds available to the ancient engineers), are not soluble in the acid solutions described, they can then be separated as a solid residue by filtration. Samples AML3 and LVL05, LVL12 (layer 2), LVL15 (layers 2 and 3), and LVL18 (layer 2) were analyzed.

1.6.10 Effect of Techniques

Chemical compositions of the matrix fractions of the materials investigated in this study were determined by means of emission spectrometry, wet chemical analyses, and TGA (volatile constituents). The matrix fractions were separated from the bulk samples by a mechanical method which involved light crushing, separation, and sieving (Roy and Langton, 1982) and/or by ultrasonic techniques. Invariably, these methods may result in minor, undetermined amounts of contamination of the matrix by aggregates present in the bulk material.

Alternative methods for determining the bulk composition (paragraph 1.6.8) for selected areas in the matrix and also for determining the compositions of individual particles in the matrix fractions were investigated and include EDX in conjunction with SEM analysis and microprobe analyses. The primary advantages in using any of these techniques are that they do not require separation of the matrix from the bulk sample, and individual particles in addition to selected areas can be analyzed. Qualitative chemical analyses of matrix particles and areas exposed on fractured surfaces were obtained by EDX/SEM analyses. A relatively thick (300 to 400Å) gold coating was required to obtain resolution at magnifications above 3,000X. As a result of this thick coating, the intensities of lower energy signals were preferentially decreased with respect to higher energy signals. Therefore, definitive compositional data for the matrix or for particles within the matrix fractions were not obtained by using this technique; however, they provided useful complementary information. Microprobe analyses were conducted on several samples to obtain quantitative compositional data for the matrix fraction. The results obtained should be interpreted with caution because of the low values computer for the total oxides present. High porosity observed on even the polished surfaces (which were required for microprobe analysis) is believed to be responsible for the loss of impinging electrons which excite the sample to produce a detectable signal, and for the absorption of the resulting energy signals by epoxy filling these pores.

Data obtained as the result of these studies were combined with knowledge obtained from numerous sources to explain the remarkable durability of certain ancient building materials. This understanding is useful in the prediction of longevity and other properties associated with aging phenomena of portland cement-based construction materials.

2 RESULTS

2.1 MACROSCOPIC RESULTS: HAND SPECIMEN EXAMINATION

Macroscopic descriptions of ancient concretes, mortars, and plasters from Greece and The Republic of Cyprus are presented in Appendix B, Tables B-1 and B-2, respectively.

2.2 MICROSCOPIC RESULTS

Petrographic data for samples collected from Greece and The Republic of Cyprus are summarized in Appendix C, Tables C-1 and C-2, respectively, and selected thin sections are discussed in Sections 2.2.1 and 2.2.2.

2.2.1 Selected Samples from Greece

Low-magnification photomicrographs of samples LVL02, LVL04, LVL08, and LVL13 are shown in Figure 2-1a to d, respectively. Samples LVL02 and LVL04 were collected from a dam near Lavrion, Greece. LVL08 and LVL13 are plasters from ore-washing basins in the ancient Lavrion silver mining district. The fabric, texture, and mineralogy illustrated in Figure 2-1a and b are typical of the plaster used to finish the inner surface of the dam. This plaster is characterized by an abundance of strained, fractured-quartz sand plus a minor amount of mafic sand which includes: pyroxene, biotite, hornblende, and plagioclase feldspar grains, and small metamorphic rock fragments in a very inhomogeneous matrix. The matrix is mottled from yellow to brown to gray and contains very-fine-grained, gray (low birefringence) patches which are round, vary in size up to 0.5 cm, and are unique to this site (upper left corner, Figure 2-1b). It was not possible to identify the phase(s) making up these areas because the very-fine grain size prohibited optical property measurements. In addition, rounded to irregular patches of slightly coarser-grained calcite, which exhibit typical carbonate extinction and birefringence, are common (upper right, Figure 2-1b). Mortars and plasters from the dam site also contained an abundant amount of opaque material, as illustrated by the numerous black areas in Figure 2-1a and b. Voids appear solid white in plane

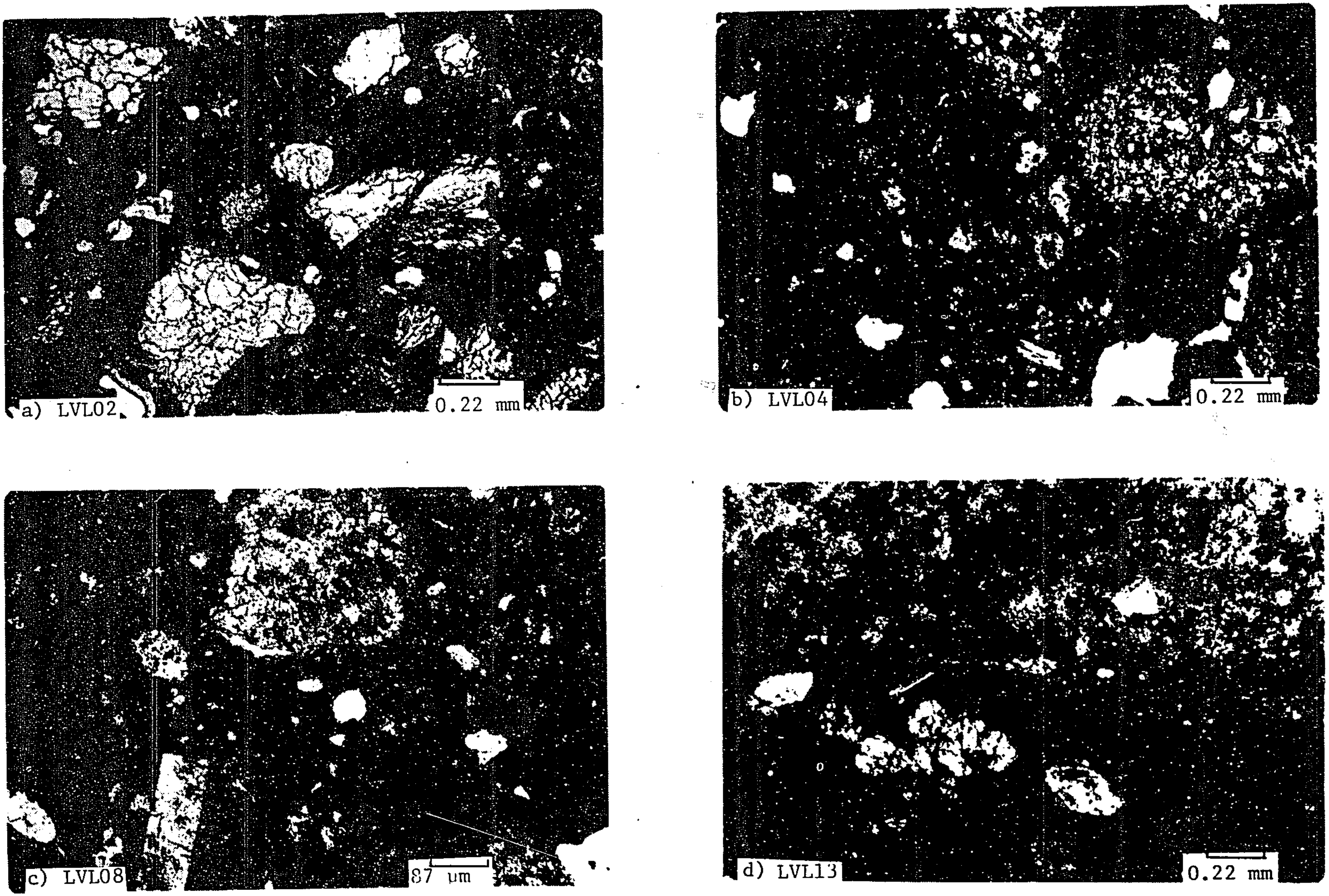

Figure 2-1. Photomicrographs of Ancient Plasters, Samples LVL02 and 04 From a Dam Near Lavrion, and LVL08 and 13 From Ore-Washing Basins in the Lavrion Mining District, Greece. (All parallel Nicols.)

light.) Matrix/aggregate interfacial reaction zones were not observed in these phases.

Low-magnification photomicrographs of samples LVL08 and LVL13 are shown in Figure 2-1c and d and illustrate a texture, fabric, and mineralogy which are typical of the plasters collected from ore-washing basins and cisterns in the Lavrion mining district, Greece. The matrix fractions of these materials are very inhomogeneous and are mottled from pale yellow to dark reddish-brown to grayish-brown. In addition to abundant dark red patches up to 0.1 mm, with diffuse to discrete selvages, areas of slightly coarser-grained calcite were also observed. Often the matrix appeared to be stained red in a web- or network-like pattern and some samples contain up to 5 percent dark red, opaque particles (less than 0.1 mm). The fine-aggregate fractions consisted of fractured and strained quartz sand plus plagioclase feldspar, augite, biotite, and other mafic crystals. The coarse-aggregate fractions were made up of angular metasediments, including schist and/or marble fragments. Matrix/aggregate interfacial reaction zones were not observed.

Some of the plasters collected from the Lavrion district are composed of more than one layer. For example, Figure 2-1d shows the interface between two plaster layers in sample LVL13. The matrix fraction of the bottom layer (upper half of this photomicrograph) is lighter in color and contains less opaque material than does the overlying plaster (lower half of this photomicrograph). It can be seen that this interface is regular and was apparently 'finished' to a flat surface prior to application of the second layer. A thin vein of secondary calcite was observed filling a fracture between these two layers, and this suggests that the interfacial region was a zone of weakness which fractured and was subsequently healed. In general, very few fractures or secondary fracture fillings were observed in the Lavrion samples.

Another example of a multilayer plaster from an ore-washing basin in the Lavrion district, LVL17, is illustrated in Figure 2-2a to d. This plaster is composed of three layers: a light-colored base plaster [Figure 2-2a (top) and c]; a moderately dark red middle plaster [Figure 2-2a (bottom), b (upper edge), and d]; and a very dark brown (opaque) exterior plaster (Figure 2-2b, center). The microtextures and coarse-aggregate fractions of these layers are similar. The primary differences can be attributed to the relative abundance of opaque particles in the fine-aggregate fractions of each layer. (The darker the color in transmitted light the higher the relative concentration of

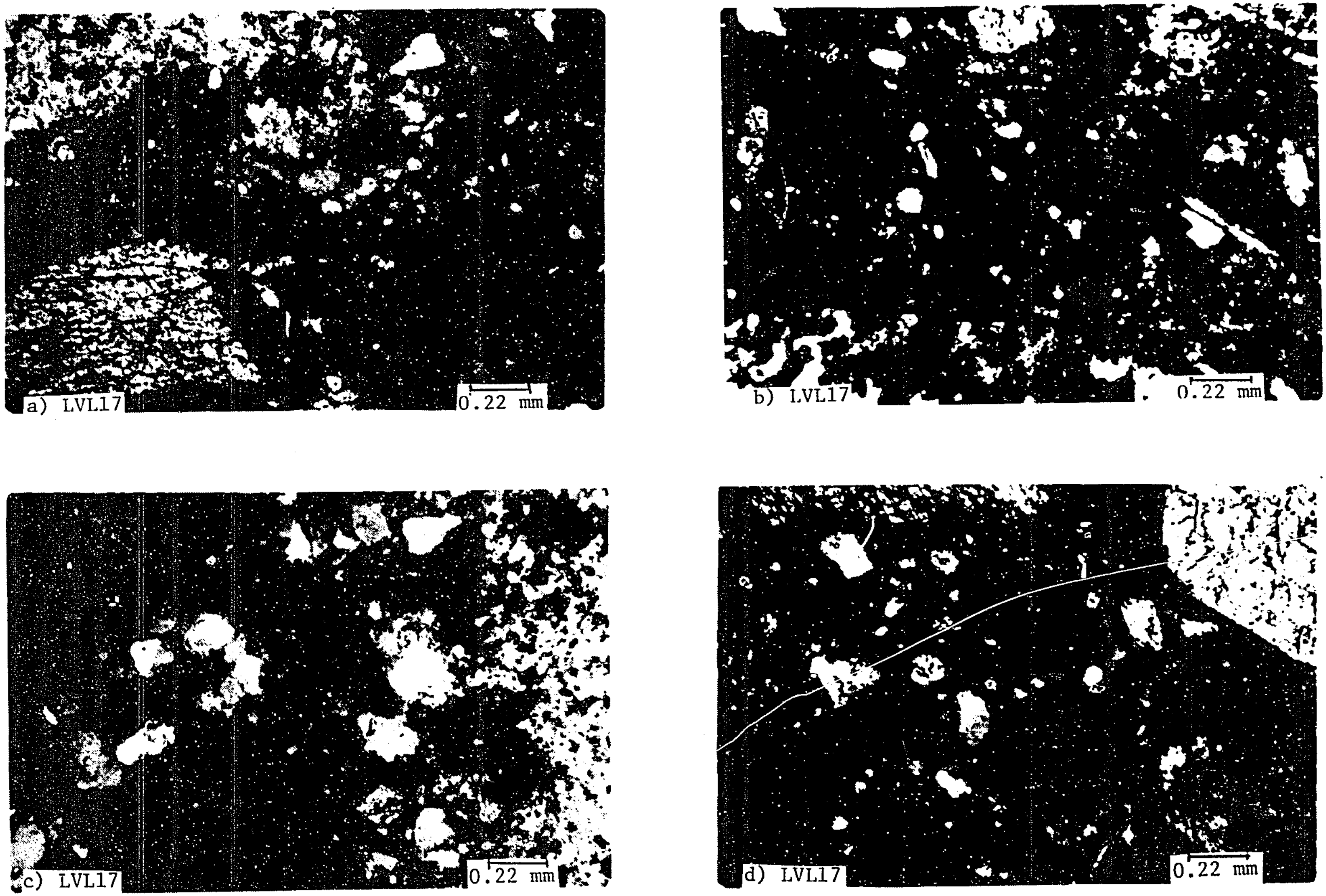

Figure 2-2. Photomicrographs of an Ancient Three-Layered Plaster, Sample LVL17, From an Ore-Washing Basin in the Lavrion Mining District, Greece. (All parallel Nicols.)

inorganic opaque particles.) The exterior surface of this specimen has recently (post-excavation) been coated with pine resin which appears opaque and porous; the pores are partially filled with secondary calcite (Figure 2-2b, bottom edge).

The contact between the bottom and middle layers of sample LVL17 is shown in Figure 2-2a and the linear expression of this interface suggests that the surface of the bottom layer was 'finished' but not 'polished' prior to application of the middle layer. The lack of a sharp contact suggests that the bottom layer was not completely set at the time the middle layer was emplaced. On the other hand, the contact between the middle and exterior layers is both sharp and shows a linear expression. These features can best be interpreted as resulting from the application of the exterior layers on a 'polished' substrate. A longer (compared to that proposed for the base plaster) curing time for the middle layer would be required to produce a hardened material capable of being 'polished'. The outer surface of the exterior layer may also have been 'polished' as suggested by its sharp, linear expression in thin section.

High-magnification petrographic studies of the matrix fractions of the Lavrion plasters revealed that they are indeed inhomogeneous, as illustrated in Figure 2-3a and b, LVL12 and LVL15, respectively. The bulk matrices appear to be composed of calcite (carbonation product of slaked lime), which occurs in areas ranging from relatively uniform and fine grained (Figure 2-3a) to irregular or rounded patches containing slightly larger calcite crystals (Figure 2-3b). The calcite matrices in all of the Lavrion samples were in general darker in color and showed lower birefringence than the matrix fractions of ancient lime plasters and mortars collected from other sites. In addition, small particles of chalcedony (amorphous silica) were common, although not abundant, in these samples, and one such particle is shown in Figure 2-3a (bright rounded particle in the center of the photomicrograph). Small dark red, opaque particles and dark reddish-brown to gray mottling were ubiquitous in the matrix of the Lavrion plasters and mortars (Figure 2-3a and b).

Photomicrographs of sample LVL18, a basin plaster from the Lavrion district through which a 'drainage' cone had been inserted, are shown in Figure 2-3c and d. The microtexture and mineralogy of the bulk plaster is illustrated in Figure 2-3c and is typical of that previously described for LVL08,

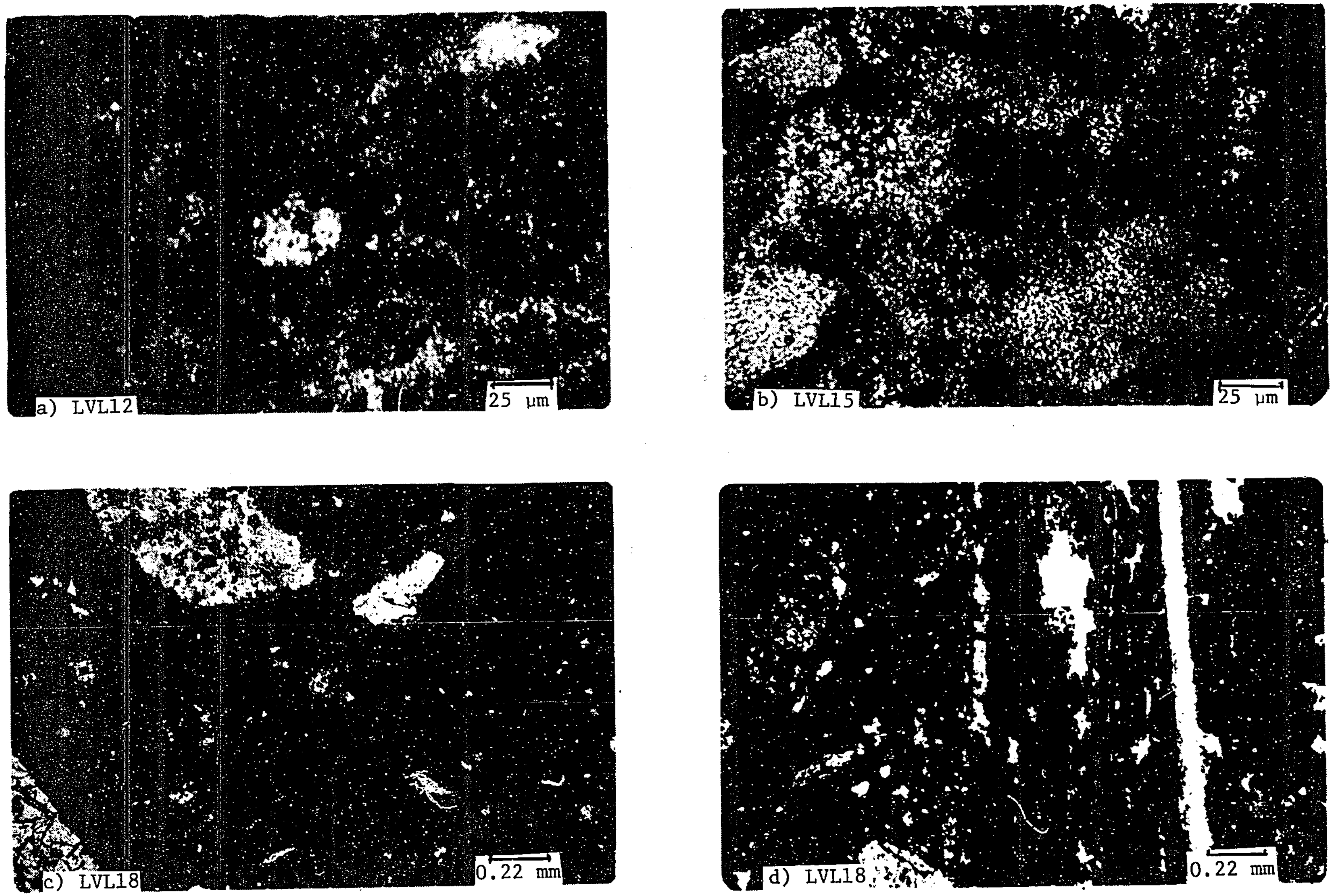

Figure 2-3. Photomicrographs of the Matrix Fraction of Ancient Plasters, Samples LVL12 and 15, and of a Plaster and Drainage Cone, Sample LVL18, From the Lavrion Mining District, Greece. (All parallel Nicols.)

LVL13, and LVL17. The microtexture of the drainage cone, shown in the right half of Figure 2-3d, is unique. It is characterized by numerous laminations which resemble growth rings or possibly diffusion (reaction) fronts. Macroscopic examinations of this cone suggested that it was manufactured through a series of at least eight plaster or paint applications. However, petrographic analyses revealed the presence of far too numerous lamellae on a scale too fine to have resulted from a man-made technique. The interfacial region between the cone and bulk plaster is coherent and suggests that the cone was inserted prior to setting of the plaster.

2.2.2 Selected Samples from The Republic of Cyprus

Photomicrographs of samples IDL02, IDL03, and KTL04, gypsum plasters from The Republic of Cyprus, are shown in Figures 2-4a to d. All of the gypsum plasters examined appear to be relatively porous and the thin sections, as seen in Figure 2-4a and b, are characterized by abundant aggregate pluck-outs. Sample IDL03 contained small, rounded, foraminifera-rich carbonate rocks, selenite blades, and uncalcined or partially calcined (and subsequently hydrated) uncrushed gypsum fragments in the aggregate fraction. The other gypsum plasters contained relatively less carbonate aggregate. These fine-grained gypsum matrices appeared clear to light grayish-yellow in plane light, displayed low birefringence, and contained patches of radiating needle-bundles up to 1.5 mm, and oriented blades up to 0.5 mm (Figure 2-4b). High magnification of the matrices revealed a variety of microtextures, as illustrated by the cross-hatched pattern made up of long-oriented needles (Figure 2-4c), and by the mosaic pattern made up of randomly oriented stubby laths (Figure 2-4d). In general, the gypsum plasters examined in this study contained a small proportion of aggregate (less than 2 mm in size) and had chemically homogeneous matrices, although the microtextures of the matrices were variable.

Photomicrographs of a variety of lime-rich plasters from The Republic of Cyprus, AML03, IDL01, KUL01, and KUL02, are shown in Figure 2-5a to d, respectively. The slaked lime originally used to make these materials has subsequently carbonated to produce very fine-grained calcite matrices. The matrix fractions of these materials are typically mottled from orange to light yellow (Figure 2-5a and d), or from grayish-yellow to brown (Figure 2-5b and c), and contain dark patches (usually red) up to 0.5 mm in size. These

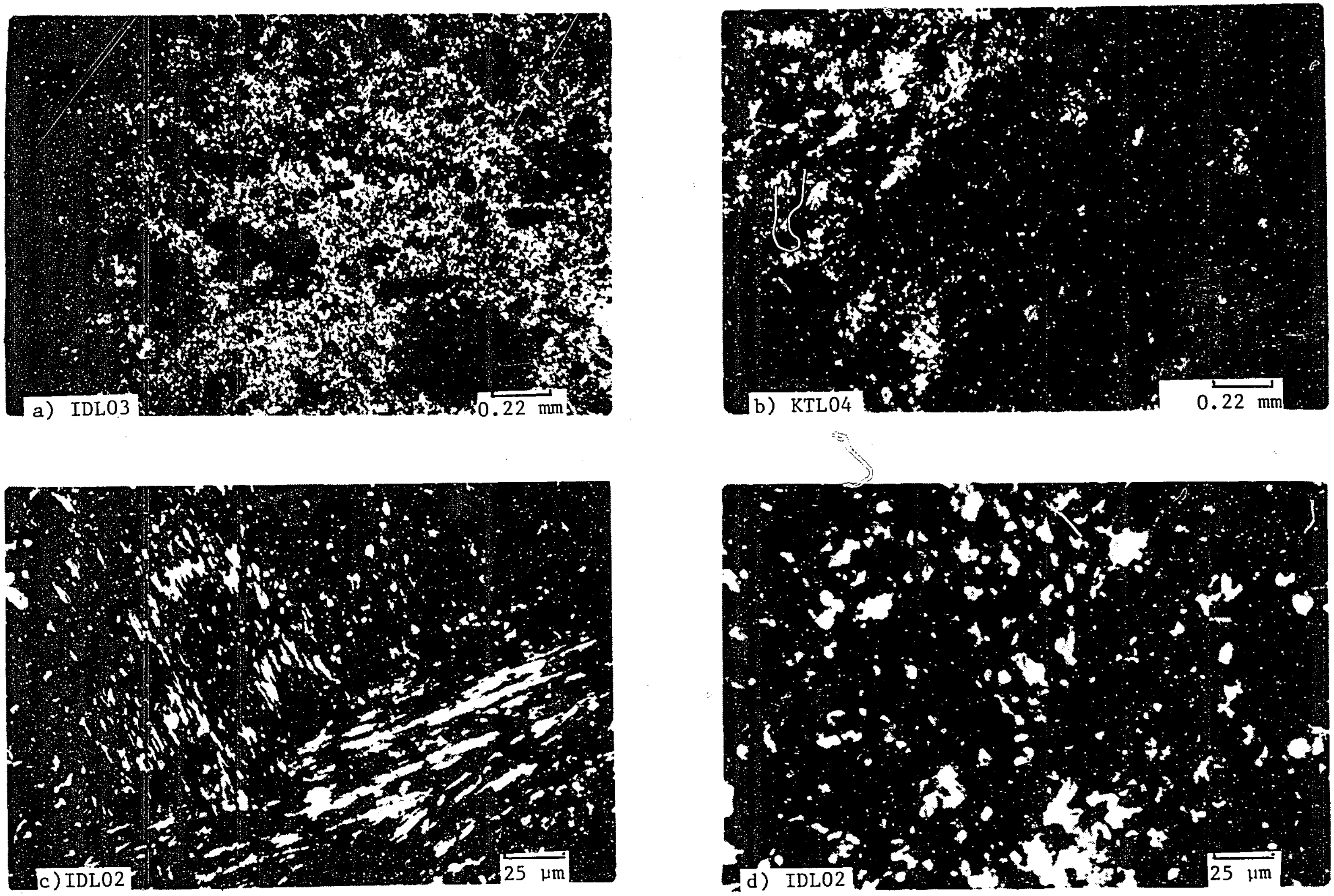

Figure 2-4. Photomicrographs of Gypsum Plasters From the Idalion, Samples IDL02 and 03, and Kition, Sample KTL04, Excavations, The Republic of Cyprus. (90-degree Nicols in a), c) and d); 70-degree Nicol in b).)

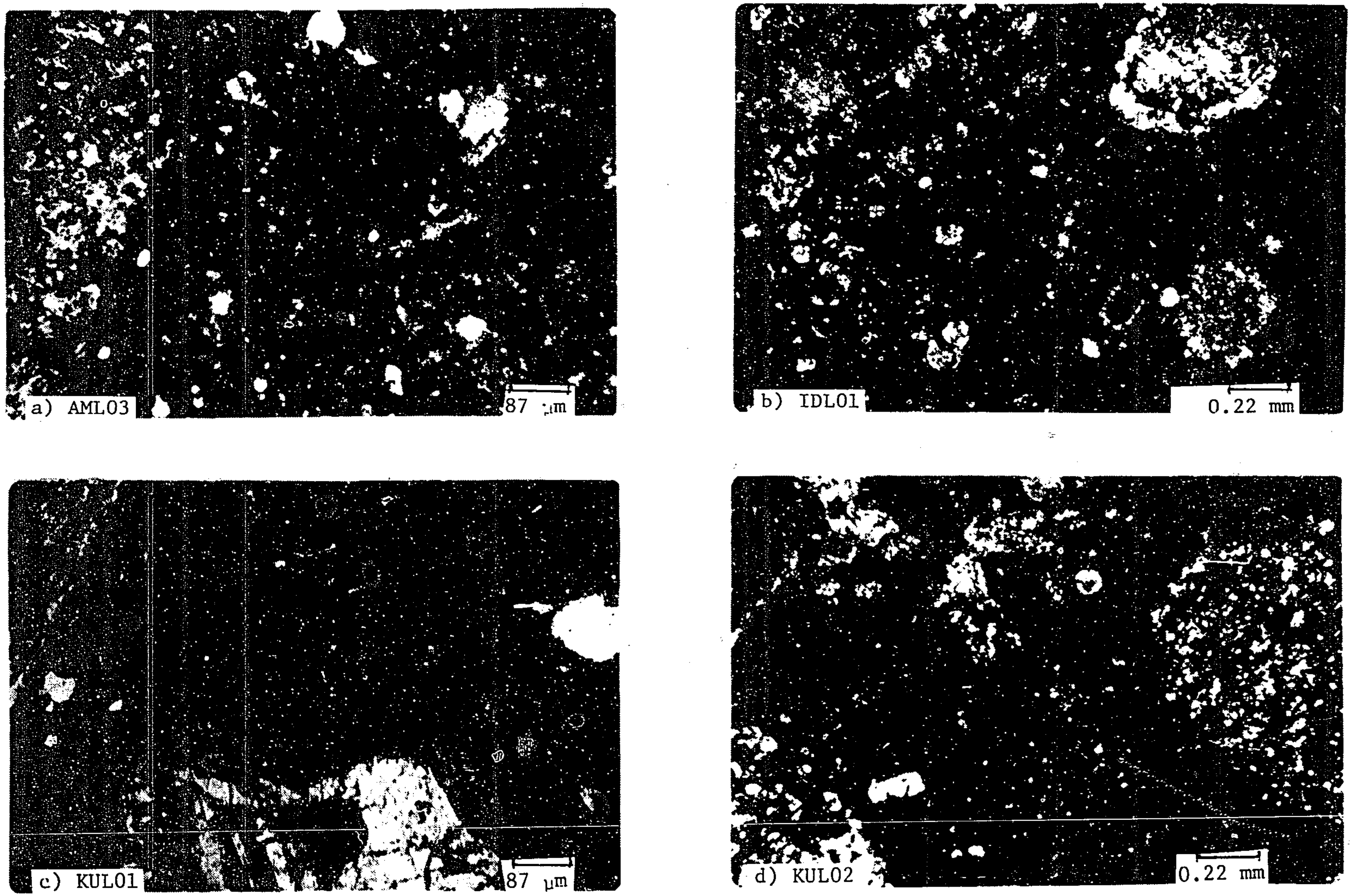

Figure 2-5. Photomicrographs of Lime-Based Plasters From the Amathus, Sample AML03, the Idalion, Sample IDL01, and the Kourion, Samples KUL01 and 02, Excavations, The Republic of Cyprus. (Parallel Nicols in a) and c); 80-degree Nicol in b); and 90-degree Nicol in d).)

patches have distinct to diffuse boundaries and a texture, fabric, and grain size similar to that of the surrounding matrix. Other patches, up to 0.5 mm, of slightly coarser-grained calcite display typical carbonate extinction and high birefringence (Figure 2-5d) and are common throughout the matrix. The coarse-aggregate fractions in the lime-rich plasters ranged from primarily igneous gravel (Figure 2-5a and c) to sedimentary siltstones and carbonates (Figure 2-5b and d), occasionally included a minor proportion of metamorphic rocks, and were rounded to subrounded. The fine-aggregate fractions consisted of quartz and/or volcanic sand. Aggregate sorting, grading, and rock type were unique to each site examined, and the aggregates were probably obtained from nearby stream channels. Interfacial reaction zones between igneous or sedimentary aggregates and the matrix phases were not observed. However, fractures such as those illustrated in Figure 2-5a and d, were often observed tracing the aggregate/matrix interfacial region. In some specimens examined, secondary calcite filled these fractures (Figure 2-5d).

Photomicrographs of sample AML02, a terra-cotta pipe with lime plaster as a joint sealant, which was collected from the Amathus excavation, The Republic of Cyprus, are shown in Figure 2-6a to d. The joint-sealant material is shown in Figure 2-6 and is composed of fine-grained calcite (carbonated slaked lime) plus less than 5 percent quartz sand. (The dark areas, holes, shown in Figure 2-6a are due to aggregates plucked out of the matrix during thin section preparation.) The matrix fraction of the sealant does contain rounded to irregular patches of slightly coarser-grained calcite which produces a somewhat uneven texture. Figure 2-6b (right edge) is a photomicrograph of the exterior surface of the pipe sealant and shows small needle- and tabular-shaped calcite crystals up to 1 mm, more or less aligned parallel to the surface, forming a thin surface rind. The interfacial zone between the terra-cotta and the sealant is shown in Figure 2-6c and d, and is characterized by: fractures parallel to the contact; secondary calcite partially filling some of these fractures; and in places, what appears to be interfacial reaction zones. Evidence for reaction between terra-cotta and slaked lime is best illustrated in Figure 2-6d (color gradation, matrix, top; terra-cotta, bottom). However, it should be noted that both the matrix and terra-cotta display discolored zones on either side of the associated fracture. Therefore, this feature may be the result of diffusion and reaction of aqueous fluids circulating along a pre-existing fracture system, rather than the result of pozzolanic reaction.

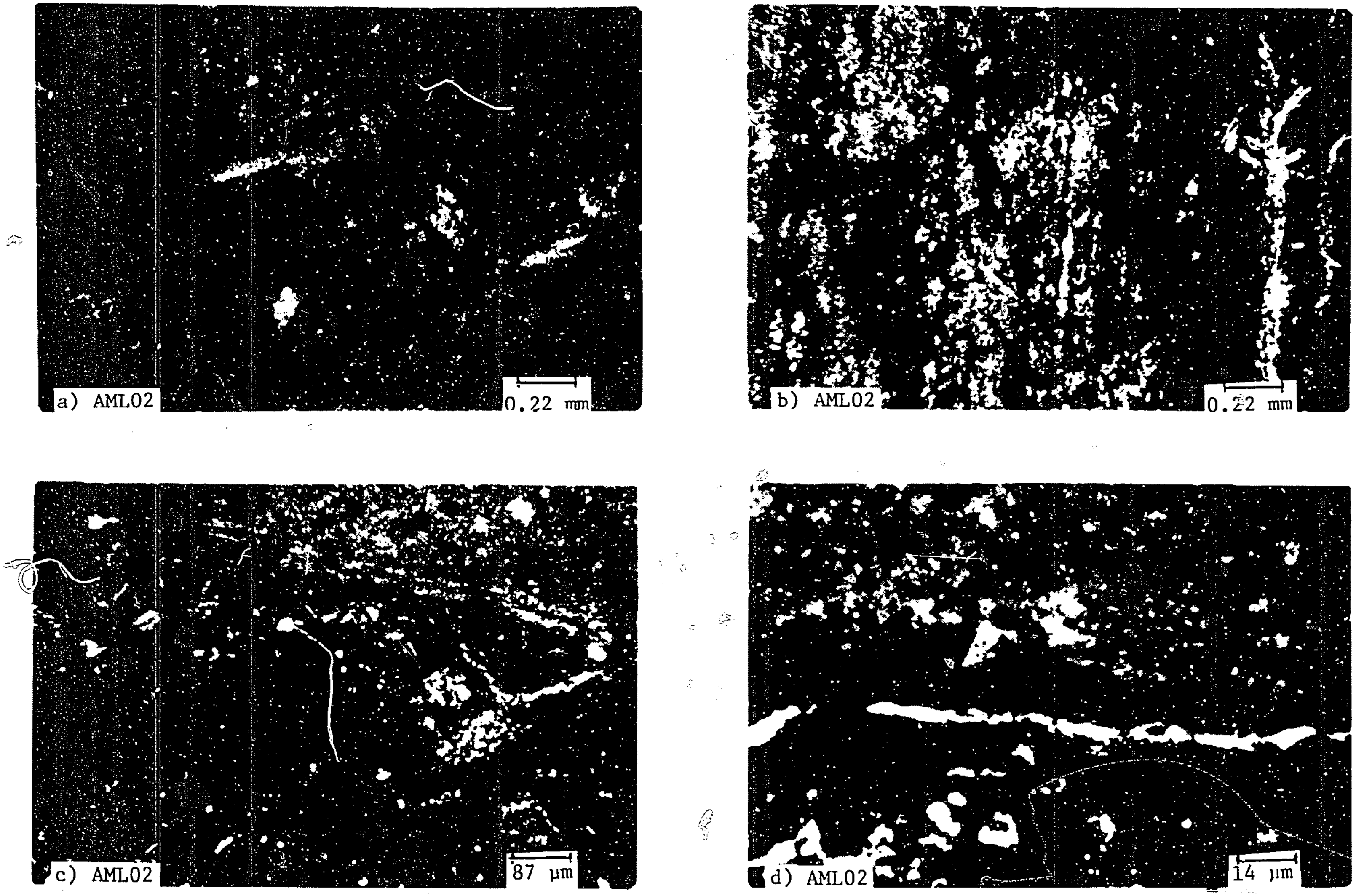

Figure 2-6. Photomicrographs of Sample AML02, a Terra-Cotta Pipe Plus Lime-Based Joint Sealant, From the Amathus Excavation, The Republic of Cyprus. (90-degree Nicols in a) and b); 65-degree Nicol in c); and parallel Nicol in d).)

Petrographic examination of a sample collected from a small basin/bin at Khirokitia, The Republic of Cyprus, revealed that this structure was a hollowed-out block of limestone rather than a lime plaster. A photomicrograph of this sample is shown in Figure 2-7a and clearly illustrates that the specimen is a poorly sorted, fossiliferous calcarenite, not a man-made material (KHL01).

Petrographic and field examination of two samples collected from the Lemba site, The Republic of Cyprus, resulted in ambiguous interpretations. A thin section of LML01, collected from what appeared to be an ancient floor plaster, is shown in Figure 2-7b. This photomicrograph resembles that of a carbonate rock, more specifically, a biomicrite containing foraminifera and algal balls, rather than a man-made material. This thin section is representative of aggregate in this building and is not representative of the matrix material. Due to the minor amount of matrix present, a representative thin section was not obtained.

Another specimen from the Lemba site, LML02, was collected from a small basin/bin which appeared to be made of a lime plaster. Figure 2-7c is a photomicrograph of this material, which is very homogeneous and composed of very fine-grained calcite.

The sample lacks tension fractures which are ubiquitous in the other lime mortars or plasters examined previously.

Figure 2-7d is a photomicrograph of a sample collected from a small bin/basin at Episcopi (Phaneromeni). This material consists of very fine-grained calcite plus less than two volume percent volcanic sand (mostly olivine). (This photomicrograph shows an unusually high concentration of olivine crystals relative to that in the total thin section.) Again, this material is relatively homogeneous and lacks tension (shrinkage) fractures.

2.3 SCANNING ELECTRON MICROSCOPE ANALYSIS RESULTS

2.3.1 Selected Samples from Greece

2.3.1.1 Samples from the Dam Site, Lavrion

Scanning electron photomicrographs of samples LVL05 (mortar) and LVL17 (plaster) collected from the retaining wall of a small dam near the town of

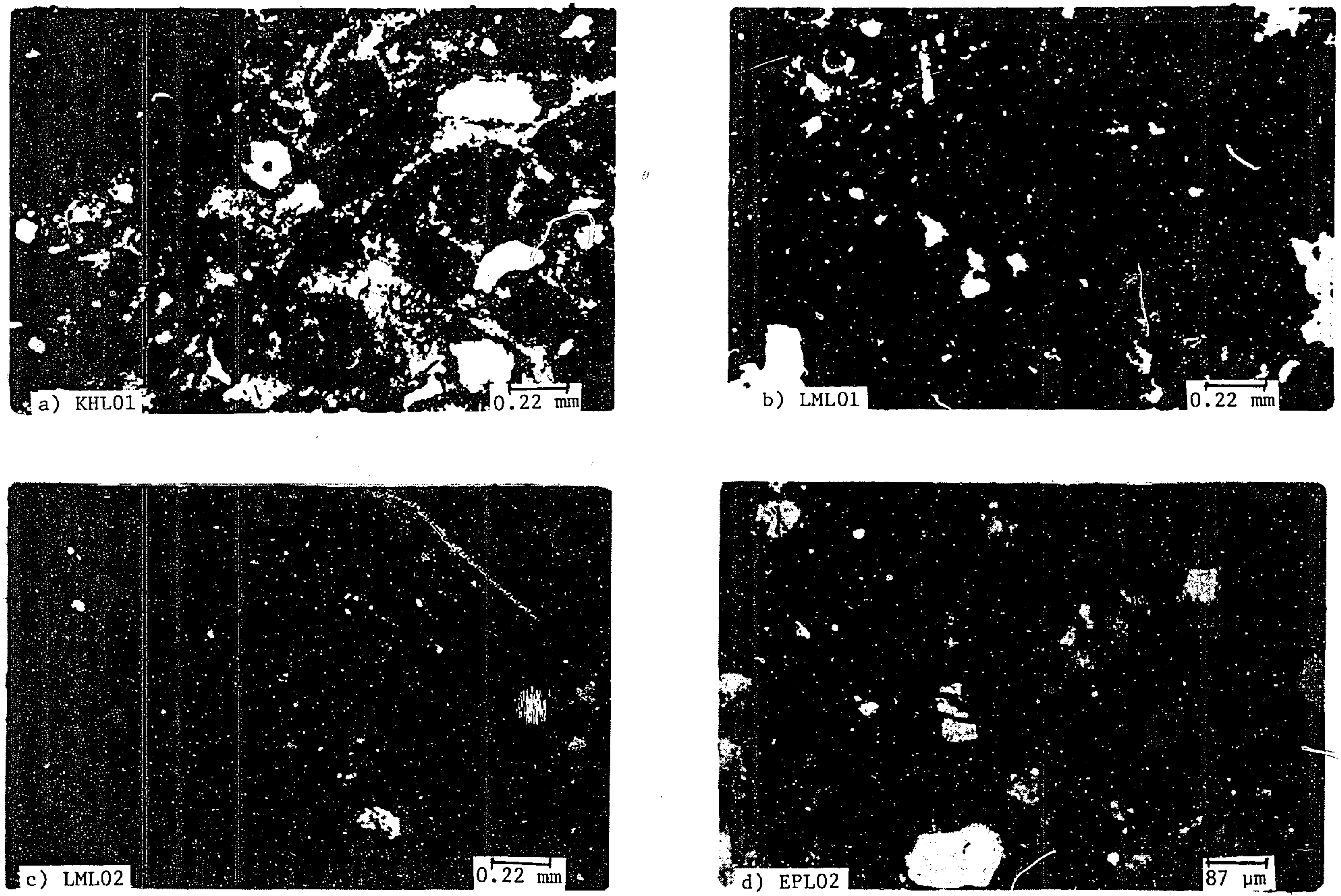

Figure 2-7. Photomicrographs of Specimens Collected From the Khirokitia, Sample KHL01, the Lemba, Samples LML01 and 02, and the Episcopi, Sample EPL02, Excavations, The Republic of Cyprus. (Parallel Nicols in a), c), and d); 80-degree Nicol in b).)

Lavrion, Greece, are shown in Figure 2-8a to d and e and f, respectively. The microstructure of the mortar, LVL05, is coherent and characterized by small, well-developed calcite crystals and massive calcite embedded in abundant, very fine-structured particles which have irregular morphologies. These particles are typically intergrown to form sponge-like masses, crumpled foils with irregular selvages and surfaces, and massive-looking features throughout the matrix (Figure 2-8a and b). An energy dispersive X-ray spectrum, typical of the fine-structured particles in LVL05, is shown in Figure 2-9 (spectrum A) and indicates the presence of Ca, with minor amounts of Si, Al, Fe, and Mg.

Radiating, tabular structures such as those shown in Figure 2-8a also appear to be intergrown with the hydrated matrix phases on LVL05. This material has a morphology similar to that commonly observed for hydrated calcium aluminate phases formed in portland cements, and EDX qualitative analysis of these tabular features resulted in detection of calcium, silicon, and aluminum. However, positive structural identification of this material has not been made, and it should be noted that these features also resemble unhydrated or partially hydrated portland cement clinker grains.

Incorporated into the matrices of LVL17 and particularly LVL05 were large chunks, up to and larger than 1 cm in cross section, of a fine-grained white phase which was identified as calcite (formed by carbonation of poorly crushed, slaked lime) and also other lumps of a fine-grained yellow phase, identified as phillipsite by X-ray diffraction. The microstructure of the calcite chunk is shown in Figure 2-8c and is characterized by a massive appearance. Few discrete prismatic or rhombohedral crystals were observed in these regions, and the interfacial regions formed between the matrix and calcite chunks were typically irregular and did not display layering or zoning. The microstructure of the phillipsite-rich chunks is very complex, as shown in Figure 2-8d. Small euhedral crystals cover the surfaces of a porous glassy-looking material (volcanic glass?). EDX analyses of various areas within these chunks resulted in the detection of silicon as the most abundant cation, lesser but approximately equal amounts of K, Ca, Mg, and Al, and minor to trace amounts of Na and Fe (spectrum R, Figure 2-9). The selvages of these chunks were usually glassy but zoning or layering of hydration products was not observed along the matrix/phillipsite interfacial regions.

Sample LVL17 is a multilayer plaster from the same structure as LVL05. The contact between two of the plaster layers is shown in Figure 2-8e and f.

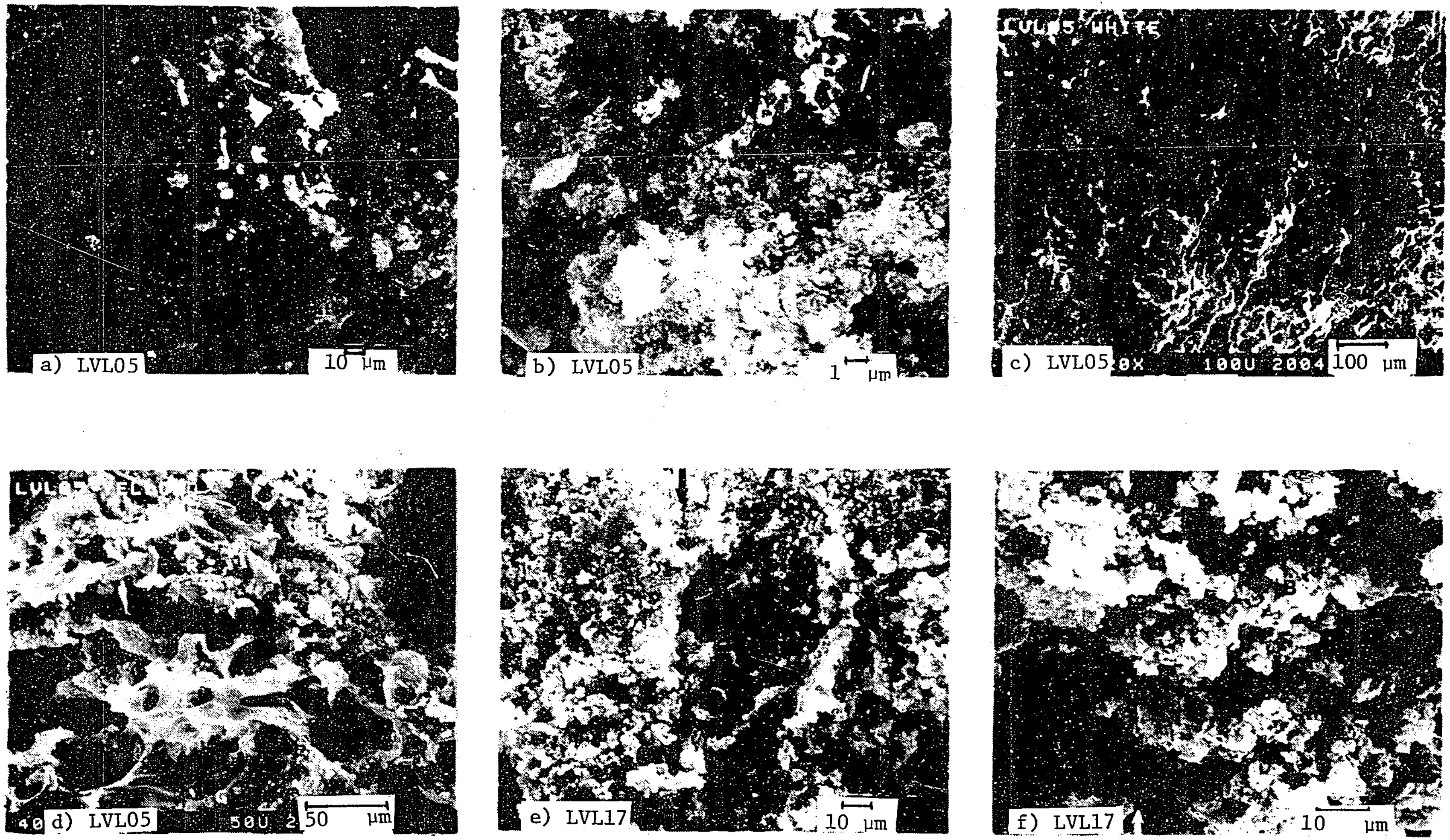

Figure 2-8. Scanning Electron (SEM) Photomicrographs (Secondary Electron Images) of a Mortar, Sample LVL05, and a Plaster, Sample LVL17, Collected From the Retaining Wall of a Dam, Lavrion Mining District, Greece.

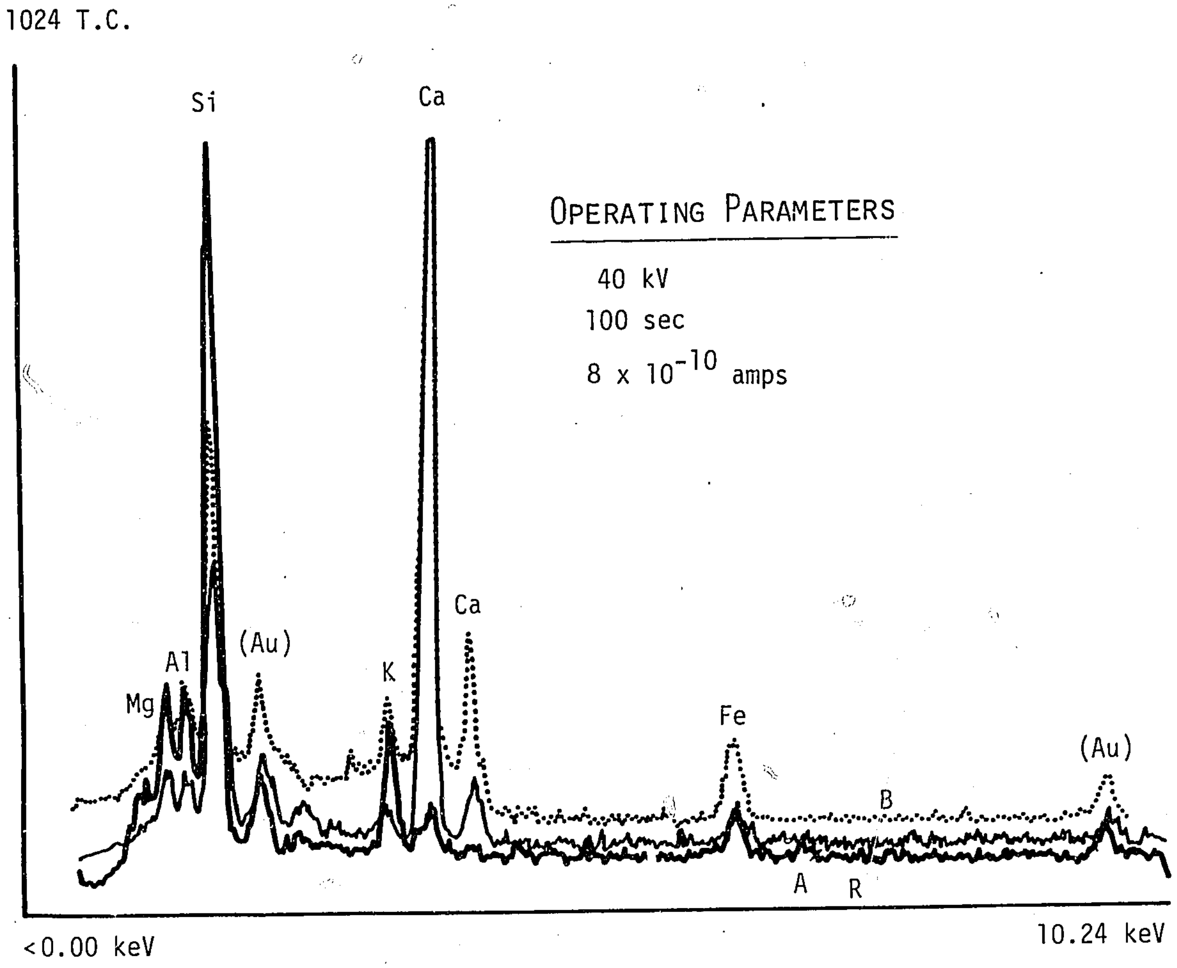

Figure 2-9. Examples of EDX Spectra of Matrix Phases in Sample LVL05. Spectrum A corresponds to the indicated area in Figure 2-8b; spectrum R to the phillipsite in Sample LVL05 (Figure 2-8d); and spectrum B to the fine structure in the matrix in Sample LVL17 (Figure 2-8f).

This interface is planar, and sharp, which suggests that the outer surface of underlying layer (right side of Figure 2-8e and f) was 'finished' prior to application of the top layer (left side of photomicrographs). This contact is marked with arrows in the secondary electron images and may even have resulted from polishing the underlying layer prior to application of the top layer.

No gross differences in the microstructures of the matrix fractions in these layers were apparent. However, the average size of the aggregate fraction in the bottom layer was coarser than that in the upper layer. The microstructures of both layers illustrated in Figure 2-8e and f are characterized by well-developed calcite crystals, most of which are 0.1-0.5 μm in size intergrown around larger calcite crystals up to 2 μm to form a coherent three-dimensional structure. A minor amount of very fine-structured particles was observed throughout portions of these layers. An energy-dispersive X-ray spectrum for the area labeled B (Figure 2-8f) is presented in Figure 2-9 and indicates the detection of primarily calcium, and lesser amounts of other cations.

2.3.1.2 Samples from Ore-Washing Structures and Cisterns in the Ancient Lavrion Mining District

Secondary electron images in Figure 2-10a and b illustrate the microstructure of the matrix in sample LVL06, a floor plaster from an ore-sorting platform in the Lavrion mining district. The matrix is composed of small calcite crystals, less than 1 μm, in addition to masses of very fine-structured, irregularly shaped particles. The sample appears to be relatively porous, although the microstructure is coherent and the calcite crystals are randomly oriented and intergrown. The calcite crystals have euhedral to platy morphologies and often appear to be growing on substrates (possibly fine aggregates), the shape of which can only be inferred on the fractured surfaces. The fine-structured particles in this sample often display an irregular colliform morphology (Figure 2-10a). EDX qualitative analyses of regions rich in this material resulted in detection of Ca; lesser amounts of Si, Fe, Al, Mg; and other cations in trace amounts. Aggregate surfaces were not exposed on fractured surfaces which means that fracture typically transects the bulk material and not the aggregate/matrix interfacial regions.

The microstructure of the matrix fraction in LVL08 and also of the inter-

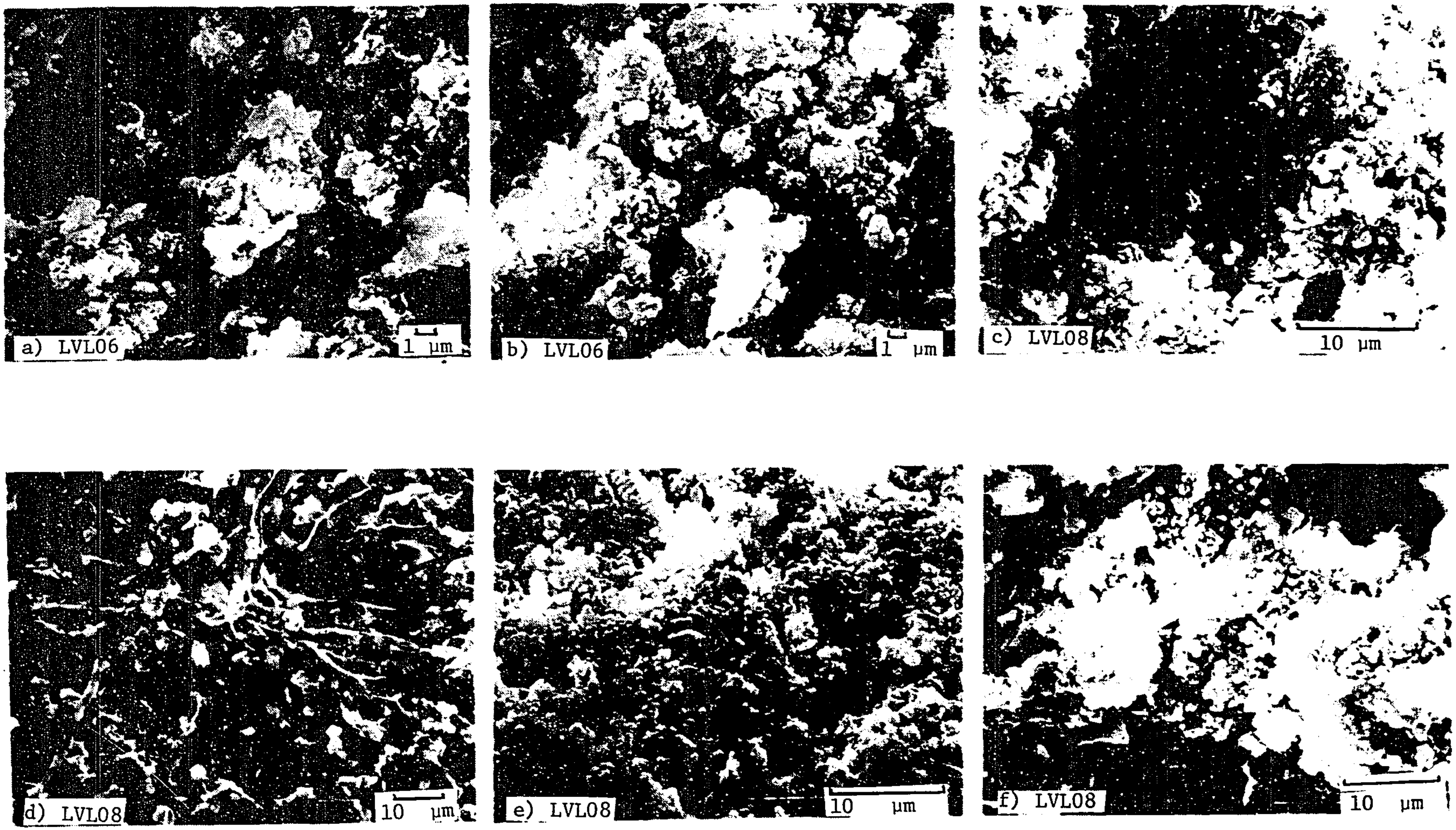

Figure 2-10. Scanning Electron (SEM) Photomicrographs (Secondary Electron Images) of Samples Collected From an Ore-Washing Facility, LVL06 and 08, in the Lavrion Mining District, Greece.

facial region formed between the matrix and an aggregate (pyroxene crystal) are shown in Figure 2-10c. Sample LVL08 was collected from a floor support of an ancient ore-washing platform. The matrix is composed of small, randomly oriented calcite crystals and the resulting texture is often lumpy, as shown here. The interfacial region illustrated in Figure 2-10c appears to be composed of a thin film-like layer covering the crystal (except for a small central portion) and an overlying layer of very fine particles intergrown to form a massive sheet. These particles are intergrown with and attached to the larger calcite crystals in the bulk matrix. This type of interfacial morphology has been observed in portland cement-containing materials and has been described by Roy and Langton (1982), Hadley (1972), and Diamond (1976).

Figure 2-10d to f illustrates another interfacial feature commonly observed in LVL08. Figure 2-10d is a secondary electron image of a quartzite aggregate coated with calcareous algal sheaths. Apparently the quartzite gravel/matrix interfacial regions were zones of relative weakness and/or high permeability. Under damp conditions, algae (green or blue-green) preferentially colonized these zones. Figure 2-10e shows the matrix side of an interfacial region; no layering or zoning were observed on either the matrix or quartzite side. The calcite crystals in Figure 2-10e have grown into voids on the irregular surface of the gravel and as a result are oriented more or less normal to the aggregate surface. Figure 2-10f illustrates calcareous algal sheaths penetrating into the calcite matrix which is shown here overlying the quartzite gravel. This cross-cutting relationship implies that the algae grew into fractures in the plaster along aggregate/matrix interfacial zones and that it was not present on the gravel at the time of mixing and construction.

Photomicrographs of sample LVL09, plaster from the interior surface of an ancient cistern, indicate that a large proportion of the matrix consists of intergrown calcite crystals 1-2 µm in size, in addition to masses of very fine-structured particles (Figure 2-11a to c). These fine particles have irregular morphologies which include ragged platelets and sponge-like masses, and the calcite crystals have prismatic, rhombohedral, and massive morphologies. The overall microstructure appears coherent and fine-grained. An example of an energy-dispersive X-ray spectrum of fine-structured particles in an area in Figure 2-11c labeled A is shown in Figure 2-12 (Spectrum A). This area is calcium-rich but Si, Fe, Mg, and Al were also detected. Figure 2-11d illustrates the film layer formed in an aggregate/matrix interfacial region in

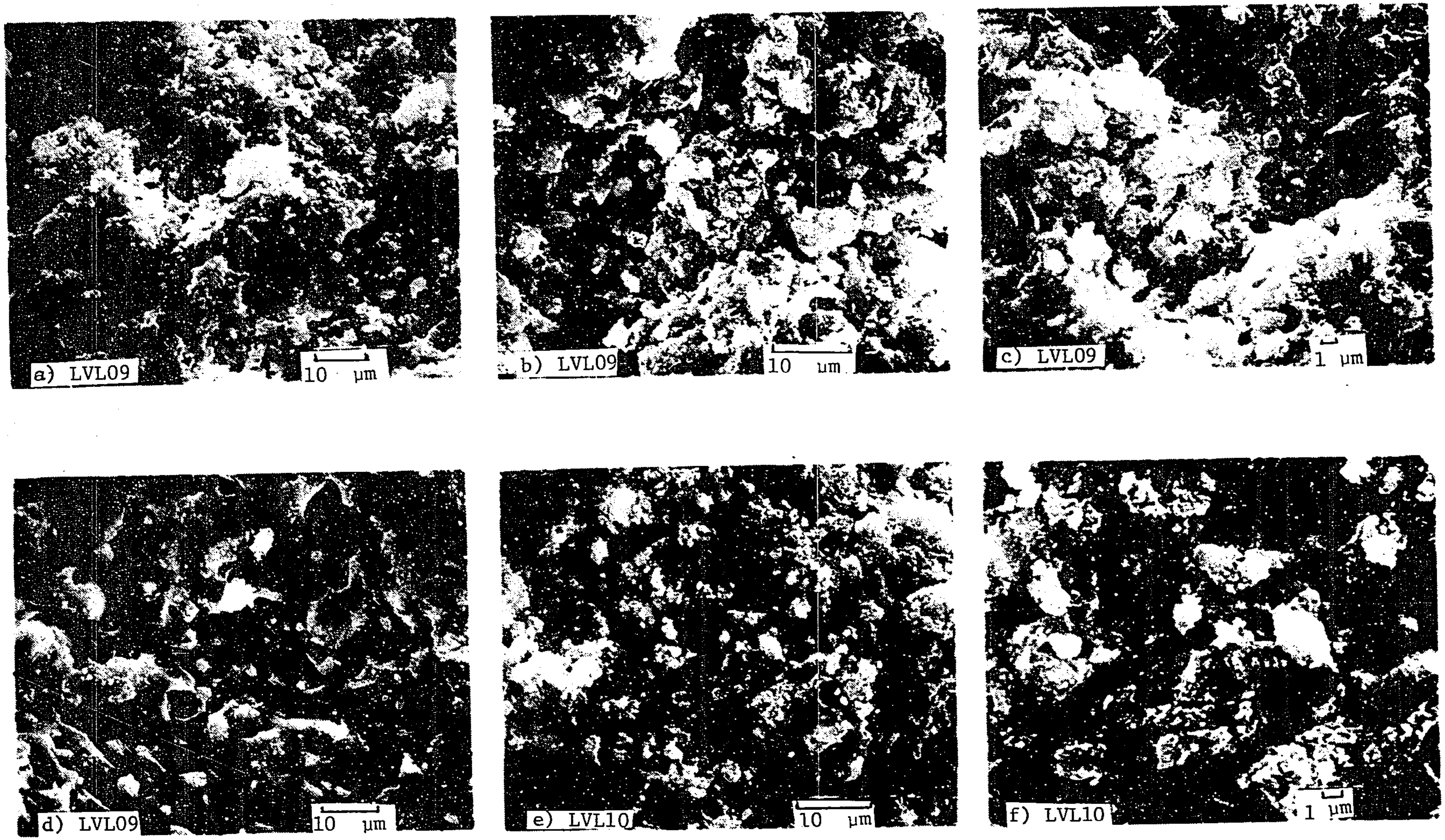

Figure 2-11. Scanning Electron (SEM) Photomicrographs (Secondary Electron Images) of Samples Collected From Cisterns, LVL09 and 10, in the Lavrion Mining District, Greece.

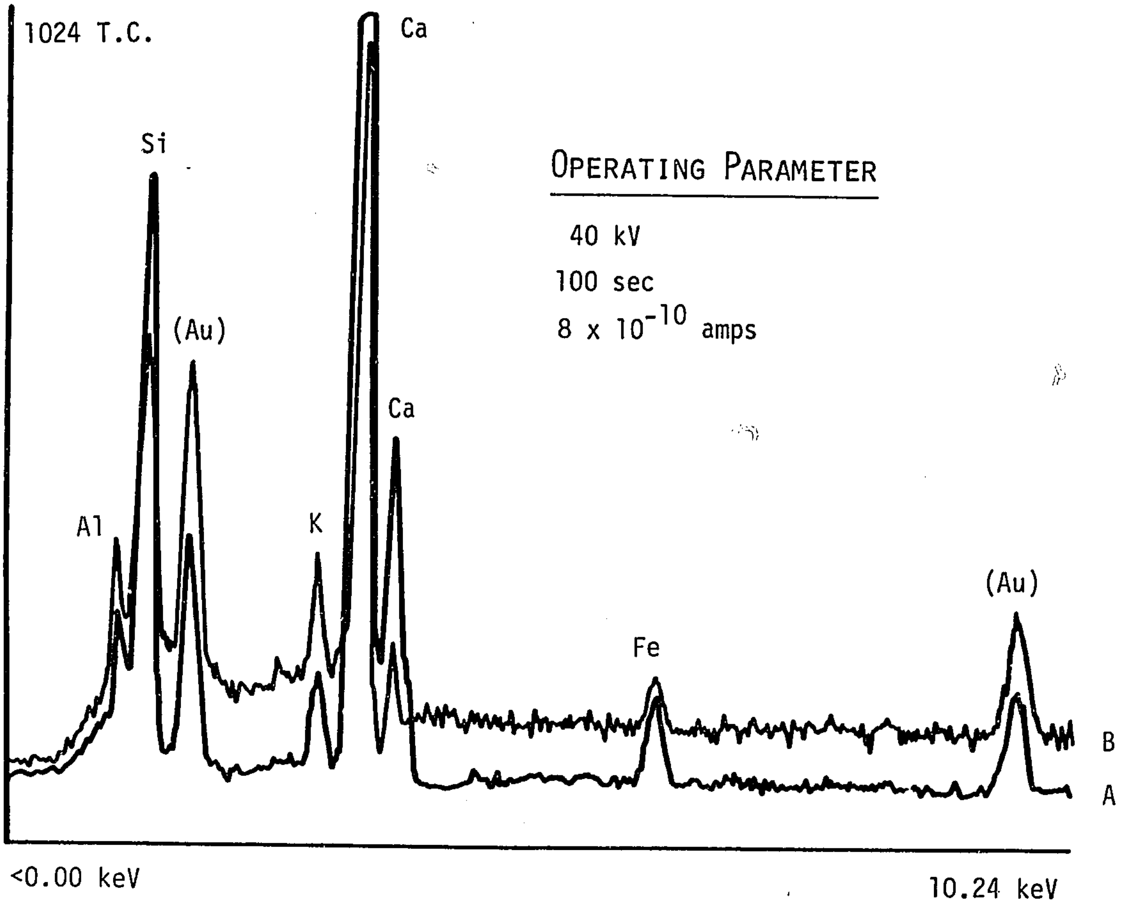

Figure 2-12. Examples of EDX Spectra of Matrix Phases in Samples LVL09 and 10. (Spectrum A corresponds to fine-structure particles in Figure 2-11c and spectrum B to fine-structure particles in Figure 2-11f, LVL09 and 10, respectively.)

LVL09. In this secondary electron image, the film layer remained attached to the bulk matrix when the sample was fractured. (The aggregate was plucked out of the surface.) This layer for the most part is massive and sheet-like, although it is porous. Also, a few small particles (either from the aggregate or matrix) appear to have remained attached to the matrix side of this sheet when it was detached from the aggregate.

The morphologies of the matrix phases and the microstructure of the cementitious fraction in sample LVL10, another cistern plaster lining, are shown in Figure 2-11e and f. These photomicrographs are similar to those described for sample LVL09, except that they contain a larger proportion of fine-structure material. This material is composed of irregular and ragged platelets, some botryoidal masses and/or sponge-like structures intergrown with calcite crystals and other fine particles. An energy-dispersive spectrum of one such area in Figure 2-11 (labeled B) is presented in Figure 2-12 (Spectrum B). Calcium was the most abundant cation detected. Substantial Si, and lesser Al, Fe, K, and Pb, were also identified in this spectrum.

A scanning electron photomicrograph of the exterior plaster layer, LVL11 (layer 3), of an ancient ore-washing basin near Lavrion is shown in Figure 2-13a. This layer consists of small calcite crystals up to 2 µm in size intergrown with fine-structure material similar to that previously described for the Lavrion samples. The calcite crystals are well developed and the microstructure appears relatively uniform and coherent. Few aggregates were observed, although calcareous algal sheaths were found on portions of this sample.

Photomicrographs of the middle plaster layer of this multilayered plaster, LVL11, are shown in Figure 2-13b to f. It is readily apparent that the microstructure of layer 2 is much more complex than that observed in layer 3 (described above). The matrix fraction of layer 2 contains well-formed calcite crystals up to about 2 µm, and other unidentified crystals with needle, platelet, or tabular morphologies. In addition, there is an abundant amount of very fine-structured material throughout the entire matrix. The most striking feature in the matrix fraction of layer 2, LVL11, is the presence and abundance of small (less than 100 µm), porous fragments identified (based on geologic inference of soil characteristics in mineralized

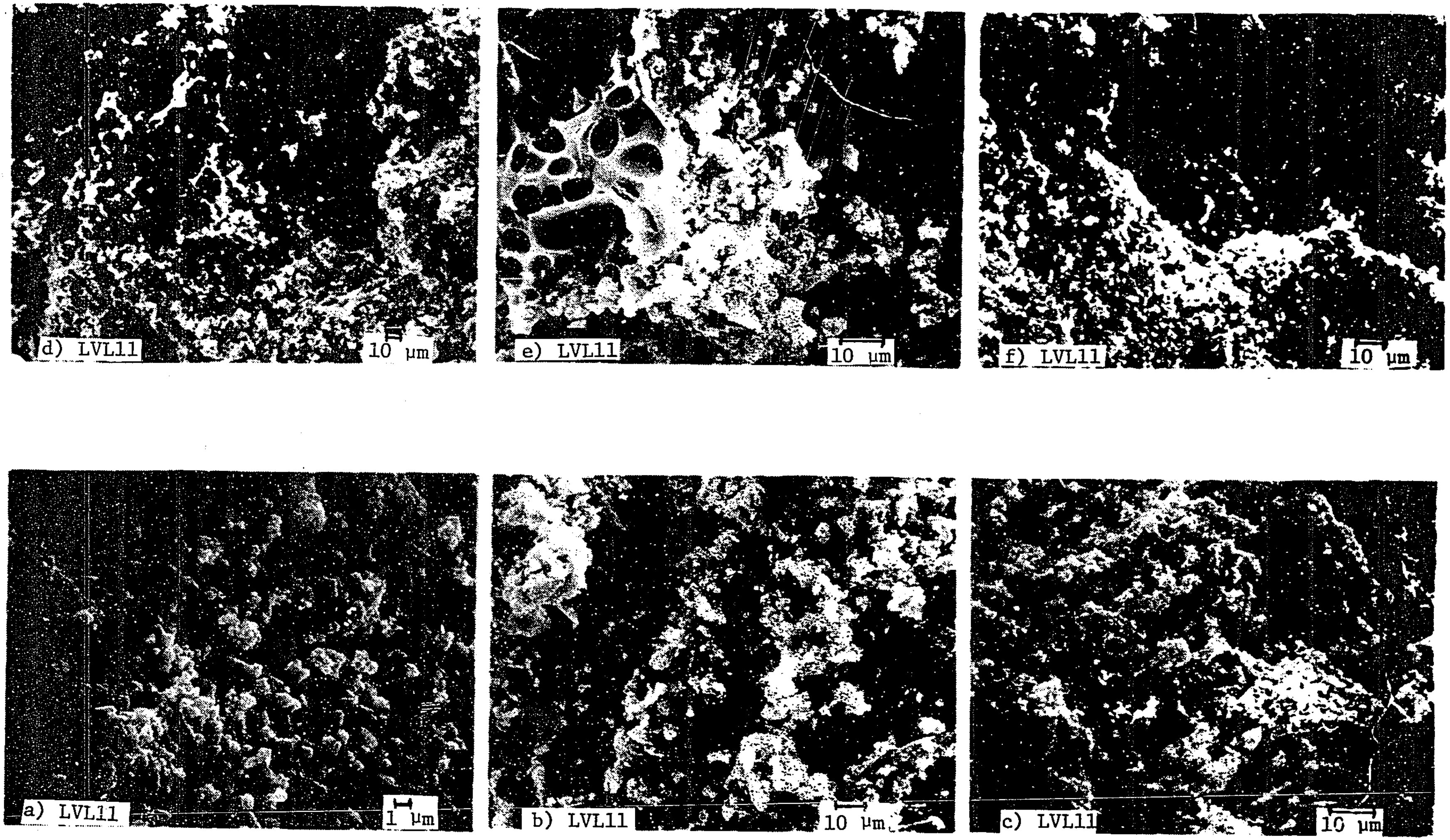

Figure 2-13. Scanning Electron (SEM) Photomicrographs (Secondary Electron Images) of Sample LVL11, the Exterior and Middle Layers of a Multilayer Plaster From an Ore-Washing Basin, Lavrion Mining District, Greece.

terranes) as gossan* fragments (Figure 2-13d and e). (However, there is a possibility that this material may be very fine slag fragments or other pozzolana material such as glassy volcanic ash.) The interfacial regions between the gossan fragments and matrix are not layered or zoned, although fine particles and crystals seem to be growing from the gossan surfaces into the matrix (Figure 2-13e); layered interfacial zones were not observed around other types of aggregates in this plaster (Figure 2-13d). The overall appearance of this sample is that of a multicomponent, very fine-grained, coherent material. The porosity also appears to be relatively low compared to other ancient plasters studied. This is in part due to the abundance of fine-structured particles.

Sample LVL12 was collected from the same ore-washing basin as LVL11. The bottom layer, layer 1 of the plaster described above, was sampled as LVL12 and the microstructure of this layer is illustrated in Figure 2-14a to f. Particle and crystal morphologies in this layer are varied and similar to those described in layer 2. Gossan (or volcanic glass or slag) fragments were also common features (Figure 2-14a and b). The microstructure of the matrix fraction is also similar to that described for layer 2, although more masses of fine-structured particles with crumpled foil morphologies were observed in layer 1. Energy-dispersive X-ray analyses of selected areas labeled in Figure 2-14 are present in Figure 2-15. The gossan fragments are silica-rich and also contain Ca, Al, K, and Fe (Spectrum A). The needles in Figure 2-14d are calcium-rich (vaterite?) and contain lesser amounts of Fe, Si, and K (Spectrum B). The fine-structured, irregular foils in Figure 2-14f contain abundant calcium and silicon and minor Al, K, and Fe (Spectrum C). The fine structure resembles some forms of C-S-H, suggesting a product of possible reaction of lime with reactive siliceous volcanic glass or gossan.

The microstructure of the matrix fraction of sample LVL13, a mortar in the wall over which plasters LVL11 and LVL12 were applied, is illustrated in Figure 2-16a to d. This matrix resembles those previously described for LVL12 (layer 3), and LVL11 (layer 2) and is relatively fine-grained and coherent.

---

*Gossan is a term used to describe the yellow to reddish deposits of hydrated oxides of iron produced near the surface by oxidation and leaching of sulfide minerals. Leaching typically results in a silica-rich, porous, sponge-like rock in surface outcrop.

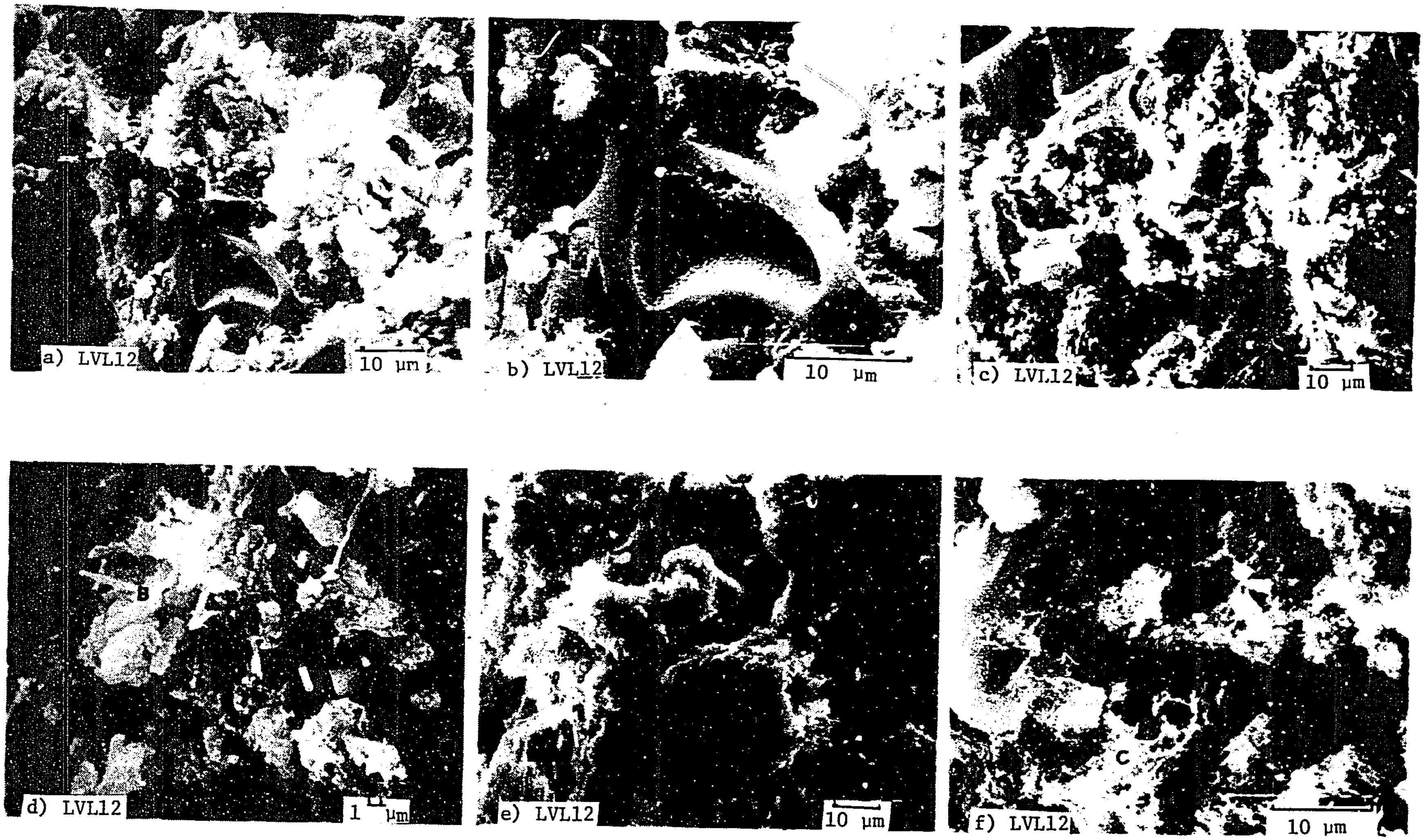

Figure 2-14. Scanning Electron (SEM) Photomicrographs of Sample LVL12, the Bottom Layer of a Multilayer Plaster From an Ore-Washing Basin, Lavrion Mining District, Greece.

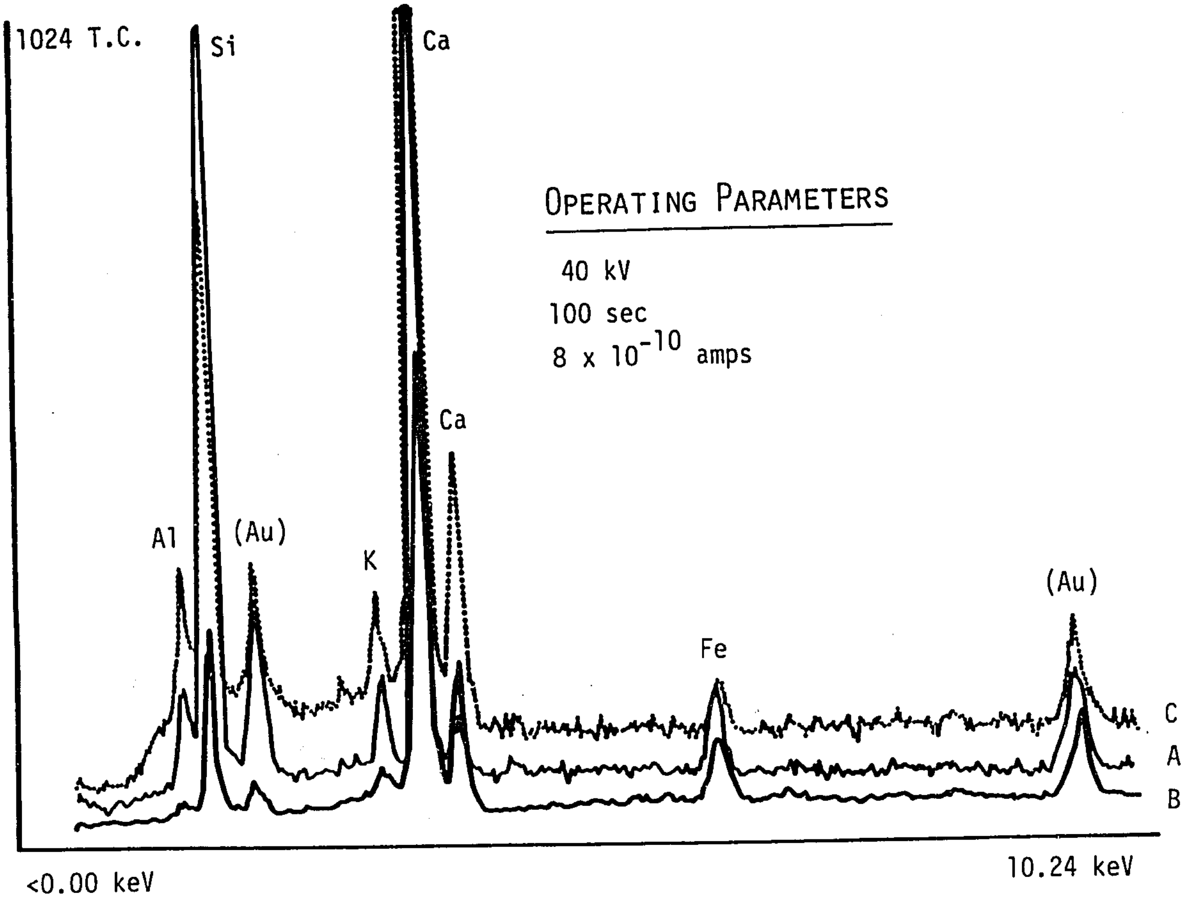

Figure 2-15. Examples of EDX Spectra of Matrix Phases in Sample LVL12, Layer 1. (Spectrum A corresponds to a gossan (or volcanic glass or slag) fragment (Figure 2-14b); spectrum B to needles in the matrix fraction (Figure 2-14d); and spectrum C to an area of fine-structured particles (Figure 2-14f).)

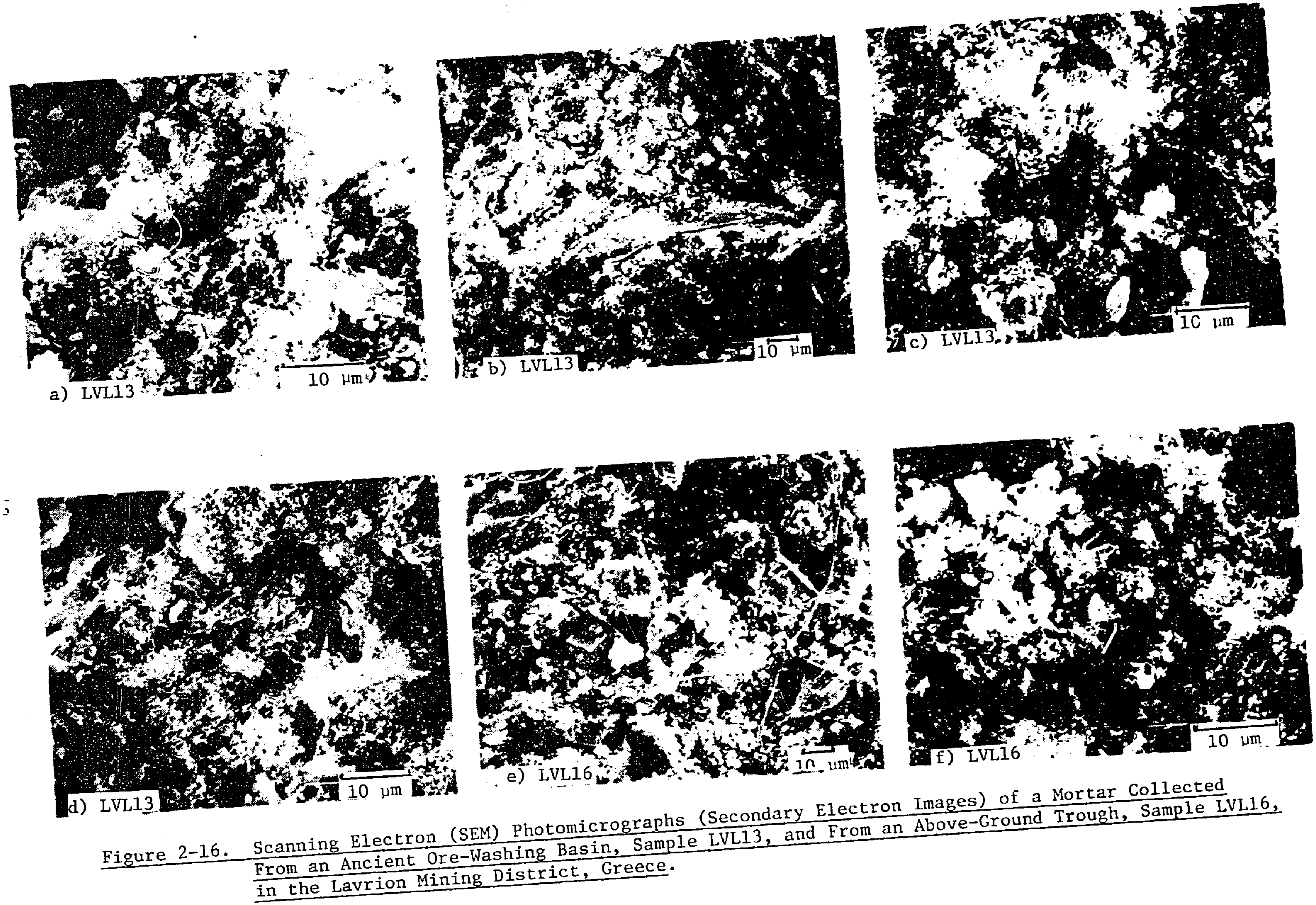

Figure 2-16. Scanning Electron (SEM) Photomicrographs (Secondary Electron Images) of a Mortar Collected From an Ancient Ore-Washing Basin, Sample LVL13, and From an Above-Ground Trough, Sample LVL16, in the Lavrion Mining District, Greece.

The matrix contains a relatively large amount of fine-structured particles (Figure 2-16b) and the interfacial regions between matrix and aggregate appear to be layered. A film-like layer overlying an aggregate is shown in the lower right of Figure 2-16b. Here it is shown attached to the matrix, fracture having separated it from the associated aggregate.

Scanning electron photomicrographs of LVL16, a plaster from the channel of an above-ground trough in the Lavrion mining district, are shown in Figure 2-16e and f. The matrix fraction of this sample contains calcite crystals, up to and larger than 5 μm in cross section (Figure 2-16e), in addition to patches of very fine-structured particles including honeycombs (Figure 2-16f). The calcite is present as well-developed crystals and also massive material. Regions within this specimen are penetrated by calcareous algal sheaths as shown in Figure 2-16e (filament-like features). EDX analysis of the fine-structured material resulted in detection of calcium, and lesser amounts of aluminum, silicon, iron, potassium, lead, zinc, and magnesium, although qualitative chemical analyses of this material were very variable. Certain particles high in lead and zinc in EDX and showing bright electron backscatter images probably correspond to the abundant small orange grains observed in hand specimens of LVL15 (layer 2) and are probably oxidized sulfides of Pb, Zn, and Fe. These particles may have been present in the carbonate rock calcined to make lime or they may have been added to the calcined lime as a soil fraction/fine aggregate fraction.

2.3.1.3 Samples from a Roman Aqueduct, Near the Amphissa-Delphi National Road

Scanning electron photomicrographs of sample ADL01, a plaster lining from the channel of an ancient Roman aqueduct, are shown in Figure 2-17a to f. The matrix fraction of this sample is relatively massive and is composed of leafy, irregular platelets, foils, and/or sheets intergrown with well-developed calcite crystals up to 2 μm in size and very fine-structured particles often intergrown into sponge-like masses (Figure 2-17a to c). The abundance of the foil- or sheet-like particles is unique to this plaster and the overall microstructure is more massive than that observed in other ancient cementitious materials examined. Energy-dispersive X-ray analysis of the matrix components resulted in detection of calcium, as the most abundant cation, in addition to minor amounts of silicon and lesser amounts of aluminum.

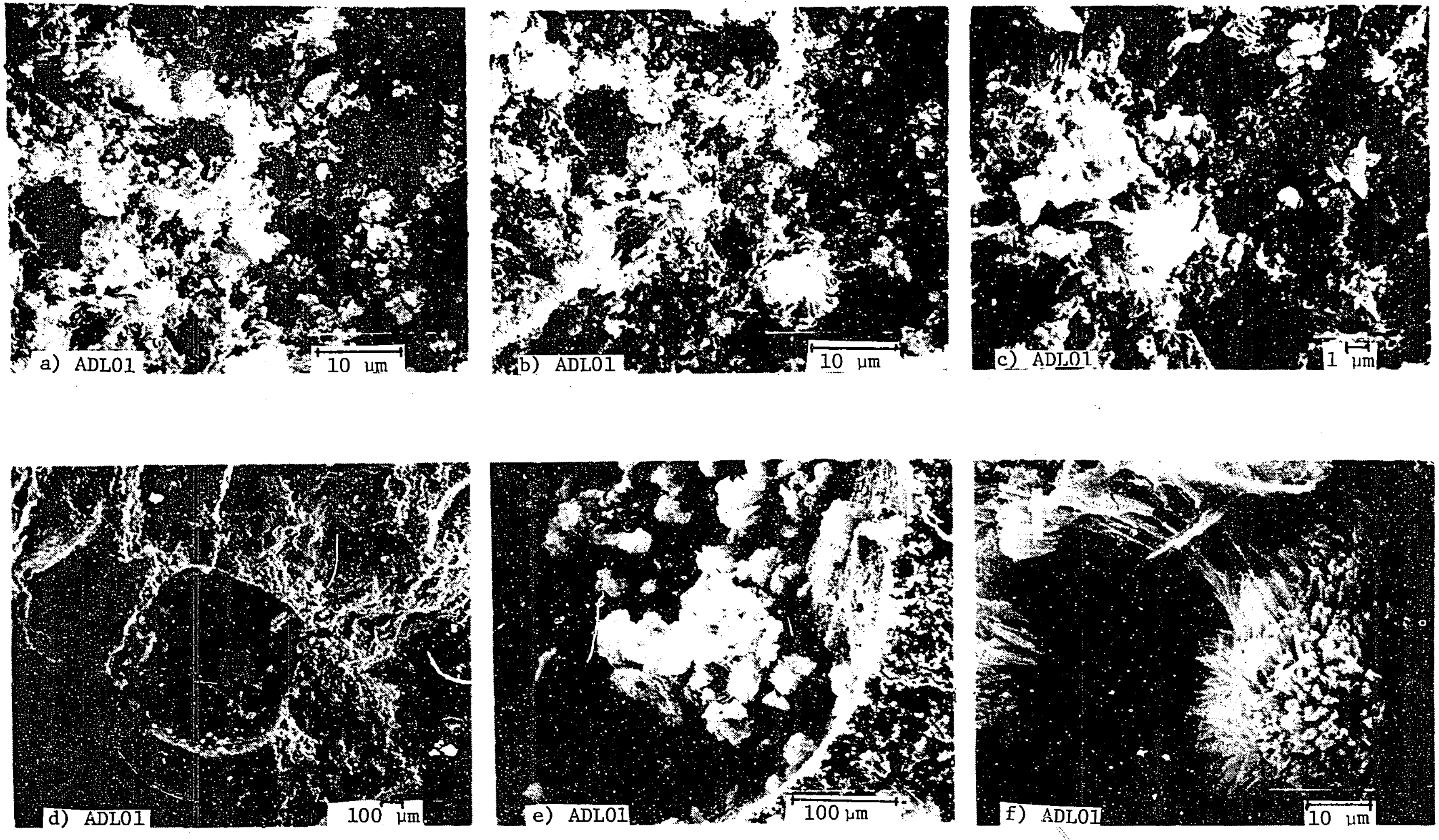

Figure 2-17. Scanning Electron (SEM) Photomicrographs (Secondary Electron Images) of Sample ADL01, Plaster Lining the Channel of an Ancient Roman Aqueduct in Greece.

A hole in the fractured surface of this sample is shown in Figure 2-17d and e. This hole formed when an aggregate was plucked out of the matrix at the time the sample was prepared for SEM examination. Bundles of small crystals can be seen growing from the matrix side of aggregate/matrix contact into a void space (crack) which was inferred to have been present between the matrix and aggregate (small pore spaces in this sample are often completely filled with these crystals). The needle habit of these crystals is clearly shown in Figure 2-17f and the EDX resulted in detection of primarily calcium (vaterite?) and minor amounts of silicon and aluminum.

2.3.2 Descriptions of Selected Samples from The Republic of Cyprus

2.3.2.1 Samples from the Amathus Excavation

Secondary electron images of the matrix in an early Christian or late Roman floor plaster collected from the Amathus excavation are shown in Figure 2-18a and b. This plaster contains both calcite crystals, 1 to 2 µm in size, and also very fine-structure particles intergrown to form a relatively porous but moderately coherent material. The fine-structure material occurs as sponge-like masses and also as more massive irregular sheets or foils, somewhat resembling C-S-H, accounting for a relatively large proportion of the matrix fraction.

A terra-cotta pipe and pipe-joint sealant, AML2, were also sampled at the Amathus excavation. The microstructure of the terra-cotta pipe is shown in Figure 2-18c and that of the joint-sealant material in Figure 2-18d. The pipe contains quartz and feldspar grains in a porous sintered or glassy-looking matrix. The sealant is mostly calcite crystals, less than 1 µm in size, intergrown into a very dense, low-porosity material. The interfacial zone between the pipe and sealant was irregular due to the roughness of the terra-cotta surface and zoning or layering in this region were not observed. Small calcite crystals grew directly on the pipe surface, and a fracture runs the length of the terra-cotta pipe/sealant contact.

Figure 2-18e is a photomicrograph of the matrix fraction of another floor plaster from Amathus, sample AML3. This sample contains a relatively small proportion of matrix compared to the amount of aggregate. In Figure 2-18e, massive calcite in addition to relatively large, up to 10 µm, calcite crystals

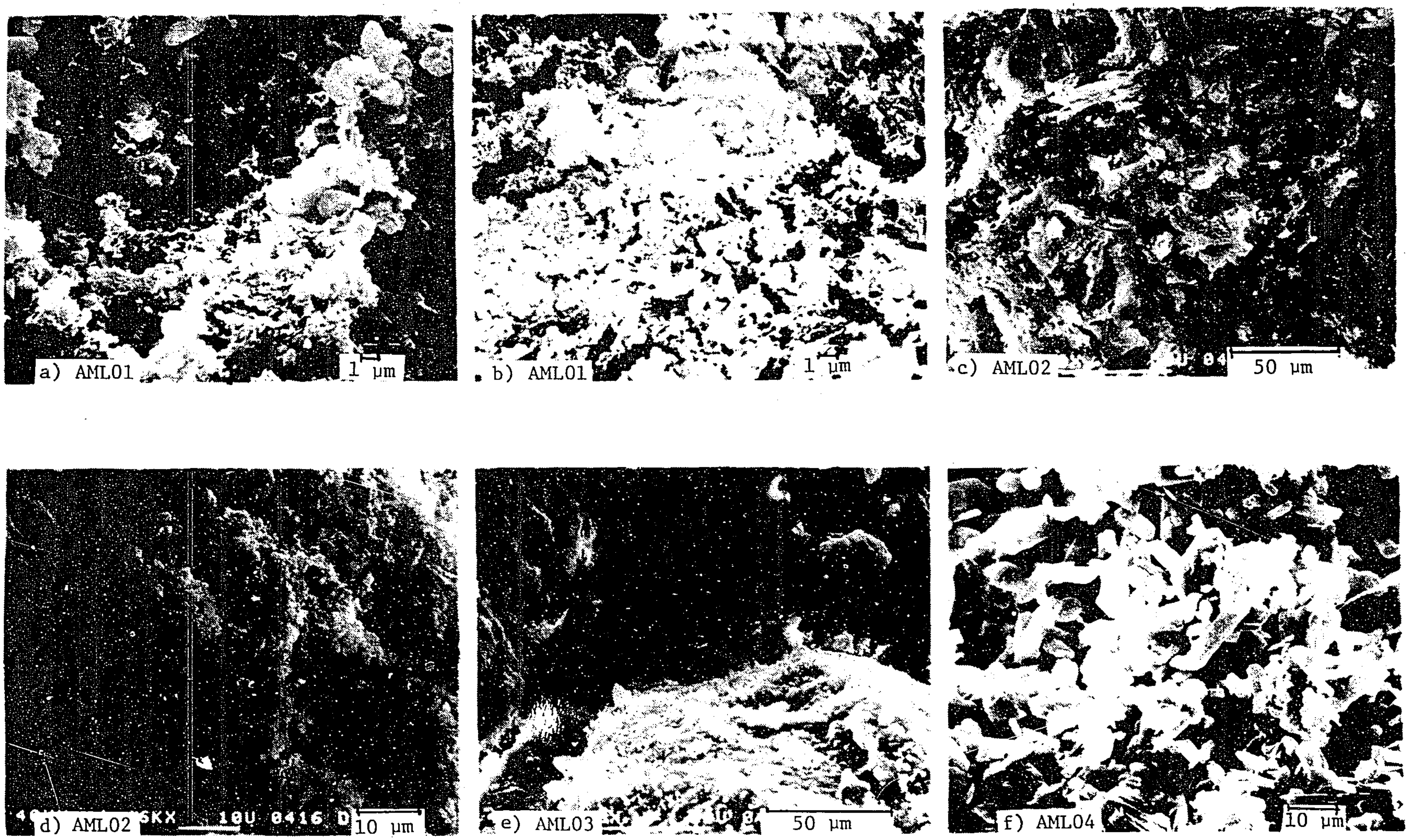

Figure 2-18. Scanning Electron (SEM) Photomicrographs (Secondary Electron Images) of Samples AML01 Through AML04, Plasters Collected From the Amathus Excavation, The Republic of Cyprus.

are shown coating rounded aggregates and cementing them into a somewhat coherent material. Small calcite crystals, up to 2 µm in size, are intergrown in other portions of this sample and cement the gravel into a weak, crumbly plaster.

Figure 2-18f illustrates the crystalline microstructure of a gypsum mortar collected from a tomb at the Amathus site. The tomb was constructed around 5500 BC and was used until approximately 200 AD. The mortar consists of randomly oriented gypsum crystals, up to and greater than 20 µm in length, which display tabular or prismatic habits and are commonly twinned as shown along the lower edge of Figure 2-18f. This mortar is coherent, although relatively porous, and the microstructure is characteristic of gypsum building materials.

2.3.2.2 Samples from the Idalion Excavation

Scanning electron photomicrographs of a three-layer plaster lining the interior surface of a rectangular bath (Roman age), IDL1 (layers 1 to 3), are shown in Figure 2-19a to f. The microstructures of the bottom-most layer (layer 1) and of the middle layer (layer 2) are similar and are illustrated in Figure 2-19a, b and c, respectively. They are characterized by the intergrowth of abundant, small calcite crystals, less than 2 µm in size, with a minor amount of very fine, irregular particles. These particles often have a crumpled-foil morphology (Figure 2-19c) and are intergrown to produce massive features. The calcite also shows a massive morphology and the resulting microstructure is relatively fine-grained and coherent.

The matrix fraction of IDL1 (layer 3) is very different from the matrices of the two underlying plasters. This exterior layer is characterized by an abundance of what resembles partially hydrated portland cement clinker grains (rounded grains in Figure 2-19e and f). These grains are 20 to 40 µm in cross section and are commonly separated from the bulk matrix by a void halo. EDX qualitative analyses of these particles resulted in detection of Ca, Si, and a minor amount of Al. The bulk matrix in this exterior plaster layer is very fine-grained (Figure 2-19d) to massive (Figure 2-19f), and the particle morphologies and microstructure resemble those observed in modern portland cement pastes. The morphology of the fine-structured phase illustrated in Figure 2-19d is very similar to crumpled foils of C-S-H in portland cement

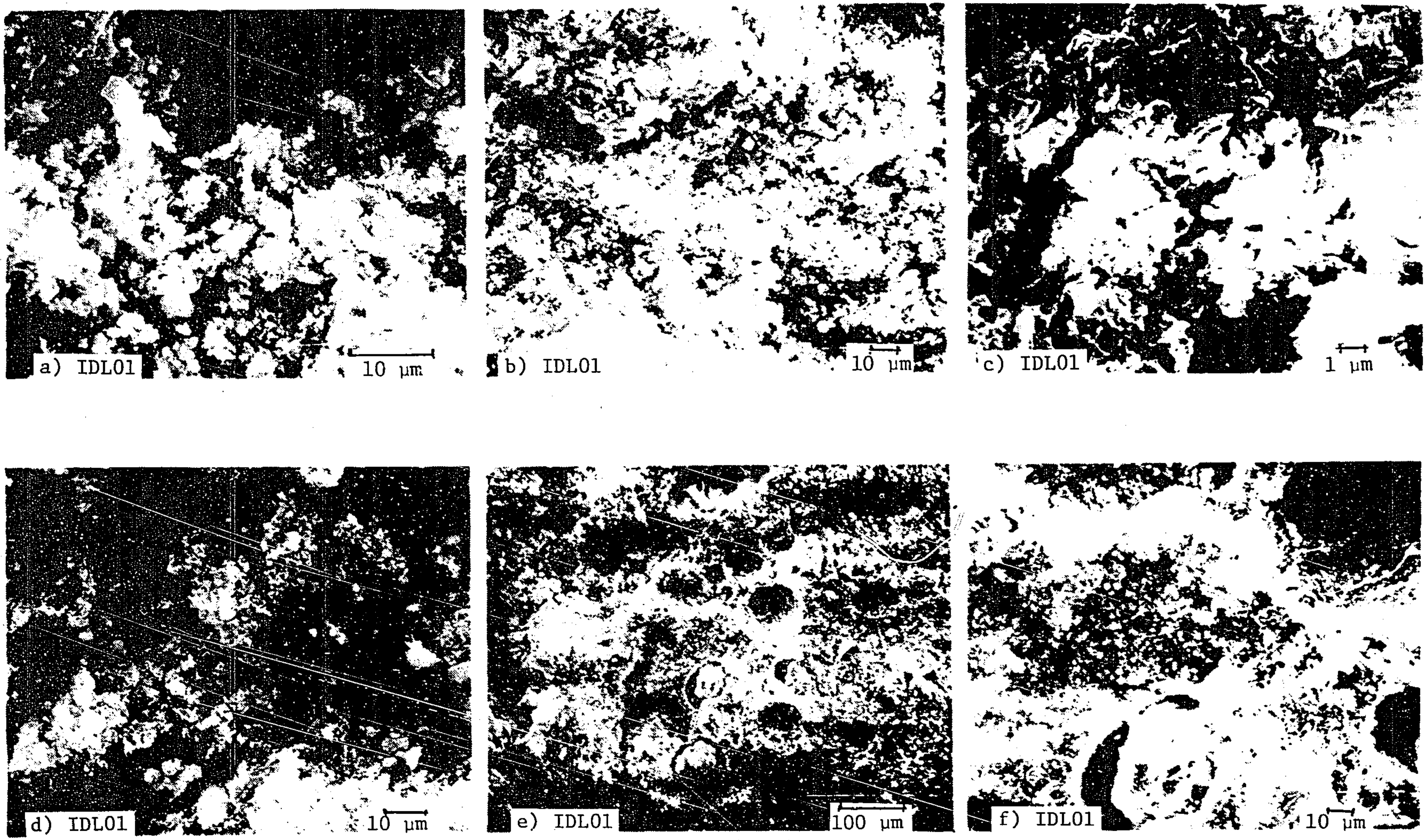

Figure 2-19. Scanning Electron (SEM) Photomicrographs (Secondary Electron Images) of a Three-Layer Plaster, Sample IDL01 - (a) layer 1; (b) and (c) layer 2; and (d) through (f) layer 3, Collected From a Bath at the Idalion Excavation, The Republic of Cyprus.

pastes. Since modern restoration and preservation of masonry structures at the Idalion excavation were being conducted at the time this sample was collected and have been in progress for several years, it is probable that the exterior layer of this rectangular bath was recently applied as a protective coating. Portland cement is known to be used in this restoration work.

Photomicrographs of a gypsum floor plaster, IDL2, and a gypsum mortar, IDL3, are shown in Figure 2-20a, b, and c, respectively. These materials are very similar and are characterized by crystalline microstructures formed by randomly oriented, intergrown gypsum prisms 5 to 10 μm and greater in length. This texture is typical of that observed in other gypsum-containing building materials examined.

2.3.2.3 Samples from the Kition Excavation

A scanning electron photomicrograph of a gypsum floor plaster from Kition is shown in Figure 2-20d. It contains crystals with prismatic or pinacoidal habits, many of which are twinned. The microstructure of this material is crystalline, relatively porous, and coherent.

Secondary electron images of KTL3, the interior plaster lining of a bottle-shaped cistern at the Kition excavation, are shown in Figure 2-20e and f. The matrix in the plaster is relatively fine grained and is characterized by the intergrowth of massive calcite and small calcite crystals with irregular platelets and fine-structured materials. In places, these fine-structured particles are formed into sponge-like masses (Figure 2-20f).

2.3.2.4 Samples from the Kourion Excavation

The microstructure of sample KUL1, a mortar from an interior wall from a structure dated at approximately second century BC, is shown in Figure 2-21a. The matrix in this mortar is composed primarily of calcite crystals less than 1 μm in size. In places, particularly around aggregates, fine-structured phases are relatively abundant and intergrown with calcite crystals. The overall microstructure is moderately coherent and fine grained.

Sample KUL2 is a two-layer plaster lining from the inside of a large rectangular 'pool' at Kourion. The contact between these layers is shown in Figure 2-21b and c. The contact is planar although not sharp, and this

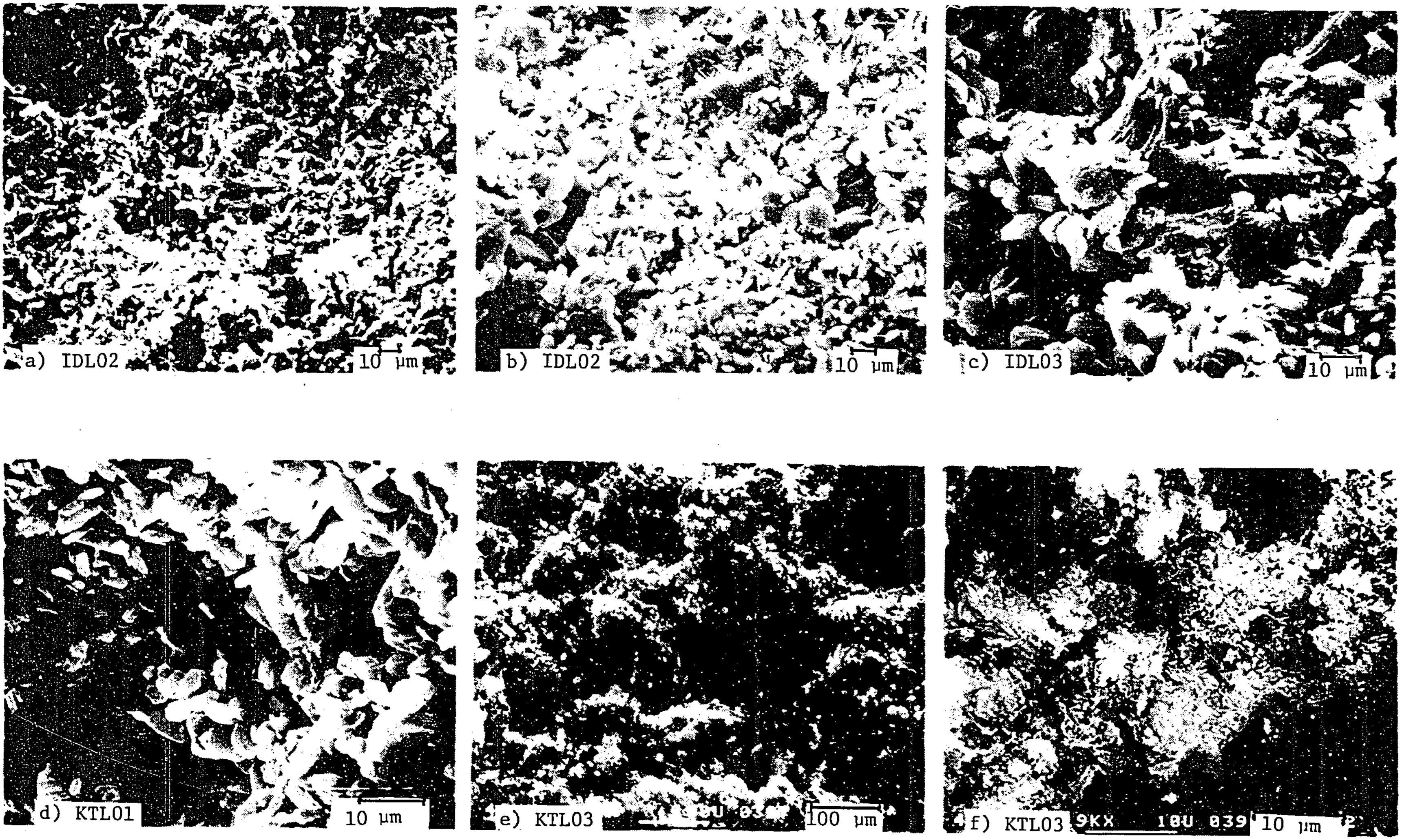

Figure 2-20. Scanning Electron (SEM) Photomicrographs (Secondary Electron Images) of Samples IDL03, KTL01, and KTL03, Collected From the Idalion and Kition Excavations, The Republic of Cyprus.

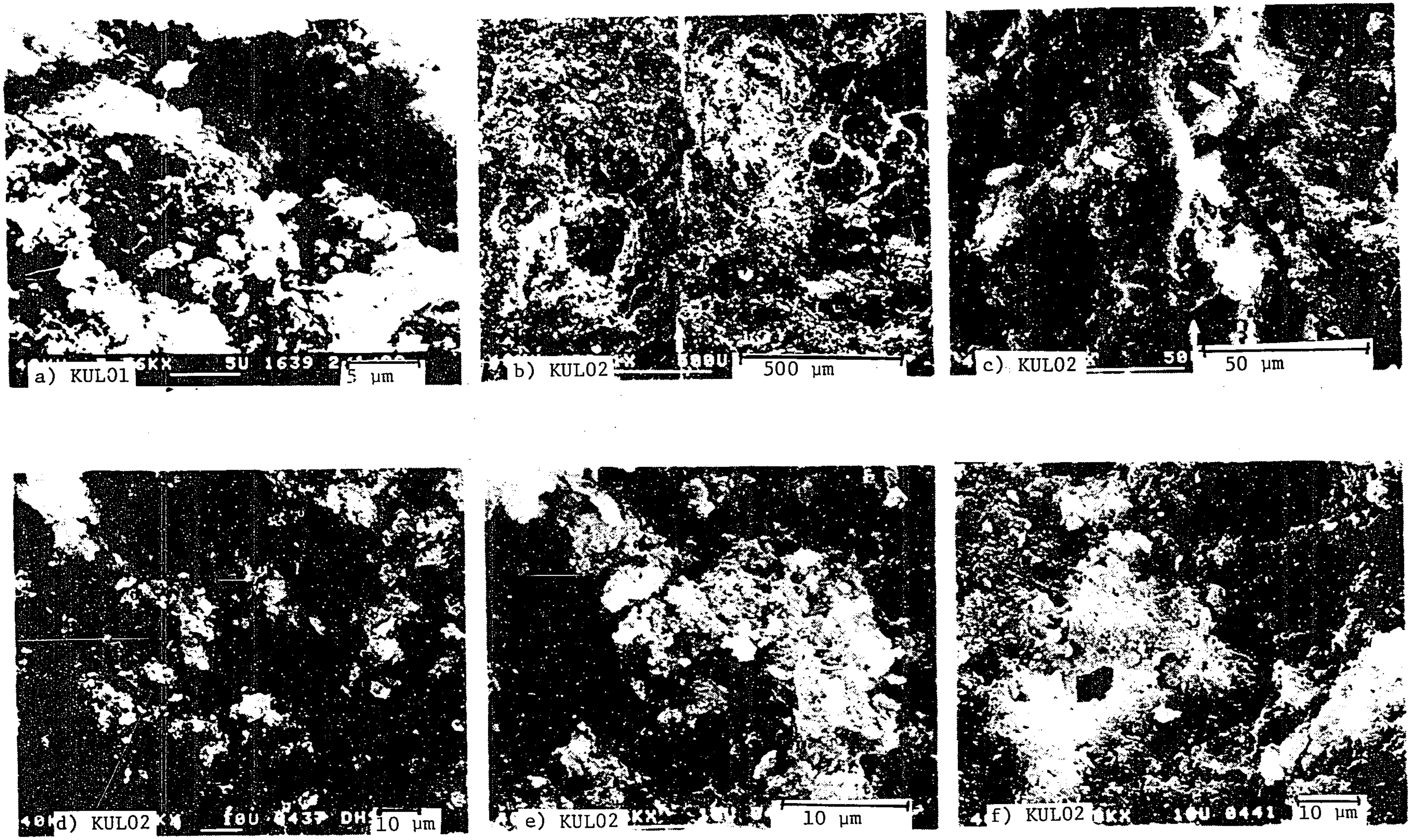

Figure 2-21. Scanning Electron (SEM) Photomicrographs (Secondary Electron Images) of a Two-Layer Plaster, Samples KUL01 and 02, Collected at the Kourion Excavation, The Republic of Cyprus.

suggests that the bottom layer was 'finished' prior to application of the exterior layer. In places, calcite crystals, up to 5 μm, were observed along the contact (Figure 2-21c) normal to the layer surfaces. The matrix of layer 2, the exterior layer, is shown in Figure 2-21d and that of the underlying plaster layer in Figure 2-21e and f. The microstructures of both layers are similar and are characteristically massive and fine grained. Calcite is the most abundant matrix phase.

2.3.2.5 Samples from the Episcopi (Phaneromeni) Excavation

Scanning electron micrographs of samples collected from Episcopi, EPL1 (hearth floor plaster) and EPL2 and EPL3 (samples of small bins or basins) are shown in Figure 2-22a, b, and c, respectively. The floor plaster is relatively friable and the matrix is lumpy in texture. The microstructure of the matrix fraction is fine grained and is characterized by small, less than 2 μm, calcite crystals intergrown with a minor amount of fine-structured material.

Samples EPL2 and EPL3 were collected from similar appearing structures (bins or basins) but their microstructures are very different. The matrix in EPL2 consists of massive calcite intergrown with small, up to 2 μm, rhombohedral or prismatic calcite crystals. Calcareous algal sheaths penetrating this sample are shown in Figure 2-22b. Sample EPL3 is shown in Figure 2-22c and the matrix fraction is composed of randomly oriented, irregular platelets, up to and greater than 10 μm in cross section, intergrown with fine-structured material. The microstructure is that of a two-phase composite material (plates and particles) and is relatively porous. EDX qualitative chemical analyses of both these phases results in detection of primarily calcium.

2.3.2.6 Samples from the Lemba Excavation

Two samples from the Lemba excavation were collected. LML1 is a floor plaster, the matrix of which is composed of small, less than 2 μm, calcite crystals and also massive calcite. The crystals are randomly oriented in portions of the sample or oriented normal to the surfaces of the massive features (Figure 2-22d). Calcareous algal filaments were also observed throughout the matrix fraction in this sample. In places, these calcareous filaments are coated with very small (less than 0.5 μm) calcite crystals

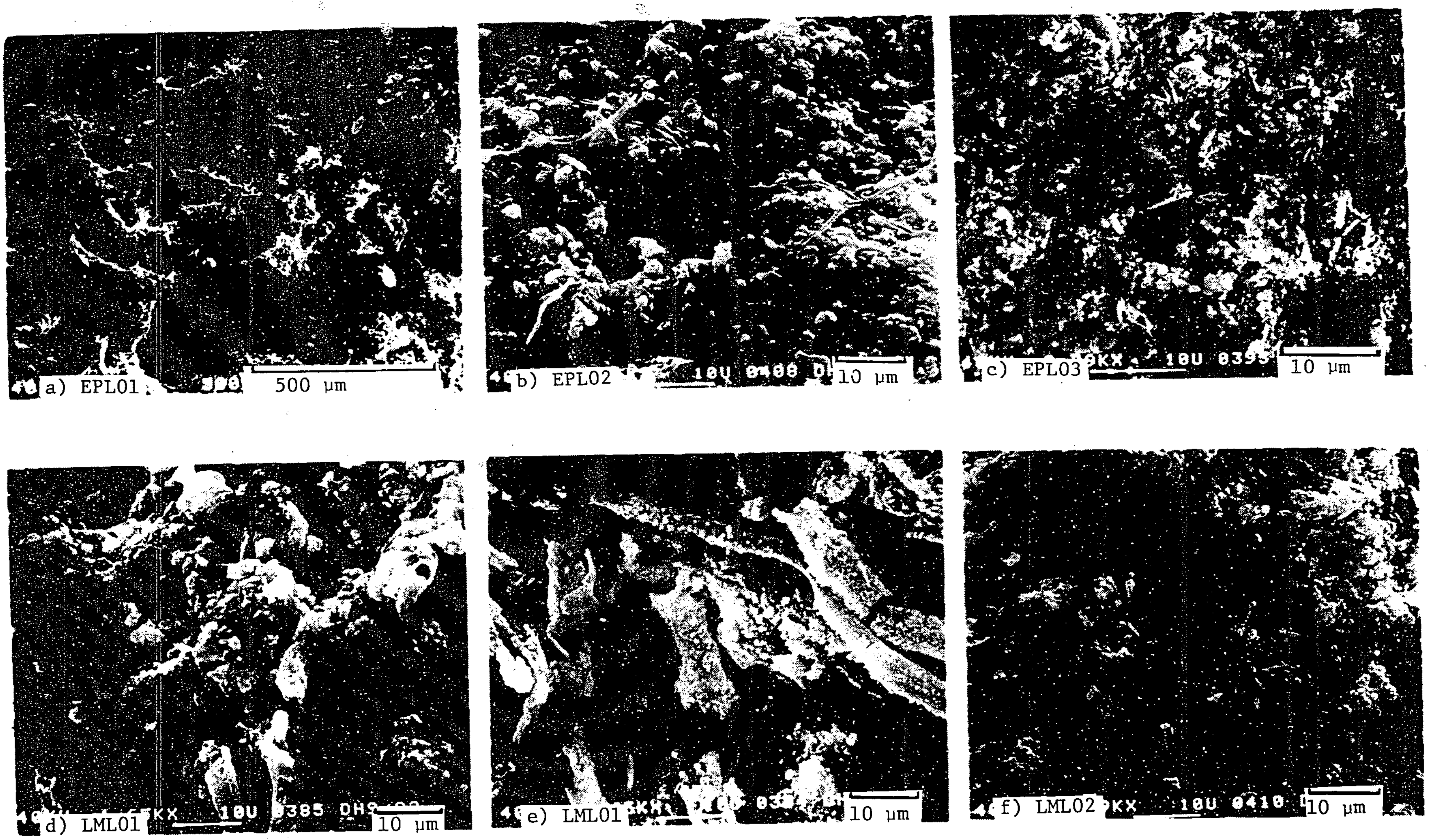

Figure 2-22. Scanning Electron (SEM) Photomicrographs (Secondary Electron Images) of Samples EPL01, 02, 03, and LML01 and 02, Collected From the Episcopi and Lemba Excavations, The Republic of Cyprus.

(Figure 2-22e), whereas other sheaths are not encrusted. This suggests that algae may have grown on this structure at some time early in its existence (at a time prior to excavation). Those sheaths not encrusted by secondary calcite may be of post-excavation origin.

Sample LML2 (Figure 2-22f) was collected from a small basin or bin structure at Lemba. The microstructure of this material is similar to that previously described for sample EPL2 and is characterized by massive calcite and calcite crystals intergrown to form a coherent material.

2.4 RESULTS OF X-RAY DIFFRACTION ANALYSIS

Results of the X-ray diffraction analyses for the matrix fraction (separated from the bulk sample by method A) of the building materials collected from Greece and Cyprus are summarized in Tables 2-1 and 2-2, respectively. Examples of powder diffraction X-ray data obtained from hydraulic hydrated lime cements, hydrated lime cements and also gypsum cement are shown in Appendix D, Figures D-1 to D-3. Comparisons of the data obtained as a result of the two separation techniques are also illustrated in these figures.

Mineralogical and phase determinations by X-ray diffraction do not permit detection of phases present in amounts less than 2 to 10 wt percent of the sample. (The exact value depends on X-ray absorption and diffraction characteristics of the particular material.)

2.5 RESULTS OF THERMAL ANALYSIS

Examples of the results for the matrix fraction of selected specimens are summarized in Table 2-3. DTA and TGA curves for the samples analyzed are presented in Appendix D, Figures D-1 to D-3. Tabulated quantitative data obtained from TGA are included in the section on chemical analyses. Confirmatory phase determinations are made from these studies, by measuring the temperature at which certain thermal effects take place, e.g., decomposition of calcite. The peak areas determine the relative proportions of different phases.

Table 2-1. X-Ray Diffraction Data for the Matrix Fractions of Ancient Plasters and Mortars From Greece.

X-Ray Code	Sample No.	Results(a)(b)
LLVL1MXRO	LVL01	CA, QU, m.PF, m.DI, AM, vm.KA
LVL2MXR	LVL02	CA, m.PF, m.QU, AM
LVL3MXR	LVL03	CA, AM, m.QU, M.PF
LVL4MXR	LVL04	CA, AM, m.QU, m.PF,M.SA
LVL4MXRS	LVL04	CA, m.QU, m.PF, AM, vm.BI
	(fracture filling)	
LLVL5MXR	LVL05	CA, AM, m.QU, m.PF, m.LA, m.HB, m.PH
LLVL6MXR	LVL06	CA, SP, QU, m.AM;
		$d = 4.477$, $I/I_o = 1.86$
LVL7MXR	LVL07	QU, CA, SP, CE, BI, m.DI, AM;
		$d = 4.9929$, $I/I_o = 6.5$;
		$d = 4.4580$, $I/I_o = 4.8$
LLVL8MXR	LVL08	CA, QU, m.BI, m.KA, m.SP, AM;
		$d = 4.4669$, $I/I_o = 3.64$
LLVL9MXR	LVL09	CA, m.QU, vm.BI, vm.PF, AM
LLVL10MXR	LVL10	CA, m.QU, m.PF, m.SP, AM, vm.BI
LVL11MXR	LVL11	CA, QU, m.BI,AM, vm.PF
LLVL12MXR	LVL12	CA, QU, BI, vm.AM;
	(layer 1)	$d = 5.954$, $I/I_o = 1.5$;
		$d = 4.456$, $I/I_o = 2.75$
LLVL12	LVL12	CA, QU, m.PF, m.SP, AM;
	(layer 2)	$d = 4.4770$, $I/I_o = 1.05$
LLVL13MXR	LVL13	CA, QU, SP, CE, m.PF, m.DI, AM, SA
LLVL14MXR	LVL14	CA, QU, SP, m.DI, m.BI, m.SI, m.PO, AM
LVL15MXRW	LVL15	CA, QU, m.PO, vm.BI, AM
	(layer 1)	
LVL15MXRP	LVL15	CA, SP,QU, m.PO, m.BI, m.SI, AM;
	(layer 2)	$d = 8.125$, $I/I_o = 2.3$;
		$d = 5.601$, $I/I_o = 1.3$

Table 2-3. X-Ray Diffraction Data for the Matrix Fractions of Ancient Plasters and Mortars From Greece (continued).

X-Ray Code	Sample No.	Results[(a)(b)]
MVL15MXRB	LVL15 (layer 3)	CQ, QU, AM $d = 2.8989$, $I/I_o = 1$; $d = 4.4759$, $I/I_o < 1$
LVL16MXR	LVL16	CA, m.QU, m.CE, vm.BI; $d = 4.4239$; $I/I_o = 2$
LVL17MXR	LVL17	CA, QU, m.CE, m.SM, m.HY, vm.KA, vm.EN, AM
LVL18AXR	LVL18	CA, m.QU
LADL1MXR	ADL01	CA, QU, AM; $d = 14.584$, $I/I_o = 3.17$; $d = 3.1992$, $I/I_o = 5.06$; $d = 1.7449$, $I/I_o < 1$

(a) Abbreviations have the following meanings: AM = amorphous material; BI = biotite; CA = calcite; CE = cerussite; DI = diopside; EN = enstatite; HB = hornblende; HY = hypersthene; KA = kaolinite; PF = plagioclase feldspar; PH = phillipsite; PO = portlandite; QU = quartz; SA = saponite; SI = siderite; SM = smithsonite; SP = sphalerite (weathered) (some may be galena); m. = minor amount; vm. = very minor amount.

(b) Phases are listed in order of decreasing amount.

Table 2-2. X-Ray Diffraction Data for the Matrix Fractions of Ancient Plasters and Mortars From Cyprus.

X-Ray Code	Sample No.	Results[(a)(b)]
LAML1MXR	AML1	CA, m.QU, vm.GY, AM
LAML2MXR	AML2	CA, m.QU, AM
LAML3MXR	AML3	CA, m.QU, AM
LAML4MXR	AML4	GY, AM
LEPL1MXR	EPL1	CA, QU, m.PF; d = 8.5073, I/I_o = 0.58; d = 5.0055, I/I_o = 1.11
LEPL2MXR	EPL2	CA, QU, PF, vm.CH, vm.IL, vm.HB
LEPL3MXRP	EPL3 (plaster)	CA, QU, vm.HB, vm.PF
LEPL3MXR	EPL3 (mortar)	CA, QU, PF, m.HB, m.CH, m.GY, AM
LEPL4MXR	EPL4	CA, QU, PF, m.HB, m.CH, AM
LCIDL1MX3	IDL1 (layer 1)	CA, m.QU, vm.PF, AM
LCIDL1MX2	IDL1 (layer 2)	CA, m.QU, m.PF, AM
LCIDL1MXRS	IDL1 (layer 3)	CA, m.QU, vm.PF, AM
LCIDL2MXR	IDL2	GY, m.CA, AM
LCIDL3MXR	IDL3	GY, CA, AM
LKHL1MXR	KHL1	CA, vm.QU
LKTL1MXR	KTL1	GY
LKTL2MXRS	KTL2	CA, m.QU, m.GY, vm.PF, AM
LKTL2S	KTL3 (surface layer)	GY, CA, m.QU
LKTL3MXR	KTL3	CA, GY, m.QU, m.PF, AM
LKTL4MXR	KTL4	GY, m.CA, AM
LKUL1MXR	KUL1	CA, m.QU, AM
LKUL2S	KUL2 (surface layer)	CA, QU, m.PF

Table 2-2. X-Ray Diffraction Data for the Matrix Fractions of Ancient Plasters and Mortars From Cyprus (continued).

X-Ray Code	Sample No.	Results[(a)(b)]
LKULMXR	KUL2	CA, m.QU, AM
LKUL2I	KUL2A (fracture filling)	CA, m.QU
LKUL3MXR	KUL3	CA, m.QU, vm.PF
LML1MXR	LML1	CA, m.QU
LML2MXR	LML2	CA, m.QU, AM

(a) Abbreviations have the following meanings: AM = amorphous material; CA = calcite; CH = chlorite; GY = gypsum; HB = hornblende; IL = illite; PF = plagioclase feldspar; QU = quartz; m. = minor amount; vm. = very minor amount.

(b) Phases are listed in order of decreasing amount.

Table 2-3. Results of Differential Thermal Analyses of the Matrix Fractions of Selected Ancient Building Materials.

Sample No.	Results
	Greece
LVL05	340-460 C = dh.Li or dc.A, 825 C = dc.C
LVL15 (layer 1)	50-120 C dh.EW, 330-370 C = dh.Li or dc.A, 835 C = dc.C, 900 C = dc.C or rexl
LVL17	50-110 C = dh.EW, 110-600 C = dh.SW, 840 C = dc.C
ADL01	50-110 C = dh.EW, 110-600 C = dh.SW, 820 C = dc.C
	The Republic of Cyprus
IDL01 (layer 3)	50-110 C = dh.EW, 120 C = dh.G, 170 C = dh.G, 200-600 C = dh.SW, 790 C = dc.C
KTL01	50-110 C = dh.EW, 130 C = dh.G, 160 C = dh.G, 815 C = dc.C

*Abbreviations used: A = carbonate (poorly crystalline?); C = calcite; D = dolomite; EW = evaporable water; G = gypsum; Li = limonite; SW = structural water; dc. = decarbonation; dh. = dehydration; rexl = recrystallization.

2.6 RESULTS OF CHEMICAL ANALYSES

2.6.1 Quantitative Analysis

Chemical analyses for the matrix fractions of the lime- and calcium silicate-based cementitious materials are presented in Tables 2-4 and 2-5, respectively (for materials from Greece and The Republic of Cyprus).

2.6.2 SEM Qualitative Analysis

Examples of qualitative chemical analyses (EDX) of the -1 µm matrix fractions which were ultrasonically separated from selected ancient composites are presented in Figures 2-23 to 2-25. The -1 µm material is essentially X-ray amorphous as discussed in Section 2.4 and was obtained from those specimens containing hydraulic hydrated lime or pozzolana/hydrated lime matrices. The qualitative analyses presented in Figures 2-23 to 2-25 (bottom) are from those areas shown in Figures 2-23 to 2-25 (top), respectively. Although the morphologies of the -1 µm particles in each sample appear uniform, the compositions of the particles may be variable. Therefore the EDX spectrum for each sample is the average analysis of the area shown.

2.6.3 TMS Results

Four peaks were distinguished in the gas-liquid chromatograms of trimethylsilyl derivatives of the matrix fractions of the ancient cementitious materials. Two of these were identified as monomer, SiO_4^{4-}, and dimer, $Si_2O_7^{6-}$, derivatives. The other two were attributed to the T-esters of $Si_3O_{10}^{8-}$ and $Si_4O_{12}^{8-}$. The derivatives of larger silicate ions were not identified due to ineffective separation by the gas-liquid chromatographic technique. Additional peaks which were observed may be due to side reactions or branching effects of the various derivatives, although mass spectrometry analyses were not performed. Data for selected samples from Greece and The Republic of Cyprus are plotted in Figures 2-26 and 2-27a as a function of relative amount of derivative versus elution time.

In addition to the ancient building material samples, two reference materials were also analyzed. These materials were an alkali-silica gel from

Table 2-4. Quantitative Chemical Analyses for Selected Ancient Building Materials From Greece.

				Layer		Layer				
				1	2	1	2	3		
	LVL05	LVL06	LVL08	LVL12	LVL12	LVL15	LVL15	LVL15	LVL17	ADL1
SiO_2, %	18.0	19.6	25.6	29.25	29.0	8.4	9.5	3.24	13.4	31.5
Al_2O_3	4.31	5.66	6.22	5.35	5.57	1.50	1.05	1.24	2.56	5.11
TiO_2	0.155	0.31	0.356	0.21	0.172	0.055	0.03	0.07	0.11	0.250
Fe_2O_3	1.7	3.26	3.72	2.95	4.39	1.53	1.17	2.19	4.27	3.22
CaO	45.1	41.6	37.3	27.0	35.8	43.5	46.0	49.3	36.0	27.3
MgO	0.84	1.87	2.69	1.157	1.33	4.55	2.75	1.80	1.38	4.30
MnO	0.064	0.115	0.136	0.098	0.118	0.143	0.158	0.548	0.453	0.0795
Na_2O	0.60	0.11	0.25	1.25	0.67	0.05	0.01	0.13	0.192	0.46
K_2O	0.84	0.43	0.73	0.95	1.10	0.07	0.047	0.22	0.18	0.54
Pb	0.4	--	--	1.9	1.0	1.6	1.7	1.0	2.4	--
Zn	0.4	--	--	1.7	1.9	0.8	1.0	1.2	4.5	--
Ba, ppm	210	1330	680	300	200	430	60	260	730	160
Cr	20	590	495	5	30	<5	<5	15	30	856
Cu	40	50	80	105	295	<5	35	65	100	80
Ni	<5	145	180	<5	15	10	<5	20	10	126
Si	120	200	240	690	450	95	75	215	120	220
V	<5	30	30	5	10	<5	<5	<5	<5	15
Zr	75	105	100	75	90	<5	10	<5	<5	60
SO_3	0.37	0.58	0.36	0.40	0.66	0.99	1.33	0.82	0.51	0.60
CO_2	23.11	16.95	14.44	18.51	14.26	25.18	28.15	24.80	24.71	16.12
$H_2O_{110\ C}$	1.53	1.62	0.91	1.0	0.6	3.18	2.35	0.33	1.16	2.77
H_2O_{total}	5.20	8.59	5.32	6.30	6.80	10.85	7.70	12.50	9.21	9.80

Table 2-5. Qualitative Chemical Analyses for Selected Ancient Building Materials From Cyprus.

	AML1 (layer 1)	AML2 (plaster sealant)	AML4	EPL2	IDL2	IDL3	KHL1	KTL1	KTL3	KUL1	KUL2 (layer 2)	LML2
SiO_2, %	23.0	6.2	0.75	25.6	0.78	0.8	4.18	1.4	23.4	9.8	16.7	12.2
Al_2O_3	5.79	1.27	0.180	5.08	0.24	0.358	0.95	0.36	5.24	2.0	2.06	2.03
TiO_2	0.243	0.05	<0.005	0.348	0.016	0.0075	0.025	0.005	0.27	0.13	0.118	0.126
Fe_2O_3	2.60	0.75	0.10	3.75	0.10	0.22	0.70	0.175	2.95	1.19	1.06	1.06
CaO	34.0	4.84	35	35.0	42.3	35.6	51.6	34.5	31.2	53.5	48.8	49.8
MgO	2.35	0.90	<0.01	2.85	0.58	0.075	0.70	0.075	2.36	2.375	1.558	3.38
MnO	0.069	0.055	0.0035	0.084	0.0163	0.01	0.044	0.007	0.094	0.028	0.043	0.0277
Na_2O	0.19	0.123	<0.01	0.61	0.04	<0.01	0.005	<0.01	0.92	0.39	0.15	0.11
K_2O	0.24	0.18	0.01	0.17	0.02	0.05	0.10	0.05	0.1	0.17	0.20	0.20
Ba, ppm	210	540	40	960	80	300	670	30	600	90	180	150
Cr	75	25	<5	290	<5	<5	10	<5	200	80	15	50
Cu	25	30	<5	<5	<5	5	10	<5	50	45	20	5
Ni	20	<5	<5	40	<5	<5	<5	<5	55	30	19	30
Sr	655	1640	615	315	570	720	1965	670	1000	400	490	650
V	30	5	<5	100	<5	<5	<5	<5	100	20	<5	5
Zr	25	<5	<5	5	<5	<5	<5	<5	35	5	5	15
SO_3	0.95	0.43	42.34	0.16	40.46	39.19	0.09	40.74	6.2	0.47	0.37	0.20
CO_2	20.74	38.10	0.34	24.10	2.03	3.48	29.55	3.77	18.2	28.20	28.60	28.17
$H_2O_{110\ C}$	3.23	0.45	0.42	0.70	0.44	0.36	3.49	0.2	0.6	0.55	0.40	1.50
H_2O_{total}	8.89	5.27	21.73	2.51	15.28	19.76	10.59	19.88	8.4	3.65	2.91	4.25

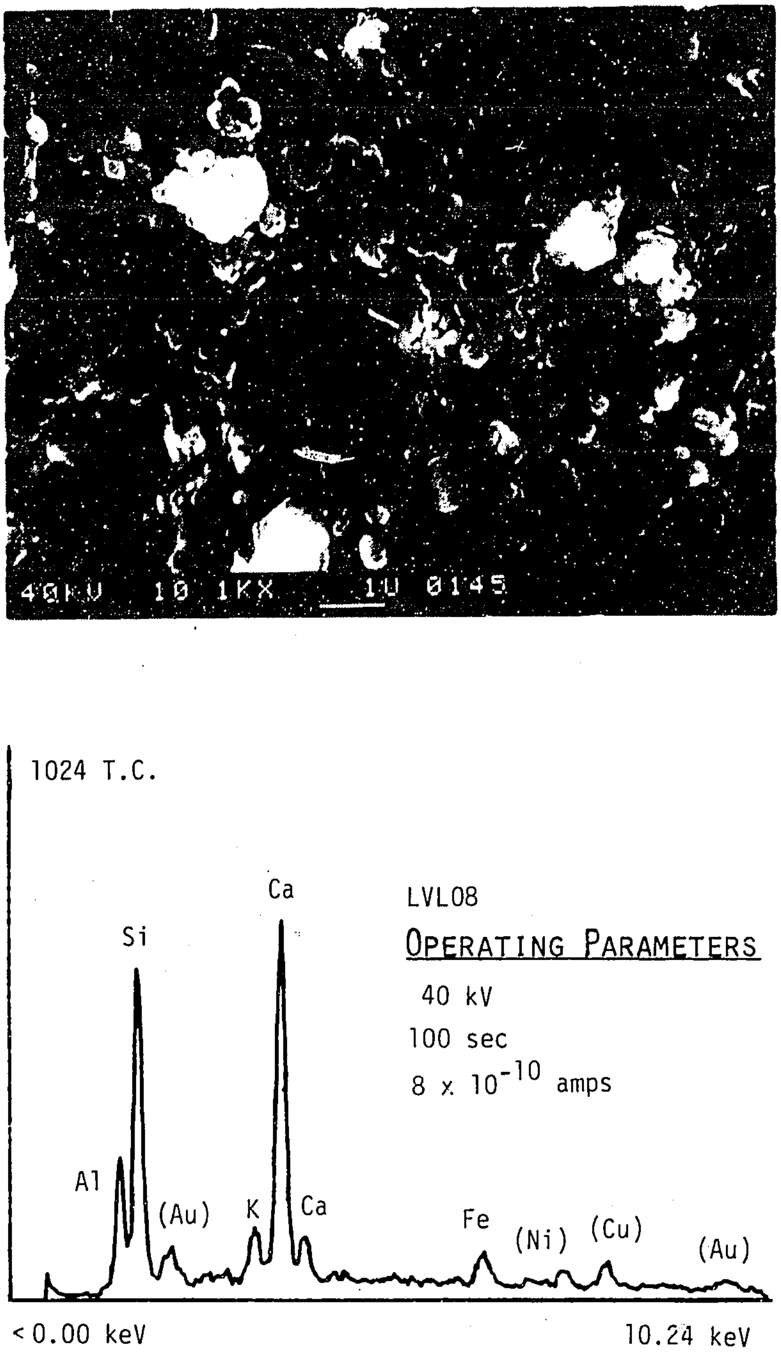

Figure 2-23. EDX Analysis of the -1 μm Matrix Fraction Ultrasonically Separated From Sample LVL08 From the Lavrion Mining District, Greece.

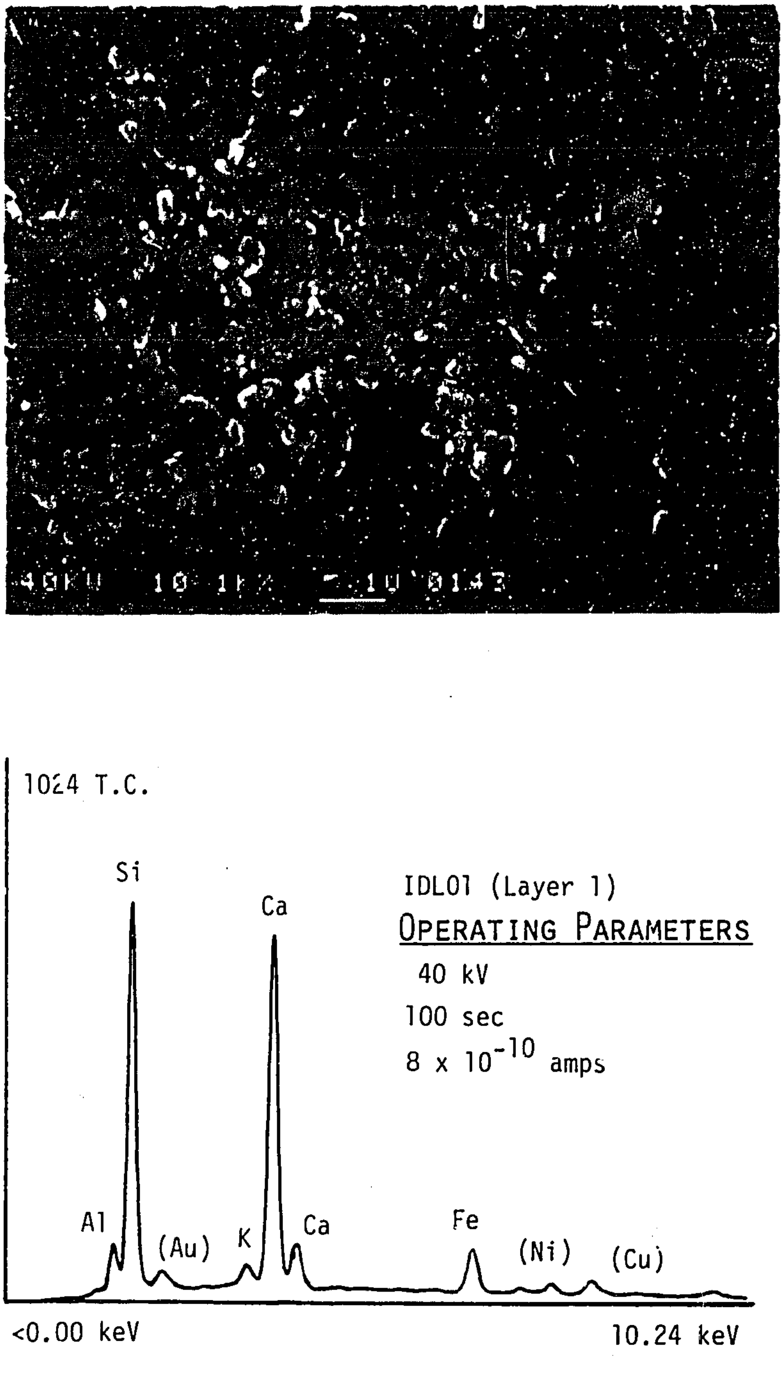

Figure 2-24. EDX Analysis of the -1 μm Matrix Fraction Ultrasonically Separated From Sample IDL01, Idalion Excavation, The Republic of Cyprus.

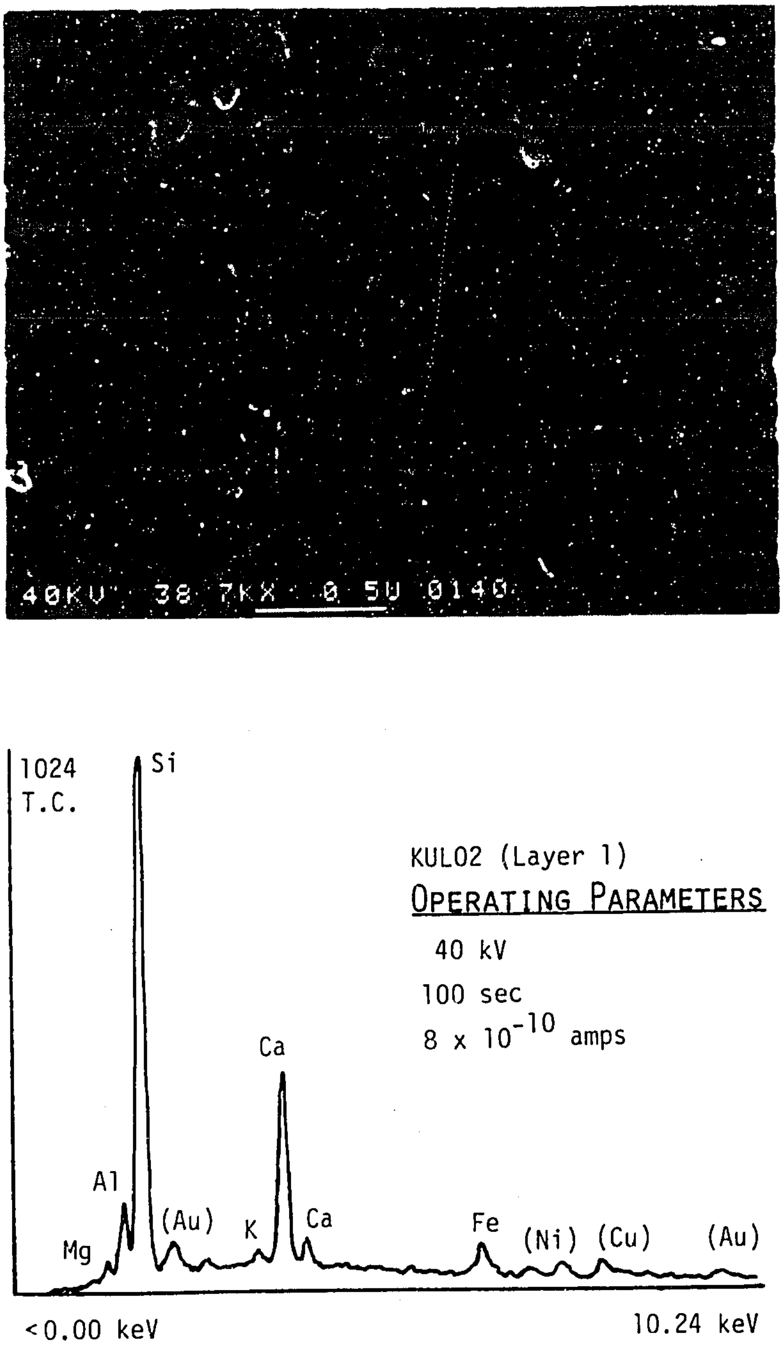

Figure 2-25. EDX Analysis of the -1 μm Matrix Fraction Ultrasonically Separated From Sample KUL02, Kourion Excavation, The Republic of Cyprus.

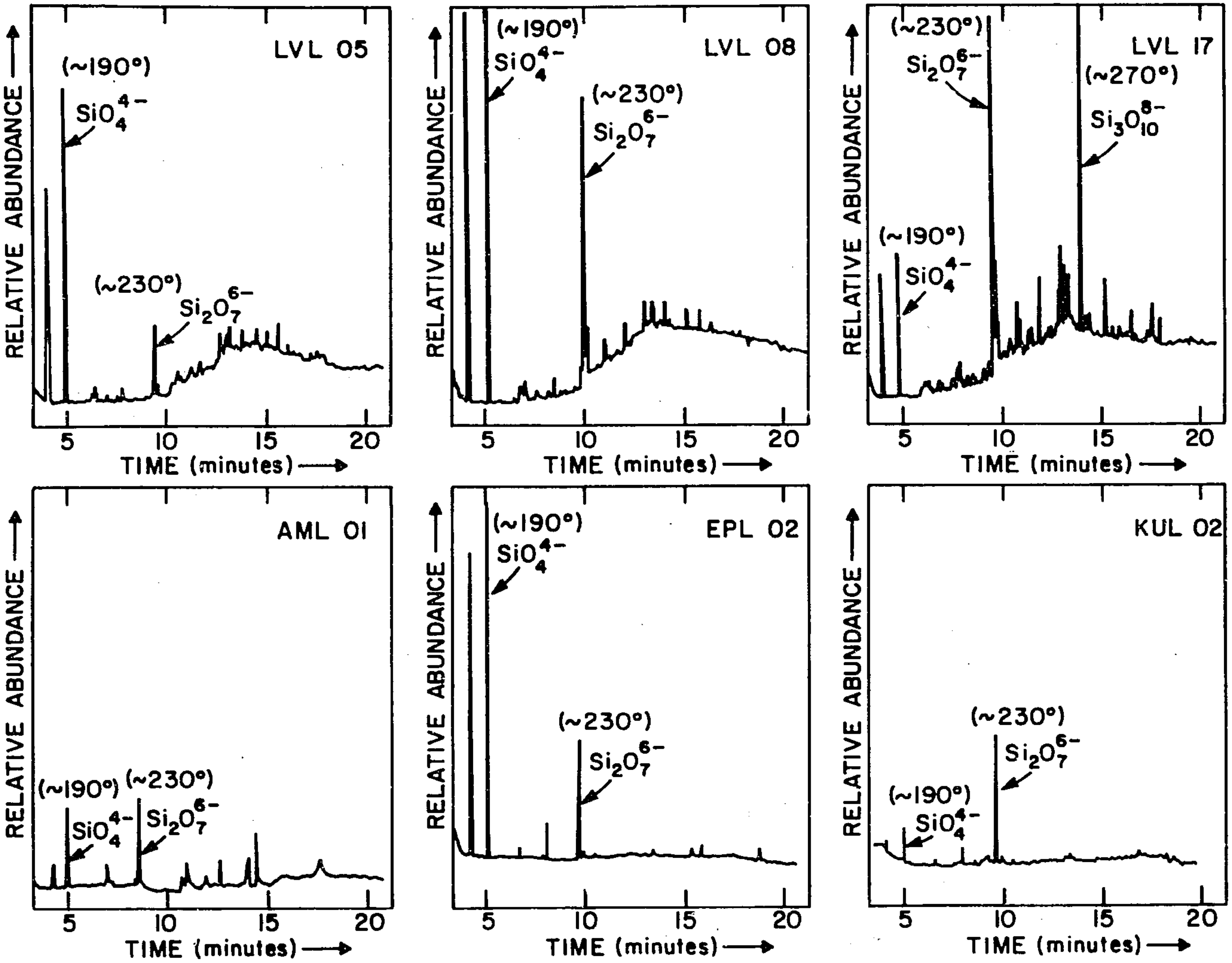

Figure 2-26. Gas-Liquid Chromatograms of the Silylated Reaction Products From the Matrix Fractions of Selected Ancient Building Materials From Greece The Republic of Cyprus.

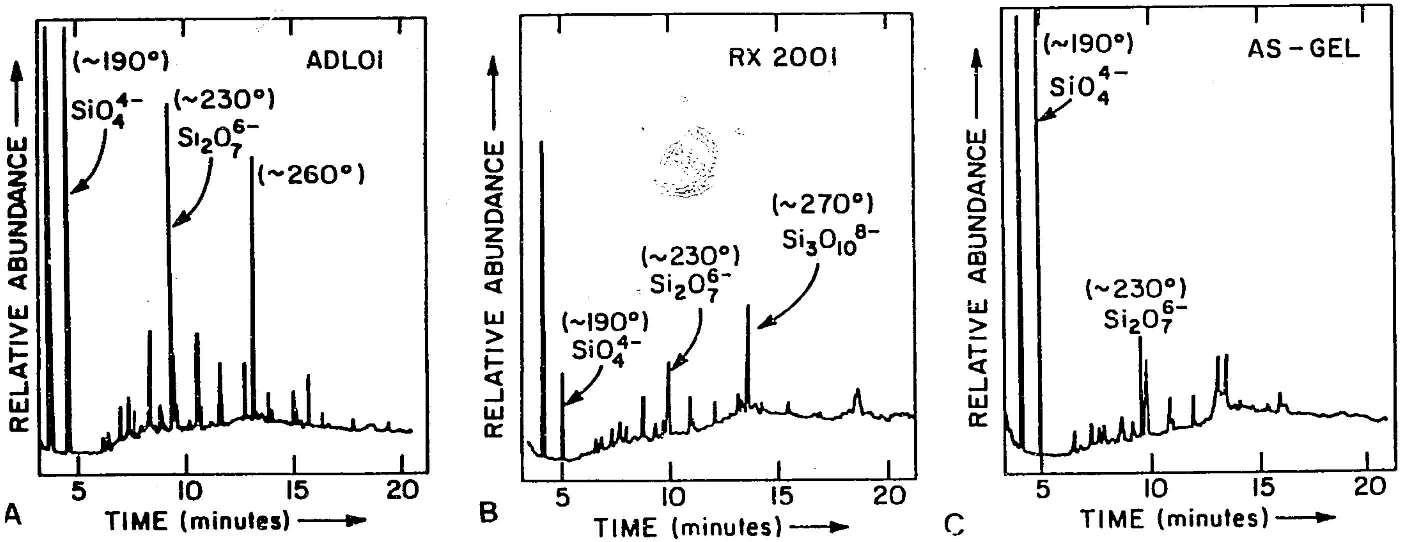

Figure 2-27. Gas-Liquid Chromatograms of the Silylated Reaction Products of (a) Mortar From Greece (ADL01) Compared with Those From (b) Pozzolan (Tuff) From Italy (RX2001) and (c) Gel (AS-GEL).

Denmark, and a fragment of volcanic ash (pozzolana ash) from Rome. These data are shown in Figure 2-27b and c.

2.6.4 Organic Analysis

A chromatogram resulting from analysis of sample AML2, pipe-joint compound from the Amathus site, The Republic of Cyprus, is shown in Figure 2-28. This pattern shows a very small amount of undifferentiated organic material that was leached from the pipe-joint material, but it is not indicative of the presence of a significant amount of organic water-proofing agents incorporated in the sample. (Gas-liquid chromatography is a very sensitive technique and the pattern illustrated in Figure 2-28 is probably the result of minor organic material in soil covering the plaster subsequent to its manufacture.)

Samples AML3 and LVL05, LVL12 (layer 2), LVL15 (layers 2 and 3), and LVL18 (layer 2) were analyzed by the acid extraction method. Organic compounds were not detected by this method in any of these samples.

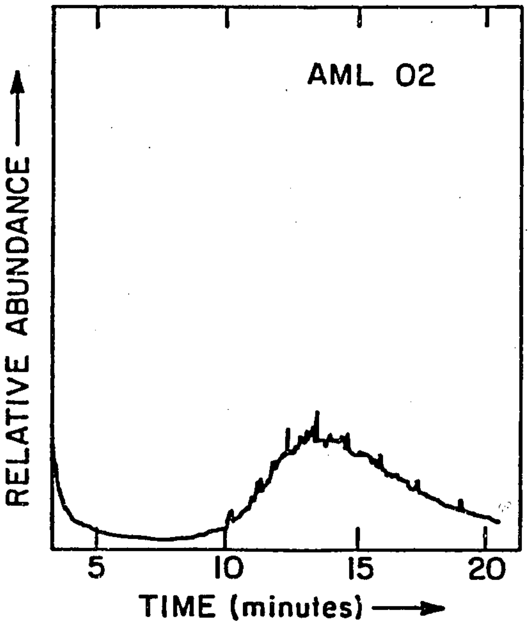

Figure 2-28. Gas-Liquid Chromatogram From Analysis of Sample AML02.

3 DISCUSSION

3.1 TYPES OF ANCIENT CEMENTITIOUS BUILDING MATERIALS

3.1.1 Gypsum Plasters and Mortars

The simplest plasters were those in which the binder phase was made by calcining gypsiferous ($CaSO_4 \cdot 2H_2O$) rocks at relatively low temperatures to form calcium sulfate hemihydrate ($CaSO_4 \cdot 1/2\ H_2O$ plaster of Paris) or anhydrite ($CaSO_4$). Dehydration temperatures for gypsum and hemihydrate are approximately 130 and 165 C, respectively. These dehydrated rocks were crushed, and water was added to the powders. The resulting hydration reactions produced a gypsum cement which was commonly used in floor and wall plasters and interior wall mortars.

Massive gypsum and selenite outcrops are common in The Republic of Cyprus, and this raw material availability is reflected by the widespread use of gypsiferous building materials on Cyprus. Specimens AML4, IDL2, IDL3, KTL1, KTL3,and KTL4, from the Amathus, Idalion, and Kition excavations, respectively, have gypsum matrices. Other specimens, such as KUL1, contain a mixture of gypsum and other cementitious phases.

3.1.2 Hydrated Lime-Based Mortars and Plasters

Lime plasters and mortars were manufactured by calcining relatively pure calcite in the form of limestone, chalk, marble, or caliche (havara or karkalla) at temperatures above approximately 800 C to produce lime. Combination of crushed lime and water results in crystallization of portlandite, $Ca(OH)_2$, which initially forms the binding phase in these materials. As discussed by Roy and Langton (1982), portlandite readily carbonates on exposure to air and most fresh groundwaters and hence, after some time, calcite becomes the binding phase.

It should be pointed out that the poor workability and nonhydraulic character of pure hydrated lime cements limited widespread use of these materials in ancient structures. However, one such type of material, opus signinium, which is a mixture of lime and fine terra-cotta fragments was used extensively enough throughout the Roman empire for Vitruvius to describe its manufacture (Vitruvius, trans. by Morgan, 1960).

At least the following samples examined in this study were classified as hydrated lime-based materials: AML1 and AML2 (pipe-joint sealant) from Amathus, Cyprus.

3.1.3 Hydraulic* Hydrated Lime-Based and Hydraulic Hydrated Lime-Based/Soil Plasters and Mortars

The use of pure hydrated lime-based plasters and mortars in ancient structures was relatively rare. This is primarily due to the limited number of outcrops of pure (99%) calcium carbonate formations. Also, the construction applications of pure hydrated lime-based materials were somewhat limited. However, siliceous and/or argillaceous carbonate rocks, containing two to ten percent amorphous or crystalline silica and/or clay, respectively, are common throughout the Mediterranean region. When calcined at temperatures above about 850 C, silica in these rocks can react with lime to form dicalcium silicate, whereas the aluminate in clays of various compositions can react with lime to form calcium aluminate phases and/or calcium aluminoferrite phases. Five weight percent reactive silica in a siliceous chalk for instance, can result in crystallization of up to 15 weight percent (approximate based on stoichiometric relations) dicalcium silicate. It is therefore reasonable to expect that many of these cementitious materials initially contained reactive hydraulic calcium silicate, calcium aluminate and aluminoferrite compounds, even in minor quantity. Hydration of calcined siliceous, argillaceous, or ferruginous carbonate rocks results in crystallization of portlandite plus formation of hydrated calcium silicate phases (poorly crystallized or amorphous) and hydrated calcium aluminate and ferrite phases. These latter phases crystallize in the presence of excess water, are relatively insoluble in water and may even harden under water, hence the term hydraulic cements. Upon exposure to air, or bicarbonate in groundwater, portlandite and the hydroxylated calcium aluminate and ferrite phases carbonate to form calcite and carbonated calcium aluminate and ferrites, respec-

---

*Hydraulic cements are cements that set and harden by chemical interaction with water and that are capable of doing so under water.

tively. With time, the calcium silicate phases may also carbonate to varying degrees.

In addition to setting in the presence of excess water, these hydraulic materials have improved workabilities (due to set retardation caused by the presence of dicalcium silicate) compared to pure hydrated lime cements. Therefore they have a much wider range of uses as plasters and mortars. In order to extend the quality of mortar or plaster which could be made with a limited amount of hydraulic cement, coarse and fine aggregate fractions were usually incorporated into these materials to produce a multimodal composite product.

Impure carbonate rocks outcrop in the vicinity of the ancient Lavrion mining district (siliceous, argillaceous, and ferruginous limestones and marbles) and also on Cyprus (siliceous chalks). All mortars and plasters collected from the ore-washing facilities and cisterns near Lavrion, Greece, were classified as hydraulic lime-based composites. Some of these specimens may contain an additional soil component possibly added to the hydraulic lime cement as an extender or to enhance hydraulic properties. Evidence for incorporation of soil (at least silt-size fraction) in LVL11 and LVL12 include: the presence of a minor amount of what appears to be fine volcanic pumice fragments, and the abundance of carbonated and hydrated phases rich in transition metal cations (iron, zinc and lead) which were probably present in the local soil. Plasters from The Republic of Cyprus which were classified as hydraulic lime-based composite materials include: AML3, IDL1, KUL1 and KUL2.

3.1.4 Others Including Pozzolana/Hydrated Lime-Based Plasters and Mortars

A few samples collected were rocks mistaken for concretes or plasters, including sample KHL1 from Cyprus. Sample ADL01 collected from an aqueduct in Greece is possibly a pozzolana/hydrated lime-based plaster. Certain others may be borderline. Other areas in the Greek islands have reported use of pozzolana-hydrated lime cements in structures of the fourth to fifth century BC (Efstathiadis, 1978), but good pozzolanic raw materials were geographically limited.

3.2 TEXTURES OF THE BULK SAMPLES; MICROSTRUCTURES AND PARTICLE MORPHOLOGIES OF THE MATRIX FACTIONS AND MATRIX/AGGREGATE INTERFACIAL REGIONS

3.2.1 Application of Techniques

Hand specimen, hand lens/binocular microscope, petrographic microscope, and scanning electron microscope and microprobe techniques were used to describe the textures, microstructures and phase morphologies of the ancient building materials analyzed in this study. Hand specimen analyses of fractured and sawed surfaces proved most useful in evaluating the relative proportions, grading, and sorting of the coarse and fine aggregate fractions in addition to the relative homogeneity of the bulk specimen. These macroscopic techniques were useful to assess the gross sample similarities, which resulted in the ability to recognize and identify samples from the same geographic regions and in some cases even from same excavation site or structure.

The maximum magnification of the petrographic microscope used in this study was approximately 1000X which proved too low for detailed analyses of the morphologies of the matrix phase. However, microtextures and in some instances matrix/fine aggregate reaction features were easily observed in thin sections. Characterization of the fine and coarse aggregate fractions was also best accomplished by petrographic techniques.

Characterization of the very fine grained matrix fractions in these ancient materials required utilization of various scanning electron microscopy techniques. Magnifications up to and greater than 20,000X permitted description of the morphologies of the matrix phases and of the microstructures in the bulk matrices and in the matrix/aggregate interfacial regions. Both fractured- and polished-surface-samples were examined by electron microscope analyses which utilized secondary electron and backscattered imagery.

3.2.2 Gypsum Plasters and Mortars

In hand specimen analyses, the gypsum plasters and mortars examined were usually white and relatively lightweight due to the low specific gravity of gypsum, 2.32, compared with 2.710 for calcite and 2.65 for quartz. These structural materials typically contained less than 10 percent fine aggregate by volume. However selenite crystal faces up to 2 mm and chunks of poorly calcined or coarsely crushed raw materials were visible.

The crystalline microstructures of these gypsum plasters and mortars were characterized by intergrown, randomly oriented crystals about 10^{-5} m in size, larger than the calcite. The morphologies of the crystals (pinacoidal or prismatic habits) ranged from equant to tabular and often displayed twinning. In thin sections they were relatively colorless, transmitted light, and areas within the matrix consisted of aligned crystals in striated, fan-like, or checkerboard patterns. Other variations in the matrix microtexture were attributed to features caused by or inherited from the coarsely crushed or partially hydrated raw material fragments. Where matrix-aggregate interfacial regions were observed, the aggregate surfaces appeared to serve as a substrate on which nucleation and growth of the gypsum crystals had occurred. These crystals were oriented more or less normal to the aggregate surfaces and were intergrown with other similar crystals in the bulk matrices. Matrix/aggregate reaction zones were not observed in these materials.

3.2.3 Hydrated Lime Plasters and Mortars

In hand specimen analyses, these ancient materials were usually white, reflecting the purity of the lime used, and were characterized by tension fractures caused by shrinkage resulting from approximately an 11 percent volume decrease associated with the reaction of $Ca(OH)_2 + CO_2 \rightarrow CaCO_3 + H_2O$ (Roy and Langton, 1982). As a result of this reaction the binding phase is converted from portlandite to calcite with time. Most of the hydrated lime-based samples examined in this study were plasters and contained less than 10 percent aggregate by volume.

The microstructures of the calcite matrices examined were crystalline, uniform and very fine grained. They were characterized by randomly oriented rhombohedra and prisms ranging from about 0.5 to 2 µm (10^{-6} m) in size. Variations in the microtexture were usually attributed to features inherited from coarsely crushed or poorly calcined raw materials. Where matrix/aggregate interfacial regions were observed, calcite crystals appeared to be growing directly from the aggregate substrates. Neither compositional nor structural zoning or layering were observed in these interfacial regions.

3.2.4 Hydraulic Hydrated Lime-Based and Hydraulic Hydrated Lime-Based/Soil Plasters and Mortars

These materials are generally multimodal plasters or mortars containing up to and greater than 70 percent (by volume) coarse aggregates and up to 70 percent of the remaining volume may consist of a fine aggregate fraction. The coarse aggregate fractions in the samples collected on Cyprus consist primarily of rounded basalt gravel. Basalt sand and quartz sand are abundant in the fine aggregate fractions. Subangular to angular schist and marble fragments, in addition to rounded pyritic metasediment and basalt gravel make up the coarse aggregate fractions in the ancient samples collected from the Lavrion mining district, Greece. Strained quartz and mafic sand constitute the fine aggregate fractions in these specimens. In addition to coarse and fine aggregate fractions, very fine aggregates (<0.05 mm) were also observed in the Lavrion plasters and mortars. Matrix color and aggregate mineralogy, angularity, sorting, and grading are generally characteristic for each geologic province from which samples were collected. Tension fractures were not obvious features in these specimens.

The matrix fractions of these hydraulic hydrated lime-containing materials generally have colors ranging from pale yellow to orange to red depending on the impurities in the carbonate raw materials and also on the color of the very fine-aggregate fractions (when present). Samples collected from The Republic of Cyprus are typically pale buff yellow. Those from the Lavrion mining district range in color from pale yellow to pale pink; most are pale orange. This orange color is directly attributable to the dispersion of very fine limonitic particles throughout the matrices in these samples. Certain ancient plasters, LVL11 and LVL12 from the Lavrion district also contained a minor amount of very fine, porous particles which were identified as fine volcanic ash (probably airborne particles from a volcanic eruption in the Mediterranean area which settled out of the air and became incorporated into the soil in southern Greece). These two types of very fine aggregate particles in the Lavrion samples are genetically very different, but both could have been incorporated into these specimens by the addition of a minor amount of locally derived soil.

The matrix microstructures of the hydraulic hydrated lime-containing samples are generally more complex and more inhomogeneous than those which were previously described for the gypsum- or hydrated lime-containing materials. Calcite crystals in these hydraulic hydrated lime matrices range in size up to about 2 μm ($2x10^{-6}$ m), and they are randomly oriented and intergrown with masses of very fine-structure particles, generally less than 10^{-7} m in size. The morphologies of the calcite crystals resemble those previously described in Section 3.2.3. The morphologies of the very fine-structure particles are irregular and can be described as platelets, foils, or needles intergrown to form sponge-like masses, botryoidal structures, or very massive features. In thin sections the matrix fractions of these building materials appear mottled, webbed, and strained. Some of these features are secondary while others were inherited from the raw materials.

Two types of matrix/aggregate interfacial zones were observed in the hydraulic hydrated lime plasters and mortars collected from near Lavrion, Greece. The first type was similar to that described for the hydrated lime plasters in Section 3.2.3; neither layered nor zoned features were apparent. This type of interfacial morphology was also observed in the samples collected on Cyprus. The second type of matrix/aggregate interfacial microstructure observed in the ancient Lavrion samples was characterized by the presence of thin film layers coating aggregate surfaces and overlain by layers of very fine particles which were intergrown with fine-structure particles and calcite crystals in the bulk matrices.

3.2.5 Pozzolana/Hydrated Lime (Hydraulic Lime)-Based Plasters, Mortars, and Concretes

Hand specimens of these materials are typically multimodal and contain up to and greater than 75 percent by volume coarse aggregates. The fine aggregate fractions in these materials often account for up to 75 percent of the remaining volume (bulk volume minus coarse- ggregate fraction).

3.3 CHEMISTRY OF THE MATRIX FRACTION

As discussed in the previous sections, the mechanically separated matrix fractions are dominated by calcite in a number of cases and gypsum in others. The extent to which this is true is shown from the calculations summarized in Table 3-1. Part a shows the residual CaO (ΔCaO) assuming that all CO_2 in the

Table 3-1. Calculation of CaO (ΔCaO) Remaining After Combining With (a) CO_2 to Form Calcite, or (b) SO_3 to Form Gypsum.*

a. Calcite calculations

Samples from Greece	CO_2	ΔCaO
LVL05	23.11	15.66
LVL06	16.95	20.01
LVL08	14.44	18.91
LVL12$^{\#1}$	18.51	3.42
LVL12$^{\#2}$	14.26	17.63
LVL15$^{\#1}$	25.18	11.42
LVL15$^{\#2}$	28.15	10.16
LVL15$^{\#3}$	24.80	17.73
LVL17	24.71	4.54
ADL1	16.12	6.78

Samples from Cyprus	CO_2	ΔCaO
AML1, layer 1 plaster sealant	20.74	7.59
AML2	38.10	-0.16
AML4	0.34	--**
EPL2	24.10	4.32
IDL2	2.03	--**
IDL3	3.48	--**
KHL1	29.53	13.97
KTL1	3.77	--**
KTL3	18.2	8.04
KUL1 layer 2	28.20	17.55
KUL2	28.60	12.35
LML2	28.17	13.91

b. Gypsum Calculations

**Samples from Cyprus	SO_3	ΔCaO
AML4	42.34	5.33
IDL2	40.46	13.98
IDL3	39.19	8.18
KTL1	40.74	5.96

*Analyses used from Tables 2-4 and 2-5.

**High SO_3 content samples; ΔCaO remainder calculated after all SO_3 is combined with CaO to form gypsum.

analyses is reacted to form calcite; and part b the residual CaO after all SO_3 has reacted to form gypsum. Although there are some assumptions in this treatment, certain trends appear clearly.

The gypsum plasters are clearly segregated in Table 3-1, part b. As indicated previously, the plaster sealant AML2 from Cyprus is $\gtrsim$ 89 percent calcite, certainly a lime plaster; while LVL12, layer 1, LVL17 and IDL1 from Greece are lime-dominated (calcite-dominated), but contain significant amounts of other components, as do EPL2, AML1 (layer 1) and KTL3 from Cyprus.

The presence of significant cementing phases other than calcite or gypsum is reflected in the existence of other major constituents, silica and alumina in particular, especially in those materials in which this is also accompanied by substantial (~10-20 percent) remaining CaO after calculation for calcite or gypsum formation. The CaO remainder indicates potential for the presence of a calcium silicate (or aluminate/aluminosilicate) cementitious phase. There are, however, some limitations in automatically assuming this.

Another method of data treatment reveals the significant groupings outside of the lime cements and gypsum cements more clearly. Compositions of the mechanically separated matrix fractions are shown in Figure 3-1, as a plot of sums of the weight percentages of CaO + MgO versus Al_2O_3 + Fe_2O_3 which were determined for the matrix fraction of selected cementitious materials collected for this study. The composition of the matrix fraction obtained by light crushing and sieving was plotted here because as a result of the particle morphology studies, it has been demonstrated that most of the matrix phases are <45 µm to >1 µm in size. These parameters were chosen for comparison purposes in order to minimize the effects of aggregate contamination and alteration or weathering. Other major and minor constituents such as SiO_2, and Na_2O and K_2O are particularly sensitive to aggregate (quartz sand, igneous rock fragments and unreacted pozzolana) contamination. It should be noted however, that only a fraction of the total oxide components are represented in this type of graph, and that a number of limitations with respect to interpreting these plots are readily apparent. For example, it is not possible to distinguish a pure lime (portlandite) cement from a hydraulic lime (portlandite plus hydrated calcium silicates) cement which may have been prepared from siliceous limestones low in clay, on the basis of $\Sigma CaO + MgO/\Sigma Al_2O_3 + Fe_2O_3$ ratios since SiO_2 is not represented. Likewise, it is not possible to distinguish cements prepared from argillaceous limestones (natural cement

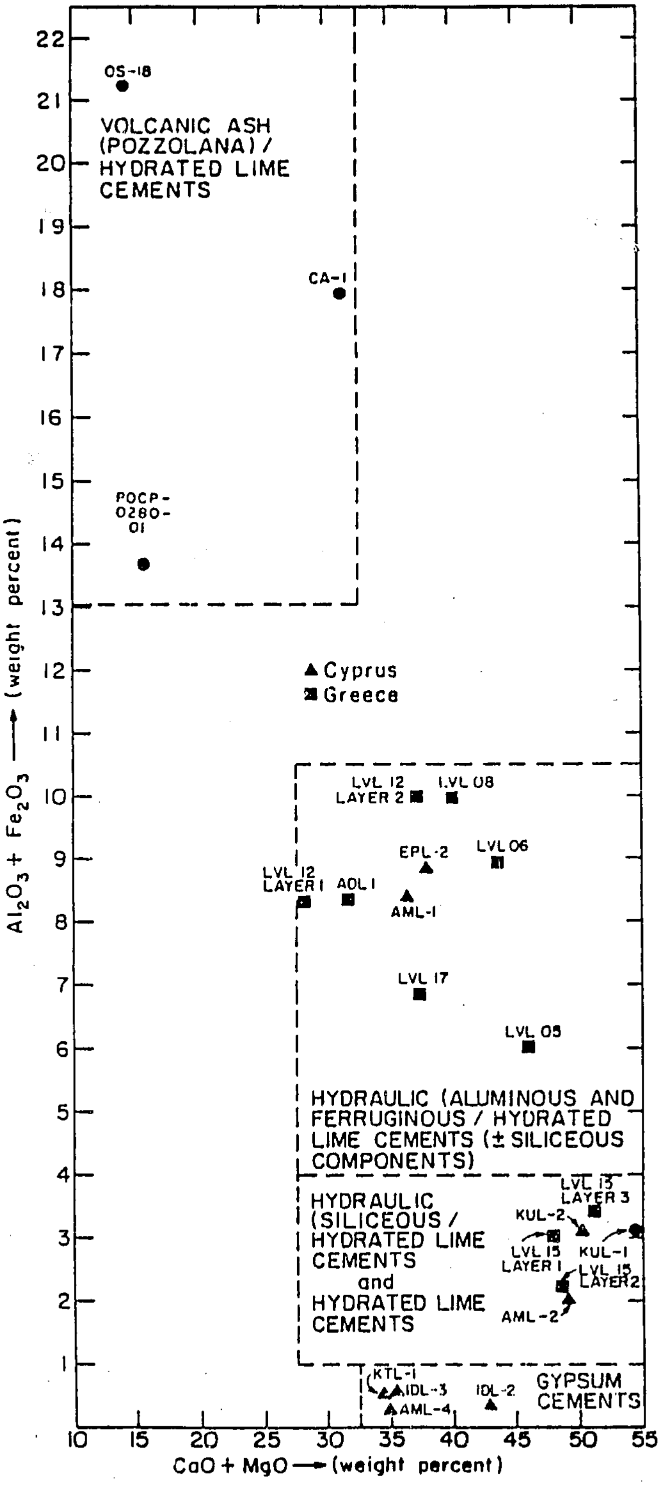

Figure 3-1. Plot of $\Sigma CaO + MgO$ Versus $\Sigma Al_2O_3 + Fe_2O_3$ for the Matrix Fractions of Selected Ancient Building Materials.

stones in which case a single material was calcined) from portland cements (prepared from a two-component raw material mix) with the same composition.

Compositional data presented in Figure 2-29 have been grouped into four categories which are consistent with cement terminology: gypsum cements; hydrated lime and hydraulic (siliceous) hydrated lime cements; hydraulic (aluminous and/or ferruginous) hydrated lime cements with and without siliceous components; and volcanic ash (pozzolana)/hydrated lime cements [one of the latter is shown from Roy and Langton (1982)]. The boundaries of the four categories are only approximate and in reality, probably overlap to varying degrees. As information is obtained on a larger number of samples, the boundaries of these categories are also expected to become better substantiated.

The ore metals lead and zinc, with exceptions, were not very abundant, and therefore apparently did not play an important role in the cementing such as reported elsewhere (Conophagos, 1982).

Gypsum cements are calcium-rich and contain less than one percent $\Sigma Al_2O_3 + Fe_2O_3$. All of the gypsum-based plasters and mortars analyzed in this study were collected from excavations in The Republic of Cyprus; and $\Sigma CaO + MgO/\Sigma Al_2O_3 + Fe_2O_3$ values for typical gypsum cement are shown in Figure 2-29. They are also low in silica. Hydrated lime cements and hydraulic hydrated lime cements in which hydration of calcium silicate phases is responsible for the hydraulic properties were used in composite materials collected from Greece and Cyprus. $\Sigma CaO + MgO/\Sigma Al_2O_3 + Fe_2O_3$ values for the matrix fractions in these materials show in Figure 2-29 that they may contain up to 4 weight percent $\Sigma Al_2O_3 + Fe_2O_3$ in addition to hydraulic siliceous components. Aluminous and ferruginous hydraulic hydrated lime-containing materials were also collected from ancient structures in Greece and Cyprus. The matrices of these materials are generally rich in both the CaO (plus or minus magnesia), Al_2O_3, and Fe_2O_3 and may contain up to 12 weight percent $\Sigma Al_2O_3 + Fe_2O_3$.

3.4 PHASE IDENTIFICATION AND PHASE RELATIONS OF THE MATRIX FRACTIONS

The hydraulic hydrated lime cements which form the binding phases in all of the ancient specimens collected from the Lavrion district, Greece, and many of the specimens from The Republic of Cyprus are composed of calcite (carbonated portlandite) plus variable amounts of X-ray amorphous calcium silicate phases. This noncrystalline material, referred to in some studies as C-S-H, exists as very fine-structure particles which may also contain aluminum, iron, magnesium and/or alkalies as determined from EDX analyses of the -1 μm matrix fraction. Minor amounts of a hydrogarnet phase were also identified in X-ray diffraction patterns of the -1 μm matrix fractions of selected specimens.

The matrices of ancient plasters and mortars collected from the Lavrion mining district are more complex than those of samples from Cyprus. For example, an X-ray amorphous hydrated iron oxide mineral (limonite) was identified by thermal analyses in the matrix fractions of the Lavrion specimens. Phases rich in Pb and Zn were identified in X-ray diffraction patterns as carbonates and altered sulfides. The presence of these components in the matrix fractions is to be expected since the carbonate rocks calcined for these cements were locally derived mineralized limestones. Phillipsite was identified in sample LVL05, a plaster from a dam near Lavrion, and it was present as chunks of zeolitic material incorporated in the matrix. The origin of this material is unknown but it is not a cementitious reaction product.

Trimethylsilylation experiments carried out on selected matrix fractions of hydrated hydraulic lime-containing materials from both Greece and Cyprus resulted in detection of silicate monomer, dimer, and minor amounts of undifferentiated polymer condensates. Neither discrete higher order polymers nor crystalline calcium silicates were detected.

4 SUMMARY AND CONCLUSIONS

4.1 SUMMARY

Mortars, plasters and concretes of unusual durability have been discovered in the remains of many ancient structures. Many have maintained mechanical integrity and could still function in their intended capacity today. The present study has characterized recently collected concretes, mortars and plasters from sites in Greece dating back to Hellenistic age (350-400 BC); and older plasters dating back to middle Bronze age (~1600 BC) and in one locality even to ~5800-5250 BC, on Cyprus. Some Roman to Early Christian age materials were also among the materials studied. Despite centuries of use and exposure to sometimes adverse environmental conditions which include atmospheric carbon dioxide, dissolved species in ore treatment liquids, and warm climatic conditions, such materials have endured, sometimes better than the stone or brick found in the same structures.

The results of these current studies of ancient materials, when integrated with information from previous work, provide insight into the long term durability of cement-containing materials, complementary to that gained from other sources such as thermodynamic (Sarkar et al., 1982) and experimental (Roy et al., 1983) investigations. These results provide the only direct long-term information on the reaction of various man-derived cementitious materials to the environments to which they were exposed.

A number of specific findings, which agree with Roy and Langton (1982) are summarized below:

1. The cementitious matrices of the materials investigated have been classified into four categories based upon chemical composition expressed in terms of $\Sigma CaO + MgO$ versus $\Sigma Al_2O_3 + Fe_2O_3$, supplemented by knowledge of the carbonate and sulfate contents. The categories are: a) gypsum cements; b) hydraulic (siliceous) hydrated lime cements and hydrated lime cements; c) hydraulic aluminous and ferruginous/hydrated lime cements (± siliceous components); and d) volcanic ash (pozzolana)/hydrated lime cements.

2. All but one of the specimens collected from Greece contain hydraulic hydrated lime cements. These plasters, mortars and concretes were primarily collected from ancient structures (~350-300 BC) including those used for washing ores and lining cisterns, in the Lavrion silver mining district: Two specimens, samples LVL01 and LVL05, were collected from a dam near the village

of Lavrion and are of questionable age. The specimen ADL01, which is a plaster from a Roman aqueduct north of Athens (~1 AD), fits the category of a pozzolana-hydrated lime cement.

3. Specimens of ancient building materials collected from The Republic of Cyprus contain gypsum cements, hydrated lime cements, or hydraulic hydrated lime cements. Samples AML4, IDL2, IDL3, KTL1, and KTL4 contain gypsum matrices and the pipe joint sealant in AML2 is a hydrated lime plaster, with no added organic material. The remaining specimens contain hydraulic hydrated lime as the binder.

4. Gypsum crystals, up to 10 μm (10^{-5} m) and greater in size constitute the binding phase in the ancient gypsum plasters and mortars. These crystals are randomly oriented, have prismatic or pinacoidal habits, and are often twinned. Composite materials containing gypsum cements show no evidence of matrix/aggregate interactions. The gypsum cements were manufactured by dehydration of naturally occurring gypsiferous rocks. Their hardening was probably the result of slaking according to the following reactions: $CaSO_4 \cdot 1/2 H_2O + 1\text{-}1/2\ H_2O \rightarrow CaSO_4 \cdot 2H_2O$. The densities of these materials were low, and they generally were relatively porous; as such, they would not be generally recommended for structures to hold water.

5. Hydrated ('pure') lime cements had limited use in ancient mortars and plasters, where they originally contained randomly oriented portlandite crystals. The lime was probably slaked before placing, and subsequent exposure to air (and water) resulted in significant carbonation of this matrix phase to form calcite crystals, 1-5 μm (1-5 x 10^{-6} m) in size, often randomly oriented, with rhombohedral or more complex crystal habits. Matrix/aggregate interfacial zoning and/or reactions were not detected in the composite materials studied here which contained hydrated lime binders. Cementitious reactions in these materials are as follows: $CaO + H_2O = Ca(OH)_2$; $Ca(OH)_2 + CO_2 = CaCO_3$.

6. Hydraulic hydrated lime cements were extensively used in ancient multimodal mortars and plasters. The cementitious products contain intergrown crystals of calcite, 1 to 5 μm in size, and fine-structure particles, <0.1 μm (<10^{-7} m) in size. The fine-structure material is amorphous to X-ray diffraction, displays irregular morphologies and microstructures, and contains Ca, Si, Al, Fe, K, Na, and Mg in variable proportions. While the presence in the

original cements of compounds such as C_2S* and hydraulic calcium aluminates and ferrites cannot definitely be proved, it is likely that they were initially present. Thus, the cementitious reactions in these materials probably took place as follows: (1) $CaO + 'C_2S' \pm 'C_3A \pm C_4AF' \pm H_2O \rightarrow Ca(OH)_2 +$ partially formed C-S-H gel ± CAH ± CAFSH. (2) $Ca(OH)_2$ + partially hydrated phases $+ H_2O + CO_2 \rightarrow CaCO_3 + C\text{-}S\text{-}H(\bar{C}) \pm CA(\bar{C})H \pm CAF(\bar{C})H$.

7. Hydrated modern portland cements contain the following phases in the approximate proportions:

$Ca(OH)_2$ ~15-20%
CAFH ~ 10% (crystalline, calcium aluminoferrite hydrate)
C-S-H ~ 70% (nearly amorphous calcium silicate hydrates).

This mineralogy differs from that observed in ancient hydraulic hydrated lime cements and pozzolana/hydrated lime cements, which contain the following phases in variable proportions:

$CaCO_3$
CAFH (crystalline)
(K,N)CAFMSH (amorphous complex hydrates).

8. As a result of increasing time and, depending on the degree of exposure to air, rain water, and ground water, modern portland cements undergo the following chemical and structural changes: $Ca(OH)_2$ and CAFH phases partially carbonate to form calcite and $CAFH\bar{C}$, and the nearly amorphous C-S-H polymerizes to form higher order condensates as discussed by Roy and Langton (1982). The C-S-H incorporates some alumina in its structure. Extended aging of the ancient cementitious materials examined in this study has also resulted in carbonation of $Ca(OH)_2$ to form calcite [because of conventional practices, much of the $Ca(OH)_2$ in porous materials was probably carbonated relatively quickly; where exposed to carbonate-containing ground waters, denser materials would proceed to carbonate slowly in the direction defined by limits of phase stabilities (Sarkar et al (1982)]. However, evidence for increased polymerization of the KNCAFMSH gel structure is not yet definitive, though further work may provide evidence of such polymerization. In fact, the presence of less strong network formers such as Al and Fe balanced by the network modifiers K and Na (in the KNCAFMSH amorphous component) may be responsible for

---

*Cement abbreviations: Oxide formulas: $C = CaO$, $S = SiO_2$, $A = Al_2O_3$, $F = Fe_2O_3$, $\bar{C} = CO_2$, $H = H_2O$, $K = K_2O$, $M = MgO$, $N = Na_2O$, $\bar{S} = SO_3$.

the limited size of polymeric structural units formed, or for the breakdown of initially formed polymers into smaller units. Current data, however, suggest there are certain advantages of the presence of Al in C-S-H or in the crystalline calcium silicate hydrate, tobermorite (Komarneni and Roy, 1983).

9. The extent of interaction of matrix with aggregate in the plasters, mortars and concretes observed was variable depending upon the specific matrix and the mineralogy and microtexture of the specific aggregate. Gypsum showed little interaction in general with aggregate, nor did hydrated lime plasters and mortars. Hydraulic hydrated lime mortars however, showed two types of matrix/aggregate interfacial regions. The first was similar to that described for the hydrated lime cements; the second was complex and was characterized by a two-layer interfacial region consisting of a film overlying the aggregate, which in turn was attached to the bulk paste by a layer of fine particles growing from the film. In these respects they resemble microstructures in modern concretes (Langton and Roy, 1980).

10. Mechanical compaction may have been used in some instances in these materials for achieving low water/'cement' ratio materials (as, e.g., when a plaster is 'worked', compressed). Although no direct evidence was found for the presence or use of organic materials as 'admixtures', in these particular materials, as is commonly done in modern concrete technology, the proper sizing of materials, and the extent of mechanical methods used appeared to achieve a similar effect. [Others e.g. have given evidence for use of organics in more recent materials. Idorn (1959) has cited evidence for use of air entraining admixtures in concrete at Provence; Miao Ji-Sheng et al (1981) for use of rice gluten, tung oil and animal blood in ancient China; and Malinowski (1979) for use of quicklime-oil expanding mixtures in Jerusalem.]

4.2 CONCLUSIONS

These investigations have provided detailed knowledge about the chemical, mineralogical, microstructural and macroscopic characteristics of some collections of durable ancient mortars and plasters. Their remarkable long-term durability is a complex function, resulting from a combination of both chemical and microstructural factors, which relate to the wise selection of materials and the skill and workmanship used in their production. Long-term durability of ancient cement-containing building materials, as compared to modern portland cement-containing composite materials, is a function of matrix mineralogy, particle size, and porosity, and aggregate type, grading, and proportioning.

Gypsum plasters, though widely used in the early materials from Cyprus, are obviously not very versatile or strong (they are largely monomineralic, mono-size fractioned, not very densely packed, and hence are quite porous), nor were hydrated lime materials generally (exceptions in the latter are those in which low porosities [very low equivalent water/'cement' ratios] were achieved probably by compaction). Eventually these two types of cements were largely superceded by the chemically different hydraulic hydrated lime based materials (or elsewhere, by lime-pozzolanic cements). The latter two categories also are generally more workable than gypsum or hydraulic lime cements, and because of the multiphase content, tend to have multi-size ranged particles, allowing better density of packing. Mechanical means for densification, indeed almost 'polishing' appear to have been used for placing layered plasters to line aqueducts or ore-washing basins, and other water-bearing structures, as they were in some Roman structures described by Malinowski (1979); the polished compacted surface helped to assure the impermeability of such structures. In modern concrete materials, small amounts of chemical admixtures are often used to achieve the same effects, more efficiently.

The microstructures of many of the ancient materials are very fine and dense. This results from the intergrowth of the minute calcite crystals formed by carbonating slaked lime, with usually somewhat lesser amounts of the finer particulate amorphous and partially crystalline complex (partly carbonated) aluminoferrite and silicate hydrates, surrounding somewhat coarser fractions of the silts and unreacted mineral and rock fragments which were intermixed. [In pozzolanic cements, which are generally more hydraulic and frequently have higher strengths, the reaction continues to take place between lime and alkalis and a silica-rich pozzolan to produce somewhat similar complex hydrated material, but generally in larger proportion (Roy and Langton, 1982).] Such fine microstructures generally give rise to greater strength. Even some of the hydrated lime cements gave durable materials, their fine microstructures giving evidence of careful preparation with a low (less than ~0.3) effective water/'cement' ratio.

The sand and larger size fraction aggregates of these durable ancient mortars, concretes and plasters contain many types of sedimentary, igneous and metamorphic rocks. The rock fractions incorporated in the materials of the

2 OF 2

current study ranged from carbonates, sandstones, shales and schists, to volcanic and pyroclastic rocks, and even some ore minerals. Some coarser mortars were found which showed excellent grading of coarse to fine fractions, which appeared to be responsible in part for their mechanical stability.

A considerable variety of rock compositions have been used, which largely reflect the rock types available locally, suggesting that it is possible to achieve reasonable durability with a number of different materials, providing chemical compatibility is maintained with the environment. However, some materials used in a particular site to line a cistern exhibited some interfacial cracking between quartzite and marble aggregate and the matrix, or between layers of plasters, part of which was later healed by infilling. In samples where cracking occurred between limestone (or marble) aggregate and the carbonate-rich matrix, it appeared that a higher water/'cement' ratio may have been used, thus permitting excessive shrinkage. Since carbonate rocks and quartz-containing sandstones are among the stratigraphic units to be sealed in a bedded salt repository environment, such observations require further detailed investigation.

By selecting samples for future studies of older and ancient concrete analogs from locations having specific rock types or aggregate sources similar to those rocks from a particular repository site (e.g., sandstones, siltstones, shales, limestones, dolomites, etc., which overlie a salt repository horizon and require sealing) or e.g. studying concretes from structures which were exposed to saline waters (sea water exposure) it should be possible to focus the comparisons more precisely to provide directly applicable information on the long-term durability of sealing materials analogous to modern concretes. It should also help to further distinguish the chemical factors, and those which are the results of microstructural and technological factors, which together contribute to assure adequate durability within the conditions imposed by the total repository environment, including rock types, groundwaters, and ambient temperature.

REFERENCES

Antiquities Department of The Republic of Cyprus, 1965. Khirokitia, A Guide (Revised Edition), Proodos Printing and Publishing Co., Ltd., Nicosia, Cyprus.

Antiquities Department of The Republic of Cyprus, 1980. Kourion, A Guide, Antiquities Department, The Republic of Cyprus, Nicosia, Cyprus.

Conophagos, Constatin E., 1980. Le Laurium (Lavrion) Antique et la Technique de la Production l'Argent, Ekdotike Hellados, SA, Athens.

Conophagos, C., 1982. 'Smelting in Ancient Laurion', Early Pyrotechnology, Eds. T.A. Wertime and S.F. Wertime, Smithsonian Institution, Washington, DC, pp. 182-184.

Courtault, B., 1979. Couplage Microthermogravimetrie - Spectrometrie de Masse Analyses Vol. 7 (11), pp. 481-488.

Department of Lands and Surveys, Cyprus, 1977.

Diamond, S., 1976. 'Cement Paste Microstructure--An Overview of Several Levels', pp. 2-30, in Hydraulic Cement Pastes: Their Structure and Properties, Proceedings of a conference held at University of Sheffield, 8-9 April 1976. Cem. Concr. Assn., Wexham Springs, UK.

Efstathiadis, Efstathios, 1978. Greek Concrete of the Three Milleniums, Research Center of the Hellenic Ministry of Public Works, Athens, Greece.

Hadley, D.W., 1972. 'The Nature of the Paste-Aggregate Interface.' PhD Thesis, School of Civil Engineering, Purdue University, West Lafayette, IN, 186 pp.

Idorn, G.M., 1959. 'Mikroskopiske Glimt af Betonteknikkens Historie' [History of Concrete Technology-Through a Microscope]. Beton-Teknik Vol. 4, pp. 119-141.

Komarneni, S., and D.M. Roy, 1983. 'Tobermorites: A New Family of Cation Exchangers', Science, Vol. 221, pp. 647-648 (August 12).

Langton, C.A., and D.M. Roy, 1980. 'Morphology and Microstructure of Cement Paste/Rock Interfacial Regions', Proc., 7th International Congress on the Chemistry of Cement, Vol. III, Communications, pp. VII-127 - VII-133, Septima, Paris.

Mackenzie, R.C., 1970. Differential Thermal Analyses, Vol. 1, Academic Press, New York, NY.

Malinowski, R., 1979. 'Concrete and Mortars in Ancient Aqueducts', Concrete International, pp. 66-76.

Miao, Ji-Sheng, Xiu-Ying Li, Rong-Kiu Cheng, and Bao-Shan Lu, 1981. 'A Preliminary Investigation of Cementing Materials Used in Ancient China', Research Institute of Building Materials, Wuhan, Vol. 9, No. 2, pp. 234-240 (June).

Ramachandran, V.S., 1969. Applications of Differential Thermal Analysis in Cement Chemistry, Chemical Publishing Co., New York, NY.

Roy, D.M., and C.A. Langton, 1982. Longevity of Borehole and Shaft Sealing Materials: 2. Characterization of Cement-Based Ancient Building Materials, ONWI-202, prepared by The Pennsylvania State University for the Office of Nuclear Waste Isolation, Battelle Memorial Institute, Columbus, OH.

Roy, D.M., M.W. Grutzeck, and P.H. Licastro, 1979. Evaluation of Cement Borehole Plug Longevity, ONWI-30, prepared for Office of Nuclear Waste Isolation, Battelle Memorial Institute, Columbus, OH.

Roy, D.M., M.W. Grutzeck, and L.D. Wakeley, 1983. Selection and Durability of Seal Materials for a Bedded Salt Repository: Preliminary Studies, ONWI-479, prepared by The Pennsylvania State University for the Office of Nuclear Waste Isolation, Battelle Memorial Institute, Columbus, OH. 157 pp.

Sarkar, A.K., M.W. Barnes, and D.M. Roy, 1982. Longevity of Borehole and Shaft Sealing Materials: I. Thermodynamic Properties of Cement and Related Phases Applied to Repository Sealing, ONWI-201, prepared by The Pennsylvania State University for the Office of Nuclear Waste Isolation, Battelle Memorial Institute, Columbus, OH.

Sarkar, A.K., and D.M. Roy, 1979. 'A New Characterization Technique for Trimethylsilylated Products of Old Cement Pastes', Cement and Concrete Res., Vol. 9, pp. 343-352.

Stager, Larence E., A. Walker, and G.E. Wright, 1974. American Expedition to Idalion, Cyprus, 1971-1972, American Schools of Oriental Research, 126 Inman St., Cambridge, MA.

Swiny, Stewart, 1979. Cyprus BC - 7000 Years of History, Ed. Veronica Tatton-Brown (contributions by V. Karageroghis and E.J. Peltenburg), British Museum Publications, London.

Tamas, F.D., A.K. Sarkar, and D.M. Roy, 1976. 'Effect of Variables Upon the Silylation Products of Hydrated Cements', in Hydraulic Cement Pastes: Their Structure and Properties, proceedings of a conference held at Sheffield, England, 8-9 April 1976, Cem. Concr. Assn., Wexham Springs, Slough SL3 6PL, UK, pp. 55-72.

Taylor, H.F.W., and D.M. Roy, 1980. 'Structure and Composition of Hydrated Cement Phases at Ordinary and Elevated Temperatures and Pressures', Proceedings of the 7th International Congress Chem. Cement, Paris, Vol. I, Principal Reports, pp. II2.1 - II2.13, Septima, Paris.

Uchikawa, H., and R. Furuta, 1980. 'Hydration of C_3S-Pozzolana Paste Estimated by Trimethysilylation', Cem. Concr. Res. Vol. 11, pp. 65-78.

Vitruvius, P., 1960. Vitruvius - The Ten Books on Architecture, translated from the Latin by M.H. Morgan, Dover Publications, Inc., New York, NY.

Webb, Jennifer, 1977. A Short Guide to the Excavatin at Kition, Antiquities Department of the Republic of Cyprus, Nicosia, Cyprus.

Znaczko-Janworski, I.L., 1958. 'Experimental Research on Ancient Mortars and Binding Materials', The Quarterly of History of Science and Technology, Warsaw, Poland, No. 3, pp. 377-407.

APPENDIX A

Site Information and Sample Identification

Table A-1. Tabulation of Location Information for Samples Collected in Greece.

Geographic Reference	Site	Site No.	Excavation Location No.	Sample No.
Lavrion	Dam	1	1	LVL01 LVL02 LVL03 LVL04 LVL05 LVL17
Lavrion	Ore-washing Facilities, Souresa Excavated by Conophagos (1980)	2	1	LVL06 LVL07 LVL08 LVL09 LVL10
	Souresa Excavations of Conophagos (1980)	2	2	LVL11
Lavrion	Ruins NW of Megala Ripari (Helicoidal Basin)	3	1	LVL12 LVL13 LVL14 LVL15 LVL16
Lavrion	Ruins near Megala Pefka (Helicoidal Basin)	4	1	LVL18
Amphissa-Delphi Junct	Roman Aqueduct Ruins	5	1	ADL01
Athens	Agora	6	1-5 corresponding to photos	AG01-AG05

Table A-2. Tabulation of Location Information for Samples Collected in The Republic of Cyprus.

PSU Site No.	Geographic Location	Excavation Site Reference	Site Location on Excavation Grid	Sample No.
1	IDALION		#E site, NW Sect, E grid	IDL1
	IDALION		#C site, SW Quad, W Grid	IDL2
	IDALION		#D site, SW Quad, W Grid	IDL3
2	KITION	Webb, (1977)	Area II at floor level III, TEMPLE #1	KTL1
	KITION	Webb, (1977)	Area II at floor level III, TEMPLE #1	KTL2
	KITION	Webb, (1977)	Area II at floor level III, TEMENOS B	KTL3
	KITION	Webb, (1977)	Area II at floor level III, TEMPLE #2	KTL4
3	KHIROKITIA	Republic of Cyprus, Antiquities Dept. (1965)	Area I	KHL1
4	AMATHUS	Site guide: Dimos Christov, Archaeologist, Republic of Cyprus; no plan obtained	Sites located on photos	AML1 AML2
	AMATHUS		Site located on photo	AML3
	AMATHUS	Site guide: Dimos Christov	Middle tomb entrance	AML4
5	PHANEROMENI (EPISCOPI)	Swiny, 1979	Site #1, Room #29, location #4744	EPL1
	PHANEROMENI (EPISCOPI)	Swiny, 1979	Site #1, Room #2, Bin #5	EPL2
	PHANEROMENI (EPISCOPI)	Swiny, 1979	Site #1, Room #13, Bin #17	EPL3
	PHANEROMENI (EPISCOPI)	Swiny, 1979	Site #1, Room #8, S. Bin	EPL4
6	KOURION	Antiquities Dept., Republic of Cyprus, 1980; excavation in progress by Dimos Christov	Sites located on photos	KUL1 KUL2 KUL3
7	LEMBA	No plan obtained	Sites located on photos	LML1 LML2

Table A-3. Field Descriptions of Ancient Building Materials and Sites for Samples Collected in Greece.

Sample No.*	Sample Description	Site Description
LVL01 1180-01	plaster (surface layer only) from interior face of dam retaining wall (E wall) 350 BC?	Lavrion, Greece; Site #1, Location #1; 1.81m from top of dam wall, 4.5 m from SE corner
LVL02 1180-01	multilayered plaster; same as above	Lavrion, Greece; Site #1, Location #1; same as above
LVL03 1180-01	multilayered plaster, same as above	Lavrion, Greece; Site #1, Location #1; same as above
LVL04 1180-01	multilayered plaster; same as above	Lavrion, Greece; Site #1, Location #1; same as above
LVL05 1180-01	multimodal mortar from between marble "fieldstones" exposed in the breached portion of the dam retaining wall 350 BC	Lavrion, Greece; Site #1, Location #1; 1.2 m from top of E retaining wall where the wall was breached to allow drainage of dam
LVL06 1180-01	multimodal concrete/floor plaster 5 cm - 10 cm thick, overlying a packed soil platform 350-400 BC	Lavrion, Greece; Site #2, Location #1; top of SW side of an elevated platform located 3.0 m from the NE side of the ore-washing basin
LVL07 1180-01	soil/schist (mud) mortar from circular platform underlying LVL06 350-400 BC	Lavrion, Greece; Site #2, Location #1; middle of SW side of platform described above
LVL08 1180-01	multimodal plaster 1.3 - 1.9 cm thick covering concave floor support 350-400 BC	Lavrion, Greece; Site #2, Location #1; SW end of floor support along NW side of ore-washing basin
LVL09 1180-01	multimodal concrete/plaster used to finish off top surface of cistern wall 350-400 BC	Lavrion, Greece; Site #2, Location #1; top surface N side of large cistern wall
LVL10 1180-01	multimodal plaster 2.5 cm thick from interior of a small cistern 350-400 BC	Lavrion, Greece; Site #2, Location #1; N side of small cistern, interior side wall, 0.6 m below top of wall
LVL11 1180-01	multimodal plaster 2.5 cm thick from exterior wall of a trough 350-400 BC	Lavrion, Greece; Site #2, Location #2; directly above outlet in NW-SE trending wall of trough above a sorting area
LVL12 1180-01	multimodal plaster 5.1 cm thick from interior wall of a wash basin 350-400 BC	Lavrion, Greece; Site #3, Location #1; 15 cm from top of central portion of SE wall of ore-washing basin

Table A-3. Field Descriptions of Ancient Building Materials and Sites for Samples Collected in Greece (continued).

Sample No.*	Sample Description	Site Description
LVL13 1180-01	multimodal mortar/plaster from between stone in wall in a trough of a wash basin ~350-400 BC	Lavrion, Greece; Site #3, Location #1; 15 cm from top of central portion of SW wall of NE corner of trough on the NE side of the wash basin
LVL14 1180-01	multilayered plaster, 2 of 3 layers 0.6 cm dk red exterior layer and 2.5 cm pink layer from interior of a trough wall 350-400 BC	Lavrion, Greece; Site #3, Location #1; same as above
LVL15 1180-01	multilayered plaster, 3 of 3 layers 0.6 cm dk red exterior layer, 2.5 cm pink layer, and 2.5 cm - 7.6 cm white layer from interior of a trough wall 350-400 BC	Lavrion, Greece; Site #3, Location #1; interior surface of SE wall of rectangular trough, 15 cm from top of wall
LVL16 1180-01	plaster from interior channel wall surface 350-400 BC	Lavrion, Greece; Site #3, Location #1; SE side of an above-ground serpentine-shaped trough interior channel wall, 5 cm from top
LVL17 1180-01	multilayer plaster (complete) from interior of dam retaining wall (E wall) 350-400 BC	Lavrion, Greece; Site #1, Location #1; 0.6 m from top of wall 6.0 m from NE corner of dam, upstream side of wall
LVL18 1180-01	plaster lining on ceramic tile cone used as a conduit through a wall in an ore-washing basin 350-400 BC	Lavrion, Greece; Site #4, Location #1; conduit in NE wall of ore-washing basin (upper portion broken away)
ADL01 1180-01	multimodal plaster and mortar from interior of the channel in a Roman Aqueduct	Amphissa-Delphi Junct., Greece; Roman aqueduct extending several hundred yards ~ perpendicular to road, sampled ~15 m from road
[1]AG01 1180-01	plaster from basin or trough 360-400 BC	Athens, Greece; Agora, Location #1
[1]AG02 1180-01	plaster from bottle-shaped cistern 350 BC - 1 AD	Athens, Greece; Agora, Location #2
[1]AG03 1180-01	joint sealant of tile pipe #A1991 (Agora Museum), maybe oxidized Pb or plaster? ~300 BC - 1 AD	Athens, Greece; Agora, Location #3
[1]AG04 1180-01	plaster from interior of a stone cistern which is tile-lined 350 BC - 1 AD	Athens, Greece; Agora, Location #4
[1]AG05 1180-01	plaster from interior of a small cistern 350 BC - 1 AD	Athens, Greece; Agora, Location #5

---

*Archive reference numbers. Abbreviated sample numbers have been used for convenience in the remainder of this text.

[1] Sample locations for these samples were photographically documented by C. Langton and samples were supplied courtesy of Dr. J. Camp, Agora Museum, Athens, Greece.

Table A-4. Field Descriptions of Ancient Building Materials and Sites for Samples Collected in The Republic of Cyprus.

Sample No.*	Sample Description	Site Description
AML01 1180-01	concrete/floor plaster 6.3 - 7.6 cm thick; from elevated platform area (~1, Roman - e. Christian)	AMATHUS EXCAVATION, CYPRUS; TEMPLE/PALACE (?); elevated platform near gate of excavation
AML02 1180-01	pipe-joint plaster (compound) from terra-cotta pipe joints (~1, Roman - e. Christian)	AMATHUS EXCAVATION, CYPRUS; TEMPLE/PALACE (?); exposed terra-cotta pipes near NW edge of excavation
AML03 1180-01	multilayer concrete from floor pre-dating AML1 (~50 BC)	AMATHUS EXCAVATION, CYPRUS; TEMPLE/PALACE (?)
AML04 1189-01	mortar from between ashlar-stone tomb (~500 BC - 2 AD)	AMATHUS EXCAVATION, CYPRUS; sampled at base of vaulted entrance to Tomb #2 (middle of 3 similar tombs)
EPL01 1180-01	plaster/concrete from floor of round hearth (~m. Bronze - 1600 BC)	PHANEROMENI (EPISCOPI) EXCAVATION, CYPRUS; Room #29 Location #4744
EPL02 1180-01	plaster from circular bin/basin (~m. Bronze - 1600 BC)	PHANEROMENI (EPISCOPI) EXCAVATION, CYPRUS; Room #2, Bin #5
EPL03 1180-01	plaster from circular bin (~m. Bronze - 1600 BC)	PHANEROMENI (EPISCOPI) EXCAVATION, CYPRUS; Room #13, Bin #17
EPL04 1180-01	plaster from circular bin (~m. Bronze - 1600 BC)	PHANEROMENI (EPISCOPI) EXCAVATION, CYPRUS; Room #28, S. Bin
IDL01 1180-01	multilayered plaster (3 layers) from interior wall of rectangular basin (~700 BC)	IDALION EXCAVATION, CYPRUS; SITE E, NW QUAD of E GRID; Bathhouse (fenced in) 3 m from paved road; sample from NE side 15 cm below top of basin wall
IDL02 1180-01	plaster from interior wall (~700 BC)	IDALION EXCAVATION, CYPRUS; SITE C, SW QUAD of W GRID; sample taken from low wall (0.3 m high) of elevated bench in central portion of the excavation
IDL03 1180-01	mortar from between limestone wall (~700 BC)	IDALION EXCAVATION, CYPRUS; SITE D, SW QUAD of W GRID; small excavation 3 m from paved road to military outpost, 1.8 m from top of wall parallel to road
KHL01 1180-01	plaster (?) circular bin/basin (~5800 - 5250 BC)	KHIROKITIA EXCAVATION, CYPRUS; Area #1, N side of foot path; Bin = 0.5 m dia.
KTL01 1180-01	plaster 2.5 - 3.8 cm thick from top of rock wall. May be top of a wall, elevated platform, or a portion of floor surface (~1200 - 800 BC)	KITION EXCAVATION, CYPRUS; AREA II at floor level III; upper surface of N side of portion of small elevated structure ~5 m North of Temple 1
KTL02 1180-01	soil mortar from between rocks forming base for sample KTL1 (~1200 - 800 BC)	KITION EXCAVATION, CYPRUS; AREA II at floor level III; sampled from 10 cm below top surface
KTL03 1180-01	multimodal plaster from inner surface lining of bottle-shaped cistern (~1200 - 800 BC)	KITION EXCAVATION, CYPRUS; AREA II at floor level III; W side of bottle-shaped cistern along W side of Temenos B
KTL04 1180-01	mortar from between limestone blocks - 2 applications of mortar are obvious from hand specimen - the outermost possibly the result of recent restoration/preservation work (1200 BC - ?)	KITION EXCAVATION, CYPRUS; AREA II at floor level III; ~2 m from ground level along W side of E wall of Temple 2

Table A-4. Field Descriptions of Ancient Building Materials and Sites for Samples Collected in The Republic of Cyprus (continued)

Sample No.*	Sample Description	Site Description
KML01 1180-01	plaster 1.2 - 2.5 cm thick from interior wall (200 - 100 BC)	KOURION EXCAVATION, CYPRUS; wall near large bottle-shaped cistern in recently excavated ancient city site N of Basilica
KML02 1180-01	plaster from interior wall of "open poor", 5 cm thick	KOURION EXCAVATION, CYPRUS: SE top corner of large "open pool" in recently excavated ancient city site N of Basilica
LML01	plaster from floor	LEMBA EXCAVATION, CYPRUS; EAST side of fenced area
LML02 1180-01	plaster (?) from small circular bin (~3500 - 2500 BC)	LEMBA EXCAVATION, CYPRUS; 0.5 m dia. basin; 0.3 m = depth in NE quad of fenced excavation

*Archive reference numbers. Abbreviated sample numbers have been used for convenience in the remainder of this text.

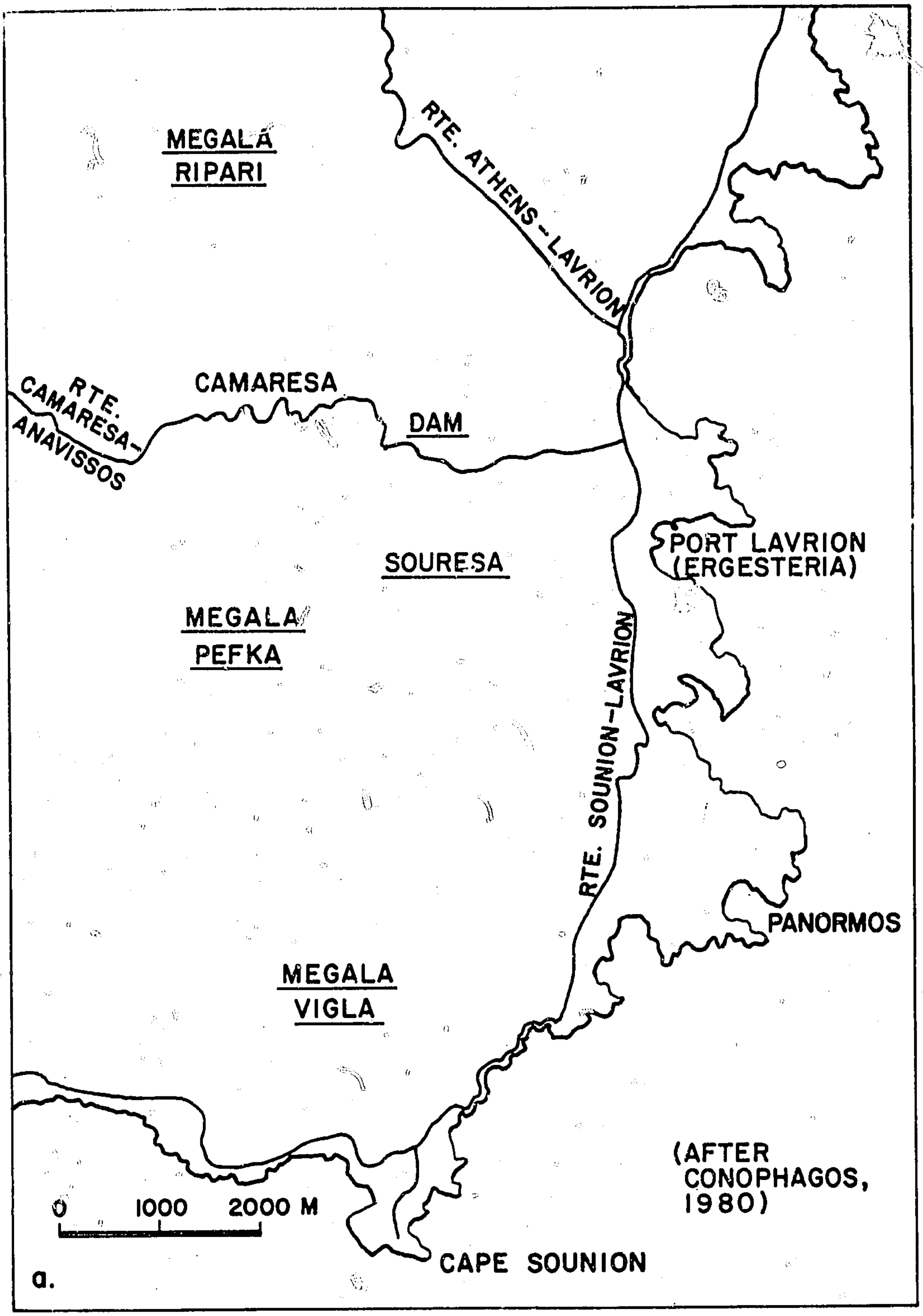

Figure A-1. a) Map of Lavrion Metalliferous Area Showing Megala Ripari, Megala Pefka, Souresa, and Dam Sample Collection Sites (Conophagos, 1980).

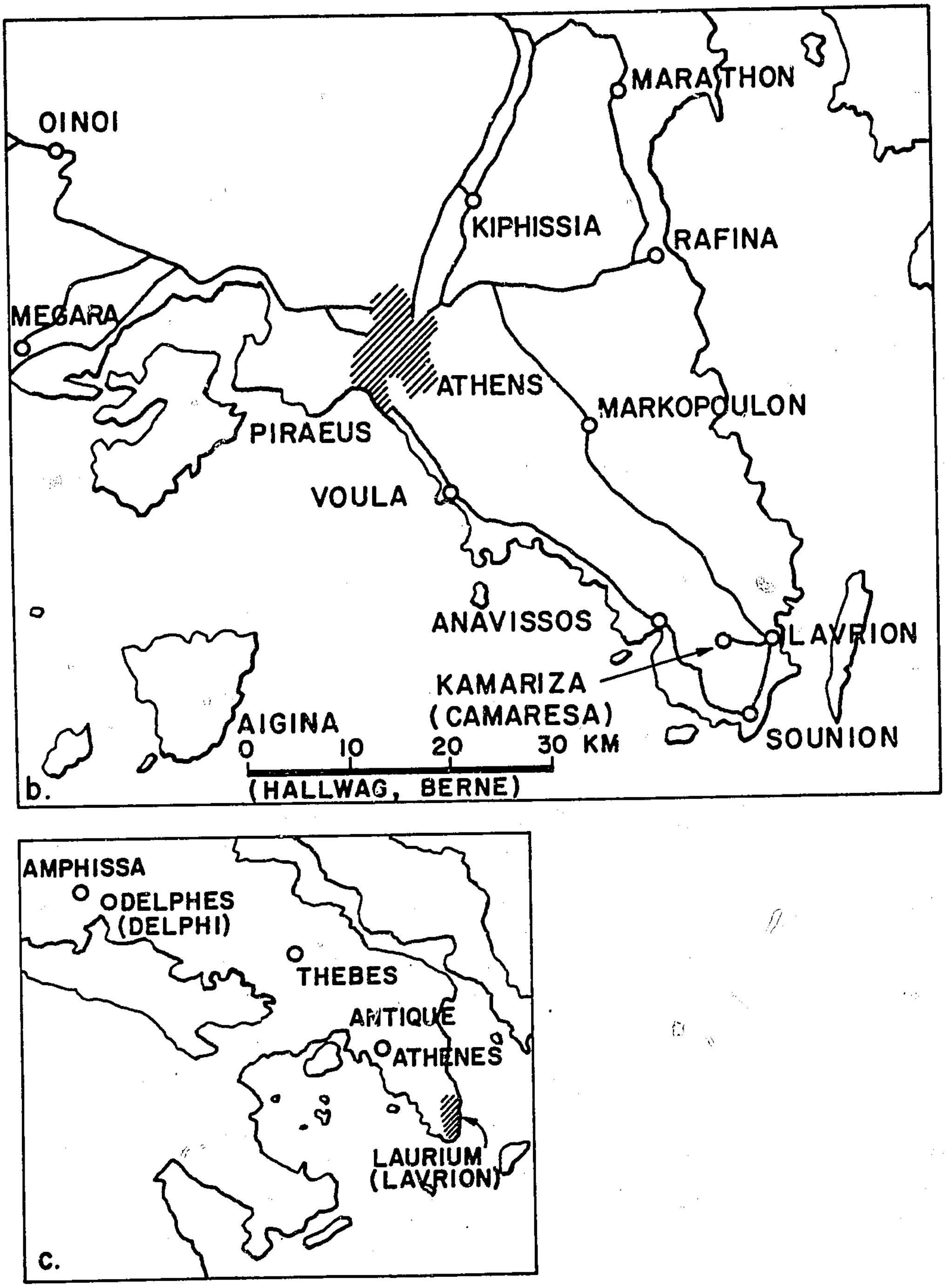

Figure A-1. **b) Modern Map of Athens-Lavrion-Sounion Area. c) Small Scale Map of Ancient Greece Showing Laurium (Lavrion)-Athens-Delphi-Amphissa Area (after Conophagos, 1982).**

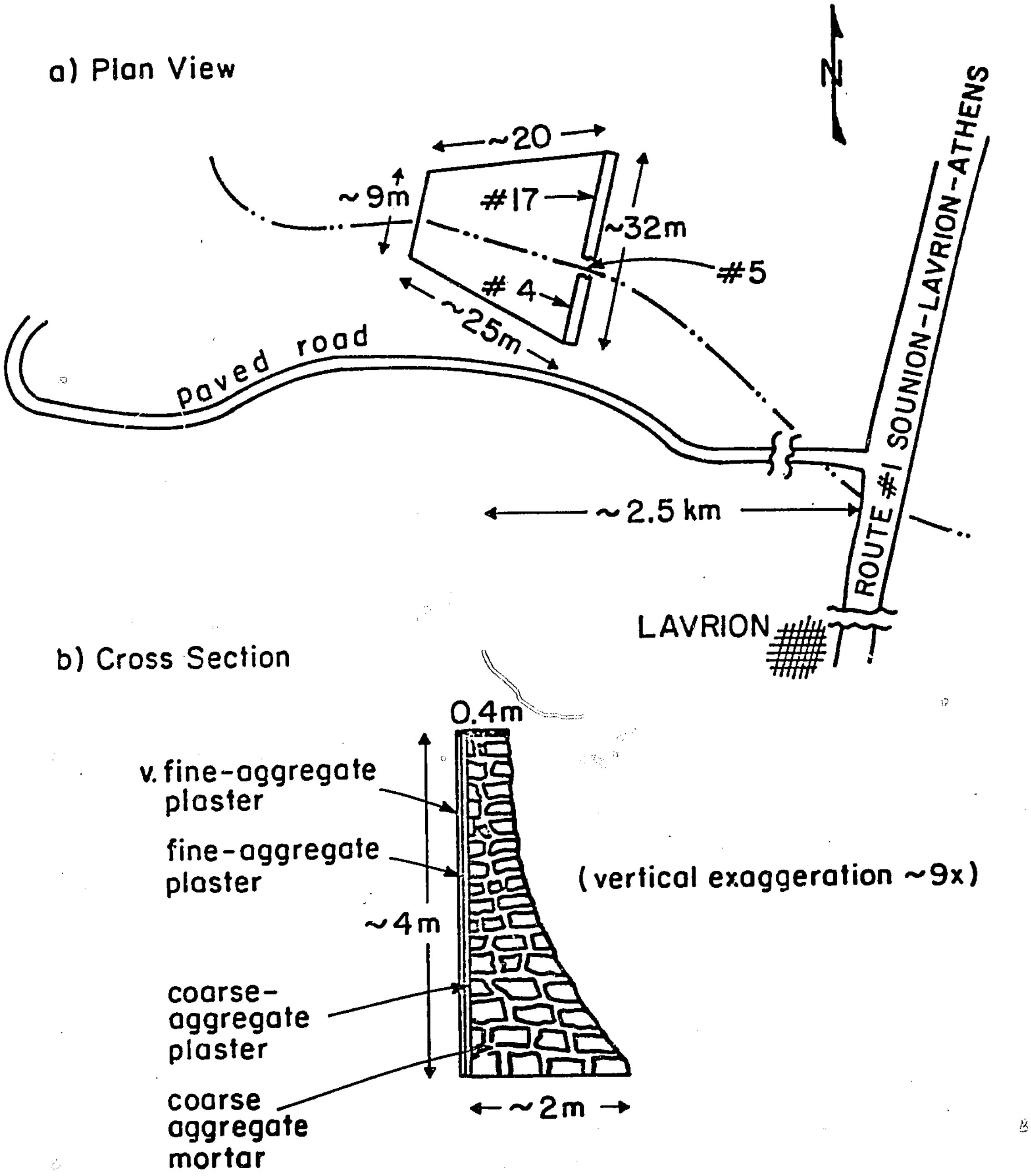

Figure A-2. Schematic Field Sketch of Site #1, Location #1, Dam Site Lavrion District. Sample locations #4, #5 and #17 are shown; numbers correspond to sample numbers in Table A-1 (not drawn to scale).

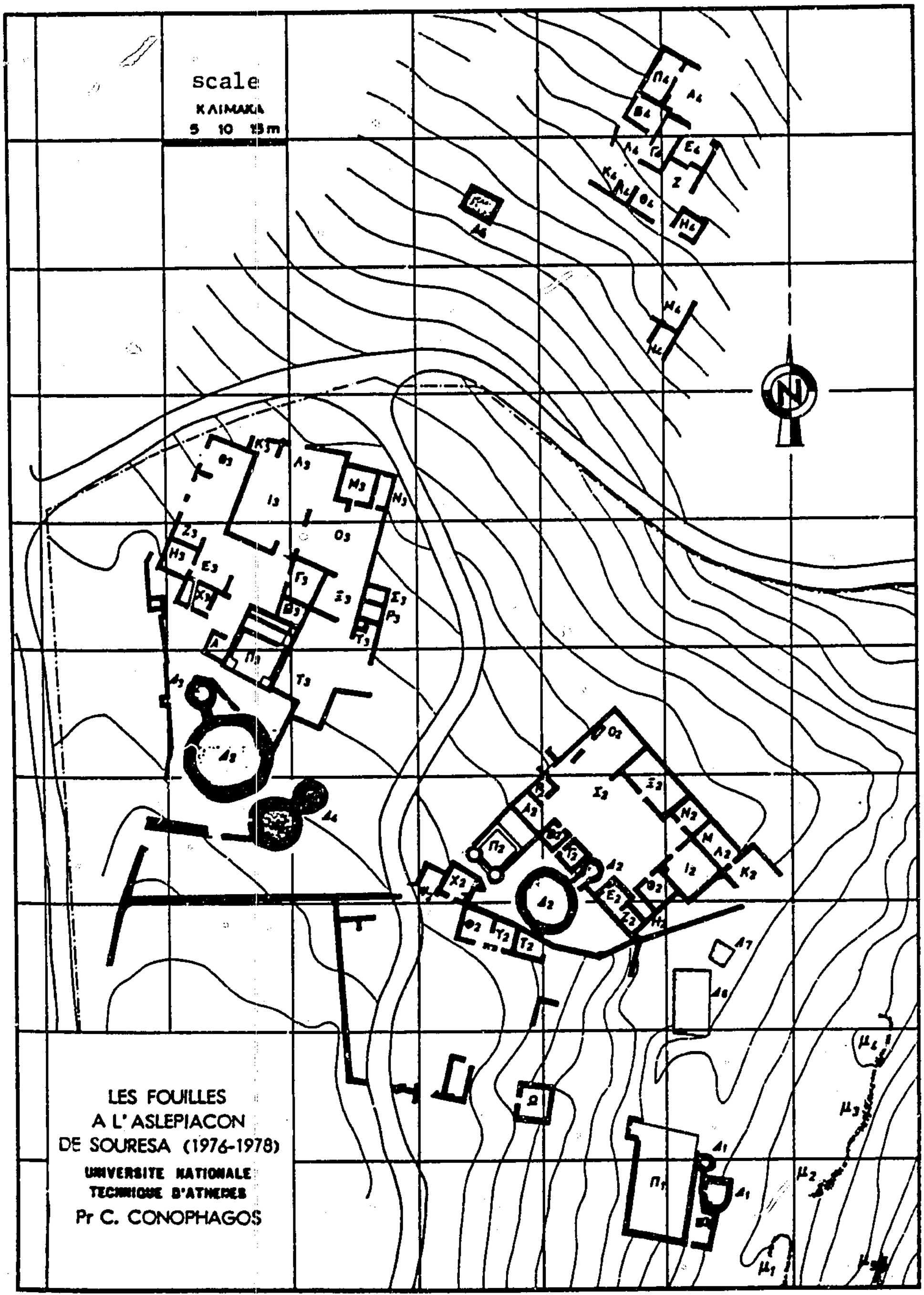

Figure A-3. Illustration of Conophagos' Excavation at Site #2, Souresa, Including Locations #1 and #2, Lavrion District (after Pr. C. Conophagos, 1980).

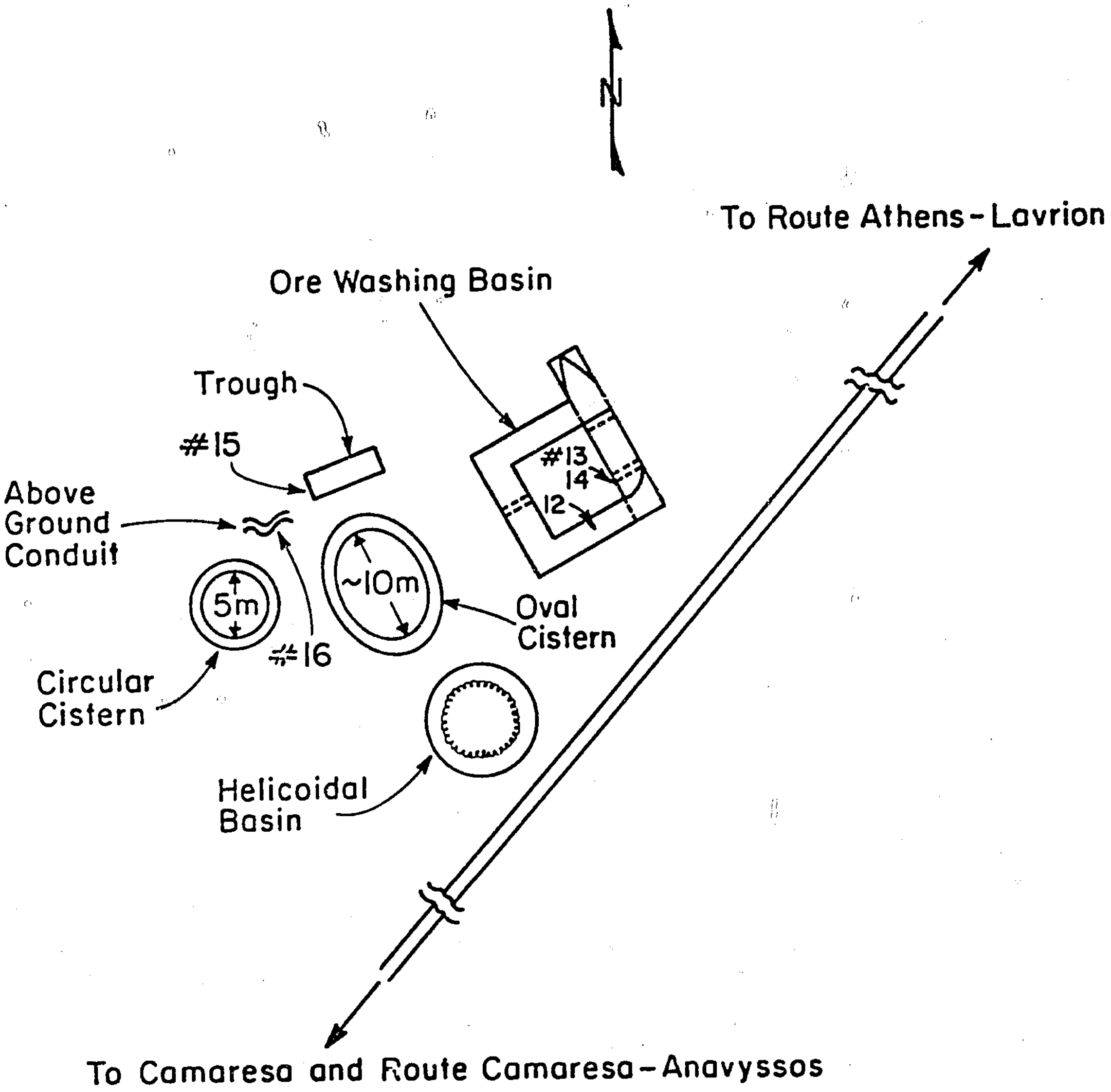

Figure A-4. Schematic Field Sketch Illustration of Site #3, Location #1 (Helicoidal Basin near Megala Ripari), Lavrion District. Sample locations are also shown and numbers correspond to sample numbers (not drawn to scale).

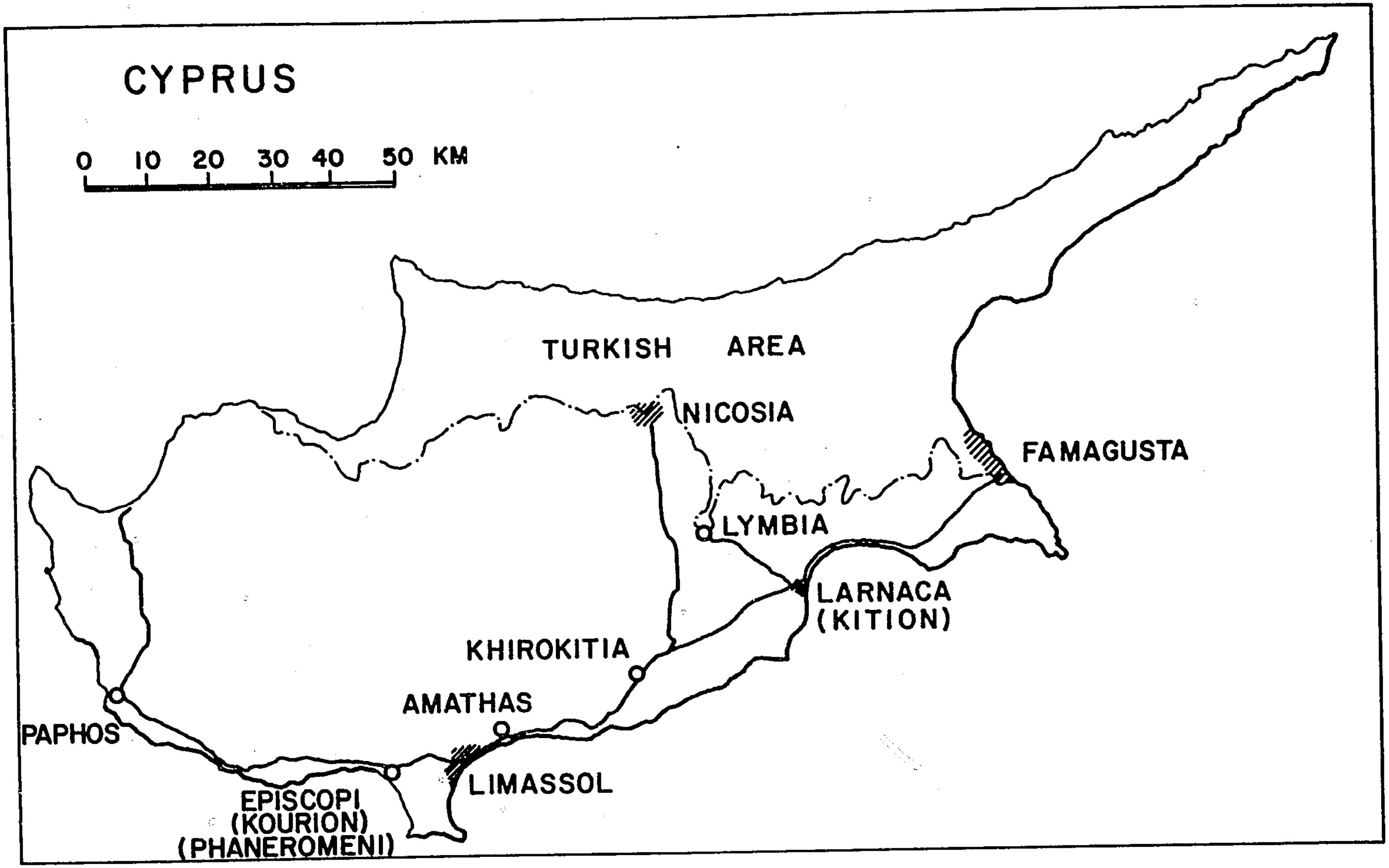

Figure A-5. Map of Cyprus. The Locations of Major Cities, Roads and Some Excavations.

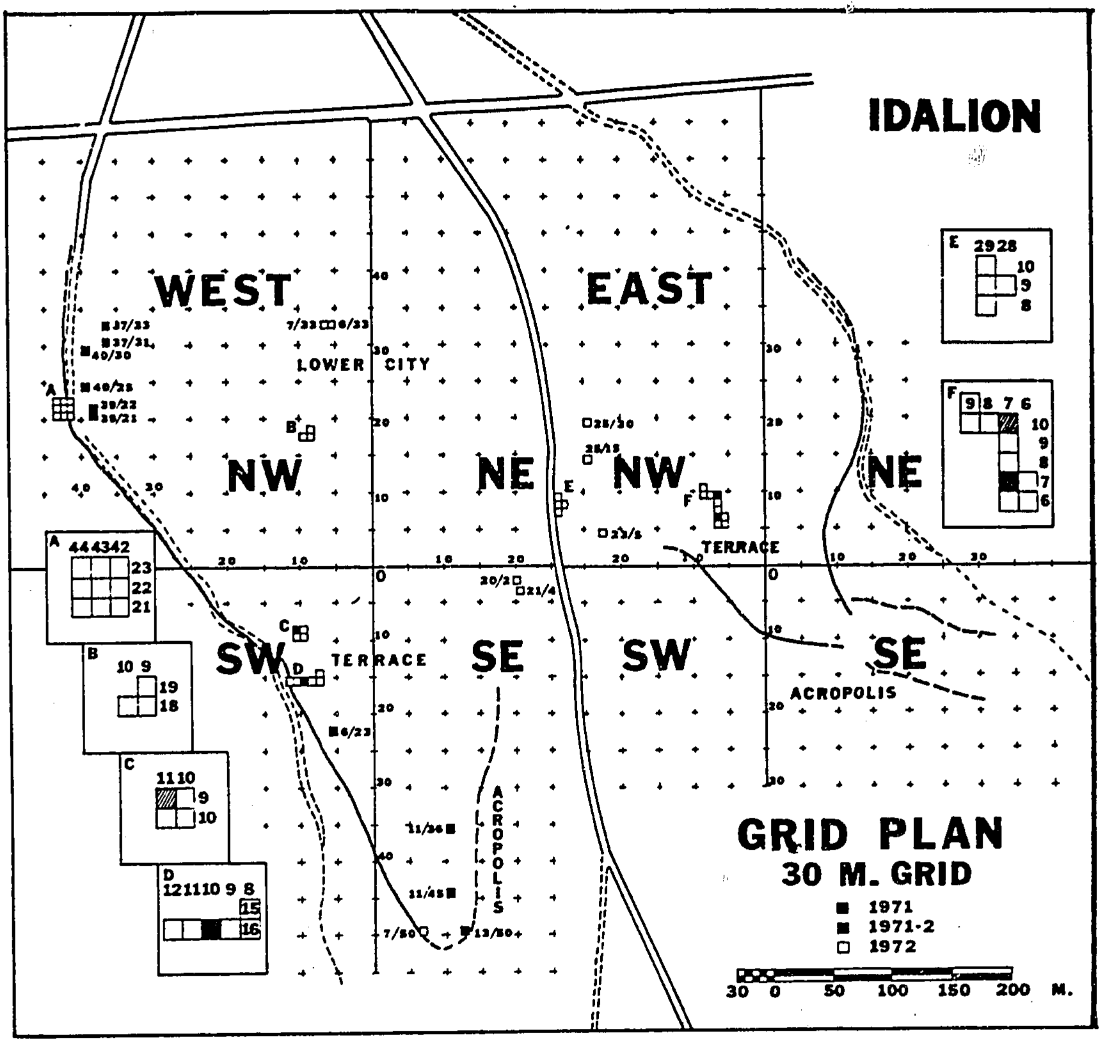

Figure A-6. Map of Idalion Excavation, and Grid Plan of the Lower City in Relation to the Two Acropolis (Stager et al, 1974). Sample location descriptions in Table A-4 are identified by grid. The West Terrace of the West Acropolis begins approximately at E-W line 7 south of zero. The East Terrace, which begins the East Acropolis, starts at the northern part of excavation Field F in E NW. E NW 23/5 and W SE 20/2 and 21/4, on the other hand, are near the southern part of the Lower City.

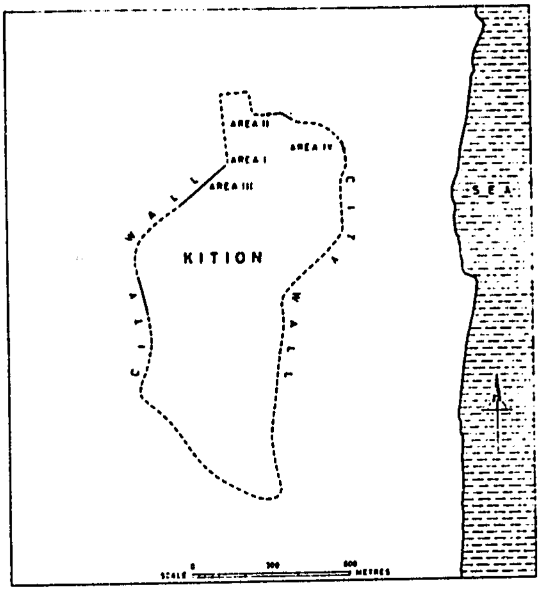

The site plan of Kition showing the city wall and the excavated Areas I—IV.

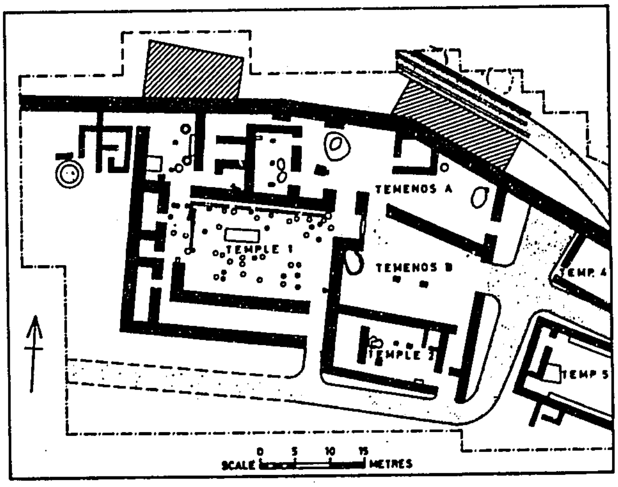

Plan II: Area II at floor III (ca.1200—ca.1150 B.C.).

Figure A-7. **Map of Kition. a) Schematic Sketch of Kition Site Showing the Locations of Excavated Areas I-IV. b) Floor Plan of Kition Area II at Floor III (Webb, 1977). Samples taken from Temple 1, Temple 2, Temenos B.**

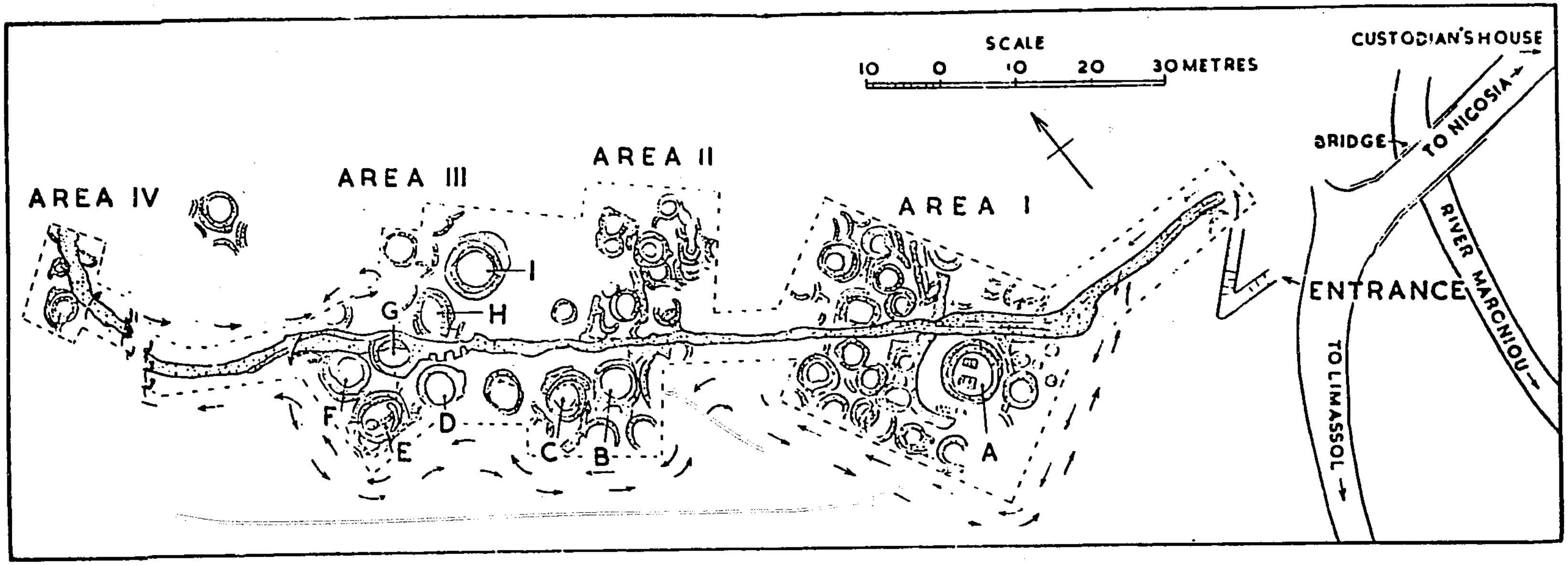

Figure A-8. Excavations at the Khirokitia Site (Antiquities Dept., The Republic of Cyprus, 1977). Samples were collected in Area I.

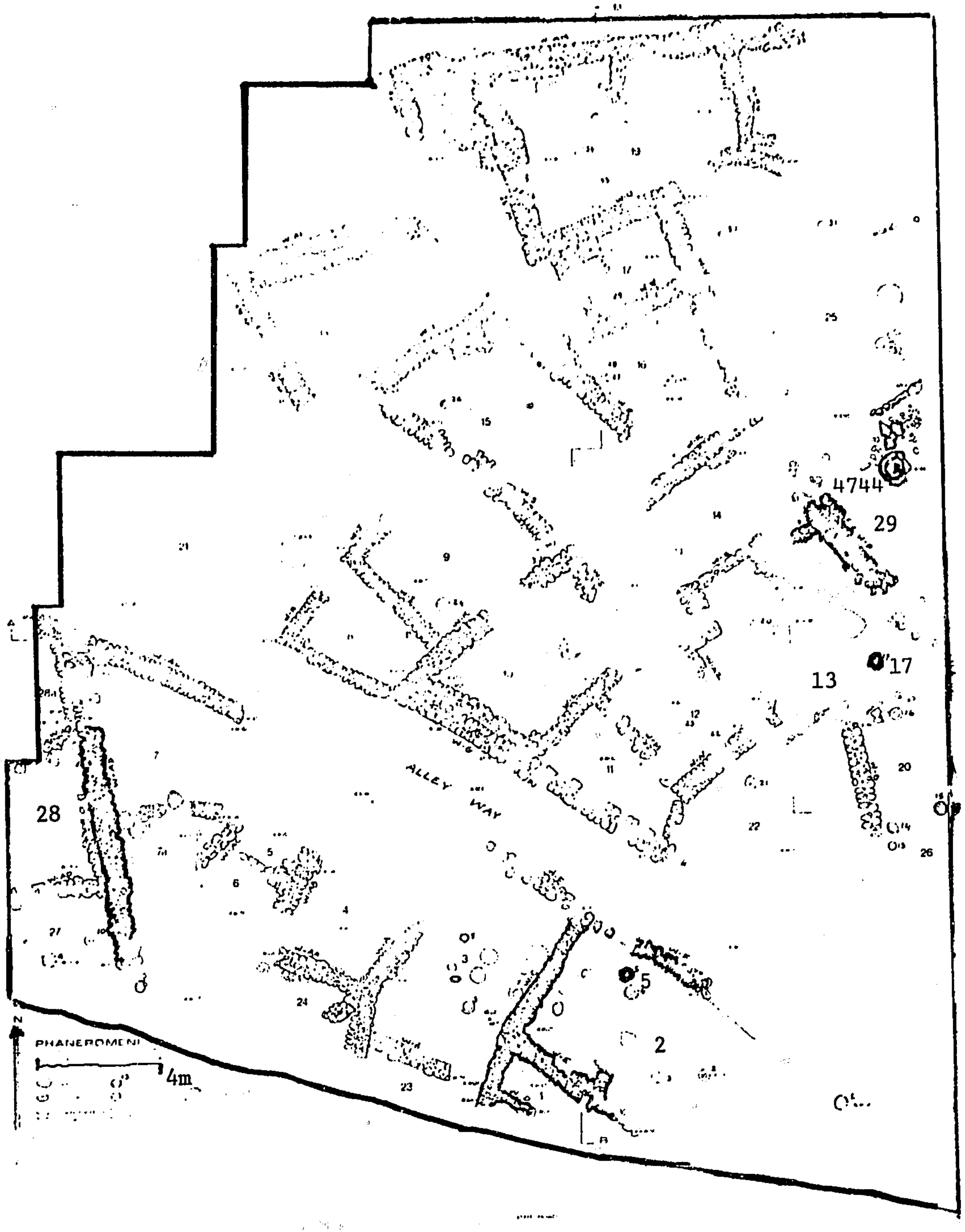

Figure A-9. Episcopi (Phaneromeni) Excavation Area A (Swiny, 1979). Rooms #2, #13, #28, and #29, and sample collection sites are highlighted.

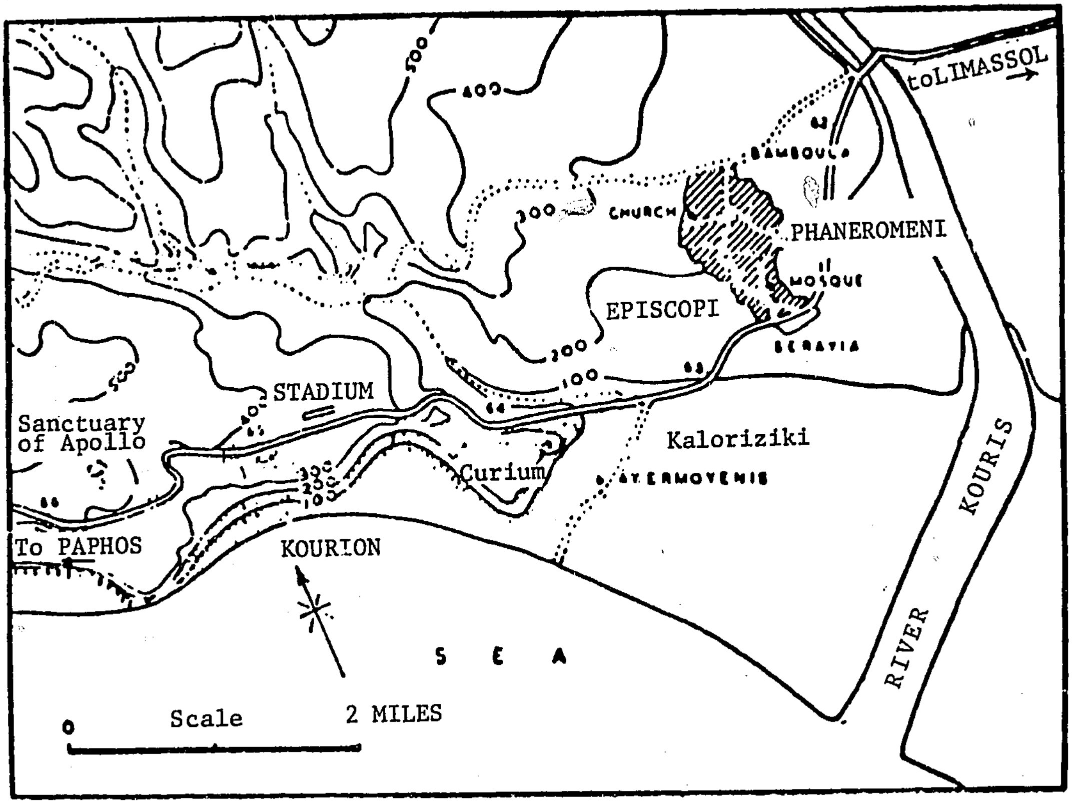

Figure A-10. Topographic Map of Kourion (Curium) Area (Antiquities Dept, The Republic of Cyprus, 1980).

APPENDIX B

Macroscopic Descriptions of Ancient Cementitious Materials

Table B-1. Macroscopic Descriptions of Ancient Plasters and Mortars From Greece.[*]

Sample No.	Matrix[†]	Aggregates	Miscellaneous
LVL01	crumbly, carbonated, pinkish gray (5 YR 8/1)	1. quartz sand <0.1 cm, subangular 2. black sand, earthy luster, rounded to subangular, <0.1 cm	~50g small broken frag.; outermost layer of a multilayer plaster; <0.2 cm thick.
LVL02 (layers 1 and 2)	m.coherent to coherent, carbonated, pale yellowish brown (10 YR 6/2) (may contain pozzolana)	1. quartz sand, rounded to subangular, <0.1 cm, ~40 2. black sand, <0.1 cm, rounded to subangular 3. carbonate frag., angular, up to 2 cm 4. metamorphic and volcanic (possibly slag) frag., subangular, <1 cm, <5% 5. chunks of massive v. pale yellowish orange material (10 YR 8/6), up to 1 cm, ~15% 6. chunks of carbonated lime, white, up to 2 cm, ~10% 7. may contain some v.fn.agg.fract.	several frag. up to 6x4x2 cm, total ~0.75 kg sample; Sample is composed of two layers of plaster; both layers were applied to an underlying flat surface, therefore each underlying plaster had a "finished" surface; upper layer ~0.4 cm thick, lower layer ~0.9 cm thick. No evidence of agg./matrix reaction; somewhat vitreous film surrounds some of the pale yellowish orange chunks. <0.25 mm thick.
LVL03 (layers 1 and 2)	coherent, carbonated, v. pale orange (10 YR 8/2)	1. quartz and black sand, <0.2 cm, ~60 to 70% 2. chunks of carbonated lime, up to 0.4 cm	10x6x1 cm (plus several smaller pieces); Sample is composed of a plaster which shows parting at the layer interface; upper layer is ~0.4 cm thick; lower layer is ~0.6 cm thick. No evidence of agg./matrix interaction. A layer <0.025 cm thick covers the entire surface. This may be a paint or it may be sec. min. It is vitreous and grayish.
LVL04	coherent, carbonated, v. pale orange (10 YR 8/2) (may contain pozzolana)	1. marble frag., angular to subrounded, up to 0.6 cm, ~30% 2. weathered and unweathered slag, black to reddish, subrounded, <0.5 cm, ~10% 3. quartz crystals <5% 4. white chunks of carbonated lime up to 0.75 cm 5. v.fn.agg.fract.	8x6x1.5 to 1.7 cm (plus several smaller pieces); Inner and outer surfaces of this plaster layer are relatively parallel which implies it was applied to a "finished" surface and its upper surface was also "finished."
LVL05	coherent, carbonated, v. pale orange (10 YR 8/2) to v. pale yellowish brown (10 YR 6/2) (may contain pozzolana)	1. quartzite and marble gravel, subangular, up to 1 cm, ~20% 2. slag (or gossan or pozzolan), up to 1 cm, ~15%, subangular 3. chunks of carbonated lime up to 3 cm, 10% 4. chunks of pale yellow massive phase up to 0.5 cm, ~25% 5. v.fn.agg.fract., <0.05 cm	8x6x5 cm (plus several smaller pieces, ~0.75 kg); Quartzite agg. often displays iron-stained surfaces; vitreous surface rims up to 1 mm thick surround yellow chunks; white and yellow chunks are relatively porous and often cellular.

Table B-1. Macroscopic Descriptions of Ancient Plasters and Mortars From Greece* (continued).

Sample	Matrix[†]	Aggregates	Miscellaneous
LVL06	sl. soft and crumbly to mod. coherent, carbonated, med. yellowish brown (10 YR 5/4) (may contain pozzolana or soil)	1. metamorphic gravel, well rounded, elongated (limonitic quartzite, limonitic gossan, marble, weathered chlorite-rich schist, quartzite), up to 1.5 cm 2. quartz and carbonate gr., <0.2 cm 3. fn.agg.frac.	12x10x6 cm (plus several smaller pieces, 1 kg; good agg. sorting; agg./matrix interfacial regions show no reaction rims; matrix may contain a significant amount of clay which would account for its tendency to crumble. Outer plaster surface is "finished"; bottom surface is irregular.
LVL07	unconsolidated soil, m. carbonated, mod. reddish orange (10 YR 6/6)	1. schist fragments, angular, up to ~3 cm	~0.7 kg soil and angular schist frag.; fn. grained, biotite- and mafic mineral-rich.
LVL08	coherent, carbonated, mod. yellowish brown (10 YR 5/4) (may contain pozzolana)	1. limonitic and non-limonitic quartzite, rounded to subrounded, <0.6 cm, ~60% 2. v.fn.agg. (may be soil) 3. quartz, feldspar and other crystals, <0.1 cm, <5%	6x4x1.5 cm (plus several smaller pieces); Agg./matrix interfacial regions show no reaction rims.
LVL09	coherent, carbonated, grayish orange (10 YR 7/4) (may contain pozzolana)	1. gravel (marble, limonitic quartzite breccia, quartzite, etc.), rounded, up to 1 cm, ~50% 2. quartz grains, rounded, up to 0.3 cm, <10% 3. terra-cotta frag., <1%, <0.5 cm, angular to rounded 4. v.fn.agg.fraction	5x5x2 cm (plus ~0.5 kg of smaller pieces); Agg. is poorly graded; agg./matrix interfacial regions show no reaction rims; sample is a plaster with outer surface "finished"; bottom surface irregular.
LVL10	coherent, carbonated, grayish orange (10 YR 7/4) to mod. yellowish brown (10 YR 5/4) (may contain pozzolana)	1. metamorphic gravel (quartzite, marble, limonitic quartzite, etc.), rounded, <1 cm, ~50% 2. limonitic gossan material, rounded, ≲0.5 cm, ≲10% 3. crystals, ≲0.2 cm, plagioclase, quartz, calcite, rounded ≲10% 4. v.fn. agg. fraction (probably gossan material)	10x6x3 cm (plus several smaller pieces); Exterior surface of this sample is coated with a thin, almost metallic, dusky brown (5 YR 2/2) substance; penetration of this substance into the sample is <1.5 mm. This may be a separate application of plaster or paint; Agg./matrix interfacial regions show no reaction rims.
LVL11 (layer 1)	coherent, carbonated, mod. yellowish brown (10 YR 5/4) (may contain pozzolana)	1. limonitic gossan, limonitic carbonate, and quartzite gravel, rounded to subangular, up to 1.5 cm, ≳70% 2. v. minor amount of sand 3. v.fn.agg. fraction (possibly soil)	10x5x1.5 (plus several smaller pieces); This is a plaster layer applied to a rough, unfinished surface; Agg./matrix interfacial regions show no reaction rims.

Table B-1. Macroscopic Descriptions of Ancient Plasters and Mortars From Greece* (continued).

Sample No.	Matrix[†]	Aggregates	Miscellaneous
LVL11 (layer 2)	coherent, brownish gray (5 YR 4/1)	1. same as layer 1	up to 0.3 cm thick; may be staining or separate application of plaster.
LVL12 (layer 1)	coherent, carbonated, pale yellowish brown (10 YR 6/2) (may contain pozzolana or soil)	1. metamorphic rock frag., mostly marble, limonitic gossan, limonitic marble, angular to subrounded, up to 0.3 cm, ≈60% 2. quartz sand 3. large chunks of carbonated lime up to 1 cm 4. v.fn.agg.fraction	20x11x3 cm and 28x15x3 cm pieces of plaster composed of two layers; layer 1 = bottom layer, contains voids up to 0.5 cm, no vug filling; Agg./matrix interfacial regions show no reaction rims. Layer 1 is ≈2 cm thick.
(layer 2)	coherent, carbonated, v. pale orange (10 YR 8/2) 30% sample vol. (may contain pozzolana or soil)	1. quartzite and metamorphic fragments <0.1 cm, angular, ≈70% 2. quartz crystals up to 1.5 cm, <10% 3. v.fn.agg.fract.	Layer 2 = top layer, ≈0.8 cm thick; very uniform and exterior surface is "finished." Interface between layers is relatively parallel to the exterior surface; bond between layers is weak and layers are easily broken apart; layer 2 shows no agg./matrix reaction rims.
LVL13	coherent, carbonated, med. reddish orange (10 YR 6/6) (may contain pozzolana)	1. limonitic gossan material, orangish to brownish, subangular, up to 0.5 cm, >50% 2. quartzite, limonitic quartzite and marble frag., rounded <0.5 cm, ≈15% 3. quartz crystals <0.3 cm, ≈10% 4. v.fn.agg.fract. (probably limonitic gossan material)	6x5x4 cm; Most of sample is a large marble agg. ≈5x5x2.5 cm; rock frag. plus quartz crystals ≈60% sample vol.; matrix contains v. fn. white speckling; no reaction rims between matrix and agg.
LVL14	coherent, carbonated	same as layers 2 and 3 of LVL15	7x3x1 cm (plus smaller pieces); layer 3 ≈0.2 cm; layer 2 ≈1 cm, same as layers 2 and 3 of LVL15.
LVL15 (layer 1)	coherent, carbonated, pinkish gray (5 YR 8/1) to v. pale orange (10 YR 8.2) (may contain a minor amount of pozzolana)	1. quartz, feldspar, fn. gr. dk. brown rounded crystals (may be sphalerite), calcite crystals, <0.5 cm, <10% 2. metamorphic rock frag. (marble pyritic chert, quartzite), angular to subangular, <0.8cm, ≈40-50% 3. chunks of carbonated lime, white, 0.2 cm - <0.05 cm 4. v. fn. orange speckles 5. may contain other v. fn. agg.	12x5x3 cm (composed of three layers). Layer 1 = bottom layer and is at least 3.5 cm thick; no agg./matrix reaction rims. Bottom surface of layer 1 is irregular, upper surface of layer 1 is parallel to exterior surface layer.

Table B-1. Macroscopic Descriptions of Ancient Plasters and Mortars From Greece* (continued).

Sample No.	Matrix[†]	Aggregates	Miscellaneous
LVL15 (layer 2)	coherent, carbonated, grayish pink (5 YR 8/2) to grayish orange pink (5 YR 7/2) (may contain pozzolana)	1. same as layer 1, except agg. size is <0.5 cm 2. more orange speckles	Layer 2 = middle layer and is 1.3 to 1.5 cm thick; upper and lower surfaces of layer 2 are parallel to the exterior surface; no parting at the layer interfaces; three-layer plaster forms a coherent unit. Some of the larger dk. brown vitreous metallic rounded agg. gr. show orange stained halos.
(layer 3)	coherent, carbonated, dk. yellowish brown (10 YR 4/2)	no agg.	Layer 3 = exterior layer and is ≳0.1 cm thick; there may have been an intermixing of layers 2 and 3 to a depth of 0.5 mm into layer 2 as evidenced by a color anomaly to this depth, or this may be an additional thin layer; exterior of layer 3 is covered with a coat of pine pitch up to 1 cm thick.
LVL16	coherent, carbonated, grayish orange (10 YR 7/4) (may contain pozzolana or soil)	1. limonitic gossan frag., limonitic breccia frag., marble, quartzite, angular to subangular up to 0.5 cm, ≳70% 2. quartz grain up to 0.2 cm, <5% 3. v.fn.agg. fraction (possibly soil)	17x10x3 cm; no agg./matrix reactions rims; angular agg. concentrated on bottom surface.
LVL17	coherent, carbonated, v. pale grayish orange (10 YR 7/4) (may contain pozzolana)	1. oxidized slag or limonitic gossan frag., orangish brown up to 0.5 cm, angular to rounded, 50% 2. fresh slag frag. vesicular, black, subangular, <0.5 cm, ≲10% 3. metamorphic frag. (including marble, quartzite, and limonitic carbonate and breccia) up to 0.5 cm 4. calcite and quartz crystals, <0.3 cm 5. v.fn.agg.fract. (probably gossan material)	12x8x2 cm (plus smaller pieces); Tendency for agg. to pluck out; no reaction rims on agg.; exterior surface is "finished"; bottom surface is irregular; agg. >70% total vol.
LVL18 (layer 1)	coherent, carbonated, grayish orange (10 YR 7/4) (may contain pozzolana)	1. quartzite and limonitic gossan gravel, rounded, ∿60% sample vol. 2. v.fn.agg.fract. 3. white chunks, <0.1 cm, ≲10%	2.5x2x1.5 cm (plus several smaller pieces); No agg./matrix interfacial reaction zones.

Table B-1. Macroscopic Descriptions of Ancient Plasters and Mortars From Greece* (continued).

Sample No.	Matrix[‡]	Aggregates	Miscellaneous
LVL18 (layer 2)	v. coherent, somewhat vitreous, dense, laminated sl. carbonated, pale red (10 R 6/2) to pinkish gray (5 YR 8/1)	no agg.	Exterior layer consists of at least 8 lamellae for a total thickness of ~2.5 mm
ADL01	coherent, mod. carbonated, lt. gray (N7) to pinkish gray (5 YR 8/1)	1. fn. basic igneous frag. (basalt), angular to rounded, 70% ≤0.1 cm, 10% ~0.1-0.5 cm 2. few quartz grains 3. v. fn agg.	13x8x5 cm (plus several smaller pieces);Abundant white linings in vugs and at agg./matrix interface.

---

*The Geological Society of America Rock Color Chart was used to designate colors as indicated by the symbol enclosed within parenthesis following each color description. The presence of carbonate phases was determined by effervescence upon contact with 5% HCl solution.

[†] Macroscopic descriptions were compiled from the samples as received. They do not take into account alteration of the samples as the result of further analyses.

[‡] The basis for describing some matrices as possibly containing pozzolana was that these matrices have textures and colors which suggest that they contain ultra-fine material similar to but finer grained than the very fine aggregate fraction (≲0.05 cm). Other coarser potentially reactive volcanic glassy fragments may have been defined as gossan.

Definition of terms: v = very; fn = fine; agg = aggregate; m = moderately; gr = grain; dk = dark; fract = fraction; frag = fragment; vol = volume.

Table B-2. Macroscopic Descriptions of Ancient Plasters and Mortars From Cyprus*†

Sample No.	Matrix	Aggregates	Miscellaneous
AML1 (layers 1 and 2)	coherent, carbonated, v. pale orange (10 YR 8/2) to lt. med. yellow (5 Y 7/6), mottled, contains discrete orangish and black speckling	1. basic volcanic rock (basalt) gravel, well rounded, up to 1 cm 2. lt.brown (5 YR 5/6), angular frag. and pale yellow brown (10 YR 6/2), angular frag. (may be terra-cotta) 3. quartz gr. <5% 4. carbonate frag.	13x12x7 cm; exterior surface is covered with a thin coating <0.5 mm thick; layer 1 (bottommost layer) less porous than upper layer (layer 2); no zoning or reaction rims in agg./matrix interfacial regions.
AML2 (plaster sealant)	coherent, carbonated, white (N9)	none	1-0.5 cm thick terra-cotta pipe joint caulking; sample is striated, which implies application of multiple lamallae.
AML3 (layer 1)	crumbly, chalky, carbonated, pale grayish orange (10 YR 7/4)	basaltic gravel, rounded, up to 2.5 cm	0.3 kg material in pieces up to 8x6x2 cm; layer 1 at least 2.5 cm thick; relatively porous.
(layer 2)	chalky to coherent, carbonated, v. pale orange (10 YR 8/2)	1. terra-cotta frag., angular, up to 0.5 cm, ≲20% 2. basaltic gravel, rounded 0.2 to 0.5 cm, ≳40%	layer 2, ≈2 cm thick; no agg./matrix reaction; relatively porous.
(layer 3)	mod. coherent, chalky, carbonated, v. pale orange (10 YR 8/2)	1. terra-cotta frag., angular, mostly 0.25 cm, up to 0.5 cm, ≳60% 2. v. fn. agg. fract.	layer 3, ≈5 cm thick; no agg./matrix reaction; contains charcoal up to 0.7 cm; relatively porous.
AML4	coherent, v. sl. carbonated, white (N9)	1. fn. agg. <5%, as orange and black speckles, <0.05 cm 2. chunks of coarse uncalcined/uncrushed gypsum, <15%	7x6x4 cm, 6x4x4 cm (plus several smaller pieces); low bulk density; somewhat crystalline in appearance.
EPL1	soft and crumbly, carbonated, v. pale yellowish orange (10 YR 8/6)	1. quartz sand and black sand, 0.1 - 0.05 cm, ≳60% 2. coarse agg.(carbonate)	≳400 gm of fragmented material.
EPL2	mod. crumbly, carbonated, v. pale orange (10 YR 8/2)	1. pale orange (10 YR 8/2), <0.1 cm to >1 cm, ≳70% sample, unidentified	9x6x3 (two pieces); matrix appears to consist of a large soil (clay) fract.
EPL3	crumbly, carbonated, grayish orange (10 YR 7/4)	same as EPL 2	6x6x3 cm; same as EPL 2
EPL4	mod. coherent to somewhat crumbly, carbonated, lt. brown	1. pale orange agg. (10 YR 8/2) up to 0.2 cm, subangular 2. pale yellowish brown agg. (10 YR 6/2), up to 0.5 cm	5x4x4 cm; matrix appears to consist of a large soil (clay) fract.; total agg. 70%.

Table B-2. Macroscopic Descriptions of Ancient Plasters and Mortars From Cyprus*† (continued).

Sample No.	Matrix	Aggregates	Miscellaneous
IDL1 (layers 1, 2, and 3)	coherent, carbonated, pale pinkish gray (5 YR 8/1)	1. basic volcanic rock frag. (basalt), up to 0.7 cm, well rounded, ≳10% 2. basic volcanic rock frag. ≲0.2 cm, rounded, ≳40% 3. quartz gr. <0.2 cm, subangular, ≳5% 4. v. small vitreous crystals, <0.1 cm, clear	12x8x6 cm three-layer plaster; Layer 1 (bottom) is ≳3 cm thick; layer 2 (middle) is ≳2 cm thick; layer 3 (top) is ≳1 cm thick; sample is relatively porous; exterior surface intermediate surfaces and bottom surface are all irregular; the layers may consequently be only the result of parting; no agg./matrix reaction features.
IDL2	coherent, v. sl. carbonated, yellowish gray (5 Y 8/1)	1. chunks of hydrated hemihydrate or uncalcined gypsum, up to 0.8 cm, <15% 2. carbonate agg., subangular, up to 1 cm	12x10x6 cm; med. density; contains large pores or air voids up to 1 cm, which suggests a low w/c; no agg./matrix interaction; no selenite crystals observed.
IDL3	coherent, v. sl. carbonated pinkish gray (5 YR 8/1)	1. chunks of hydrated hemihydrate or uncrushed gypsum, rounded to subangular, ≲30% 2. carbonate agg., <5%	10x10x5 cm; med. density; relatively porous.
KHL1	coherent, carbonated, yellowish gray (5 Y 7/2)	none	12x12x5; probably a rock; contains abundant fossils plus a few clastic gr.
KTL1	coherent, v.v.sl. carbonated, v. pale orange (10 YR 8/2)	1. few quartz gr., <5%	9x8x4 cm (plus one large piece of a rock composed of selenite crystals); This is a gypsum plaster over selenite; matrix contains abundant transparent vitreous crystals, ≲0.1 cm.
KTL2	crumbly, carbonated, v. pale orange (10 YR 8/2)	1. basaltic gravel, rounded, up to 1 cm, ≃60%	5x4x3 cm; no reaction between agg. and matrix.
KTL3	coherent, carbonated, med. yellowish brown (10 YR 5/4)	1. basaltic gravel, rounded, up to 0.5 cm, ≳25% 2. marble and quartz, rounded, up to 0.5 cm, ≳10% 3. quartz sand, ≳0.05 cm, up to 20%	≳0.5 kg of frag. up to 6x3x1 cm; Texture is grainy/sandy; carbonate is present in pores and fractures between agg. and matrix.
KTL4	coherent, weakly carbonated, v. pale orange (10 YR 8/2)	1. selenite crystals ≲20%, up to 2 mm 2. quartz sand, up to 2 mm	12x8x5 cm; pores up to 5 mm are common; patches of lime and gypsum up to 2 mm in dia. are common.
KUL1	coherent, carbonated, v. pale orance (10 YR 8/2)	1. basalt gravel, up to 5 mm, ≲50 % 2. volcanic sand, fn.gr., ≲10% 3. few quartzite frag., rounded	13x5x5 cm; no agg./matrix zoning observed; porous.

Table B-2. Macroscopic Descriptions of Ancient Plasters and Mortars From Cyprus*† (continued).

Sample No.	Matrix	Aggregates	Miscellaneous
KUL2 (layer 1)	coherent, carbonated, v. pale orange (10 YR 8/2)	1. basic volcanic frag., up to 0.6 cm, v. well rounded, <40% 2. basic volcanic sand, $\sim$0.1 - 1 mm, <20% 3. quartz sand, well rounded, <5% 4. carbonate frag., subangular, <5%	30x9x5 cm, 10x7x5 cm, and 12x5x5 cm pieces. Two-layer plaster; layer 1 (bottom layer) is 3.5 - 4 cm thick and the top surface is even and planar ("finished"); relatively porous and fractures are common; agg./matrix reactions were not observed.
KUL2 (layer 2)	v. coherent, m. carbonated, pale red (10 R 6/2)	1. fn. red agg., <0.1 mm, <40% 2. quartz and basic volcanic sand, <0.1 mm, <10%	layer 2 is $\gtrsim$0.5 cm thick, and has a "finished" exterior surface; the fn. red agg. may be crushed terra-cotta; fractures and extensive carbonation were not observed.
LML1	coherent, carbonated, lt. grayish orange (10 YR 7/4)	1. quartz sand, $\lesssim$0.1 cm, rounded, $\gtrsim$70% 2. carbonate rock frag., color and texture similar to matrix except where differential weathering has taken place	$\gtrsim$0.5 kg material as large as 5x3x1 cm; no agg./cement reaction.
LML2	coherent, carbonated, v.v. pale orange (10 YR 8/2)	1. no agg. in plaster sealant 2. terra-cotta pipe contains quartz crystals and sand <1 mm	3x2x1 cm; pipe sealant/terra-cotta contact is fractured; plaster sealant shows texture and striations which conform to the pipe surface

---

*The Geological Society of America Rock Color Chart was used to designate colors as indicated by the symbol enclosed within parentheses following each color description. The presence of carbonate phases was determined by effervescence upon contact with 5% HCl solution.

†Macroscopic descriptions were compiled from the samples as received. They do not take into account deterioration of the sample upon further analysis.

Terms defined as in Table B-1.

APPENDIX C

Microscopic Descriptions of Ancient Cementitious Materials

C

Table C-1. Microscopic Descriptions of Ancient Plasters and Mortars From Greece.

Sample No.	Matrix^{+}	Aggregates^{++}	Miscellaneous
LVL02	fn. gr.; lt. yel.-br. mottled to lt. orange-br. (calcite matrix)	1. quartz and feldspar sand gr., ≈40% of sample 2. quartzite and schist frag., <0.3 cm	matrix displays bf. typical of fn. gr. carbonate crystals; reaction zones between matrix and agg. were not observed
LVL03	fn. gr.; dk. red.-br. mottled to dk. br.-red.; diffuse to discrete patches of fn. gr. calcite	1. marble frag. 2. quartzite frag. and quartz gr., strained 3. fn. gr. schist frag.	same as above; patches of calcite display typical bf. and extinction and the crystals are sl. larger than those in the bulk matrix
LVL04	v. fn. gr.; lt. yel. to red.-yel.; diffuse to discrete patches throughout	1. schist frag. ≈40%, subangular 2. marble frag., ≈20%, subangular 3. calcite-rich schist frag., subangular	same as above; patchiness in matrix is caused by diffuse areas with sl. differences in gr. size; patches are occasionally rimmed with a dk. stain; some agg. are rimmed with med. gr. calcite which is probably filling pre-existing fractures
LVL05	v. fn. gr.; yel.-br. mottled to red.-br. to clear; patches of orange to br. material; subrounded up to 2 mm of an unidentified phase and corresponding to lt. yel. chunks (in hand specimen)	1. carbonate frag., fn. gr., red staining around selvages 2. schist frag. 3. few calcite crystals	same as above; matrix is characterized by extensive mottling in a rounded to subrounded pattern; few charcoal frag.
LVL06	v. fn. gr.; red.-br. to gray-br. to yel. to clear; v. mottled into rounded and irregular-shaped patches; rounded patches of v. fn. gr., gray, unidentified material	1. schist and quartzite up to 1 cm; rounded 2. marble, coarse gr.	mottling pattern suggests that the original plaster was composed of chunks of material and was v. inhomogeneous; many patches have dk. selvages; reaction zones between matrix and agg. were not observed; matrix displays bf. and extinction typical of fn. carbonate
LVL08	v. fn. gr.; dk. red.-br. to lt. br.-yel. to clear; v. mottled and patchy	1. schist and quartzite frag., rounded, ≈40% 2. fossiliferous mudstone frag. 3. fn. gr. limestone frag.; rounded 4. quartz gr. 5. v. fn. opaque grains	lighter areas in the matrix display typical calcite extinction and bf. and are coarser gr.; agg. selvages do not exhibit staining or reaction; this sample is characterized by ≈10% red opaque particles <0.4 mm and by red webbing in portions of the matrix
LVL09	v. fn. gr.; dk. red-br. to orange-br. to gray-br.; v. mottled; patches of unidentified material v. fn. gr., grayish, rounded	1. carbonate rock frag. containing coarse calcite and strained quartz gr., >90% slide 2. few small quartz gr.	chunks of unidentified material are characterized by extensive webbing and mottling (gray to red to yel.-br.); no reaction zones on agg. were observed
LVL10	v. fn. gr.; red-br. with dk. red-br. webbing and mottling; patches of yel.-br. fn. gr. crystals and rounded patches of a v. fn. gr. unidentified material	1. quartzite, med. gr. marble, and schist frag., well rounded 2. quartz and feldspar sand gr. and also small biotite and pyroxene crystals, ≈5-10% 3. opaque phases, ≈5%	some agg. are rimmed with calcite which probably filled pre-existing fractures; agg./matrix reaction zones were not observed

Table C-1. Microscopic Descriptions of Ancient Plasters and Mortars From Greece (continued).

Sample No.	Matrix†	Aggregates††	Miscellaneous
LVL11 (layer 1)	v. fn. gr.; lt. yel.-br. with rounded patches of dk. red-br. up to $\gtrsim$0.21 mm $\gtrsim$5% matrix; rounded patches of sl. coarser calcite	1. fossiliferous carbonate frag. 2. schist frag. containing strained quartz, mica, clays, m, carbonate angular 3. dk. red-br. opaque phase, $\lesssim$0.5%	same as above; overall patchy appearance due to inhomogeneity in comp. and gr. size; patches of unidentified fn. gr. material previously described
(layer 2)	v. fn. gr.; dk. red-br. mottled to v. dk.br. and orange-br.; abundant med. gr. calcite patches with diffuse to discrete boundaries and also abundant patches of the unidentified phase (fn. gr., gray) with discrete boundaries	1. same as above 2. dk. red-br. opaque phase, $\gtrsim$5-10%	same as above; this layer is characterized by numerous tension fractures perpendicular to the plaster surface. Randomly oriented fractures are filled with calcite; calcite also observed filling fractures around agg.
(Surface stain)	v. fn. gr.; v. dk. br. to black, opaque	none	thickness of this layer is $\gtrsim$4 mm although black staining does penetrate layer 2 to a depth of at least 0.5 mm
LVL12 (layer 1)	v. fn. gr.; red-br. mottled to dk. red-br. to lt. yel.-br.; patches of sl. coarser crystals display carbonate extinction and bf.; large rounded patches of the v. fn. gr. unidentified phase some of which show sl. darker rimming and discrete boundaries	1. quartz, plagioclase, feldspar, and pyroxene crystals 2. schist frag. 3. quartzite frag. 4. fn. to med. gr. carbonate frag.	this slide shows a gradation in the size and type of agg. perpendicular to the plane of the plaster surface; agg. fraction in the portion furthest from the surface is composed primarily of rock frag.; whereas, the overlying portion is composed primarily of quartz gr. and other crystals; there is no gradation or change in the matrix and hence an interface was not observed. This pseudolayering may be indicative of agg. settling.
(layer 2)	same as above	1. marble frag., med. gr. 2. schist frag. 3. quartzite frag. 4. red opaque frag., $\gtrsim$5% 5. charcoal frag.	
LVL13 (layer 1)	v. fn. gr.; dk. red to br.-red mottled to grayish-br.	1. marble frag., angular 2. quartz gr., angular 3. calcite crystals	surface onto which the exterior layer was applied was "finished" (flat and parallel to exterior surface); there is a thin zone at the interface between the two layers which may be due to intense carbonation
(layer 2)	same as above; rounded patches of v. fn. gr. unidentified material with discrete boundaries are common	1. marble, angular 2. schist, angular 3. iron stained quartz gr. and calcite crystals	
LVL155 (layer 1)	fn. gr.; yel.-br. to lt. red-br.; extensive mottling; diffuse patches of gray-br., $\lesssim$5%	1. marble frag., coarse gr. 2. carbonate breccia and skarn frag. 3. schist frag. containing biotite and hornblende 4: strained quartz gr.	areas containing sl. coarser crystals in the matrix display typical carbonate bf. and extinction; red-br. irregular patches are too fn. gr. and too opaque for optical measurements; in places contact between layers 1 and 2 is characterized by elongated dk. br. linear features up to 1 mm oriented parallel to the plane of the interface and are identical to the dk. webbing in layer 2

Table C-1. Microscopic Descriptions of Ancient Plasters and Mortars From Greece (continued).

Sample No.	Matrix[+]	Aggregates[++]	Miscellaneous
(Layer 2)	fn. gr.; yel.-br. to red-br.; diffuse irregular patches and webbing of gray-br. ≳20%; abundant red opaque particle, irregular shape, ≲10%	1. same as above 2. opaque particles (crystals) ≲2% 3. v. small calcite and quartz crystals	some areas are stained red (appear to be limonitic patches); matrix has a variety of textures; sl. coarser gr.; carbonate patches are common
(layer 3)	v. fn. gr.; v. dk. red-br.; uniform texture	1. quartz gr. <5%	interface between the thin exterior layer and the middle layer (2) is characterized by a v. fn. band of carbonate material up to ≳1.5 mm thick; under high mag. this zone is made up of a network of randomly oriented (in some places radiating) calcite crystals.
(pine pitch residue on surface)			There is a thin layer of carbonate crystals between the exterior surface of layer 3 and the pine pitch residue coating the surface; v. fn. gr. calcite is disseminated throughout the pine pitch residue which is basically amorphous, opaque, and appears to contain dk. br. webbing
LVL16	v. fn. gr.; lt. yel. mottled to gray-yel.; patches of sl. coarser gr. calcite up to ≳0.2 mm which display typical carbonate bf. and extinction; discrete, rounded, orange patches up to ≳0.2 mm	1. large calcite crystals up to 0.4 cm 2. marble frag., angular to subangular 3. feldspar and strained quartz crystals 4. quartzite frag. with abundant opaque minerals 5. siliceous gossan frag. v. fn. gr. calcite, fracture filling	same as above
LVL17	fn. gr.; lt. gray-yel. to dk gray-yel. to red-gray; mottled and patchy; fn. opaque grains ≳2-5%	1. marble frag., med. gr., subangular 2. schist frag., subangular to angular 3. quartzite frag.	matrix is relatively inhomogeneous but most of it displays carbonate optical properties; matrix contains distinct patches of med. gr. calcite ≳5% in addition to v. small quartz gr. and other crystals
LVL118 (layers 1 and 2)	v. fn. gr.; med. to lt. br. mottled to dk. gray-br.; patches of red opaque material, fn. gr. gray-br. material, and also sl. coarser gr. calcite with diffuse to discrete boundaries	1. quartzite, containing strained quartz gr., rounded 2. micaceous schist, rounded to subangular 3. strained quartz gr. and calcite crystals	exterior layer (2) consists of numerous (more than 10) lamellae which appear to be v. fn. gr. "growth lamallae" or consecutive alteration features; these lamallae do not appear to be the result of multiple applications of paint or plaster
ADL01	fn. gr.; lt. yel. to yel.-br.; carbonate bf. and extinction; ≲20% sample	1. limestone frag., fn. gr., fossiliferous and non-fossiliferous 2. sandstone 3. siltstone 4. weathered igneous frag. 5. anhydrite (fossiliferous)	this sample appears to be v. coherent and displays a dense microstructure

---

*Abbreviations are standard for petrographic descriptions.

[+] Except where indicated otherwise, the matrix fraction of these materials is composed of calcite plus other unidentified phases which are too fine-grained for optical property determinations.

[++] Aggregates are listed in decreasing order of relative abundance.

Table C-2. Microscopic Descriptions of Ancient Plasters and Mortars From Cyprus.

Sample No.	Matrix	Aggregates†	Miscellaneous
AML01 (layer 1)	fn. gr.; gray-yel. to clear; mottled with diffuse to distinct red patches (gray-yel. areas are v. fn. gr.) (calcite matrix)	1. basalt frag. containing plagioclase, olivine and pyroxene crystals, rounded with weathered surfaces 2. carbonate frag. containing foraminifera ± algal mats, rounded 3. carbonate frag., subangular to angular, iron stained 4. igneous frag., fn. gr., iron stained	calcite crystals and fracture fillings are common; matrix displays typical calcite extinction and bf.; foraminifera are present as fn. agg. throughout the matrix
AML02 (terra-cotta pipe)	v. fn. gr.; dk. red-orange	1. carbonate frag. containing foraminifera, rounded up to $\approx$2 mm 2. carbonate frag. containing algal mats, mottled and webbed dk. br., elongate angular to rounded 3. quartz, olivine, feldspar, biotite crystals up to $\approx$0.21 mm, $\approx$5%	fabric of the terra-cotta is aligned parallel to the form of the pipe; tension cracks are developed parallel to curved exterior surfaces of the pipe frag.
(pipe/plaster interfacial region)	color and gr. size are gradational between terra-cotta matrix and sealant matrix		interfacial zone is up to 0.42 mm and has a fabric parallel to the terra-cotta surface; this fabric is primarily due to secondary calcite stringers and fractures
(plaster joint sealant)	v. fn. gr.; clear to yel.; carbonate bf. (calcite matrix)	1. quartz gr. up to 0.21 mm 2. foraminifera up to 0.21 mm 3. biotite crystals up to 0.21 mm	thin stringers of calcite fill fractures; a salvage of alternating lt. yel. to dk. yel.-br. lamallae is present along the outer surface. Outer-most layer consists of tangled needles or fibers (biaxial neg., low bf. phase) $\approx$0.1 mm thick
AML03 (layer 1)	v. fn. gr.; lt. yel.-br. mottled to med. br. with red-br. patches (calcite matrix)	1. foraminifera; some are replaced by med. to coarse gr. calcite	areas containing fossils are surrounded by regions of a darker color but same texture as the matrix, selvages are distinct to diffuse; the nature of this "agg." is unusual and unresolved; the darker patches may be Ca_2SiO_4 "ghosts" or chunks of lime subsequently hydrated and recarbonated, or partially calcined limestone subsequently recarbonated. The central portions of many of these areas have been preferentially plucked out
AML03 (layer 2)	v. fn. gr.; br. yel. mottled to gray-yel.; carbonate bf.; diffuse red-orange stained patches (calcite matrix)	1. carbonate frag. foraminifera-rich ± algal mats, iron stained (dk. to med red) 2. qtz. gr. <5%	calcite fracture fillings and other areas of fn. to med. gr. calcite are possibly fossils or fossil frag.
AML04	v. fn. gr.; clear to lt. yel.; low bf. checkerboard texture in places (gypsum matrix)	1. selenite crystals $\lesssim$1 mm, $\lesssim$5%	v. small tabular equant, and/or needle-shaped crystals result in mosaic and checkerboard textures; this plus low bf. are indicative of a gypsum plaster/mortar

Table C-2. Microscopic Descriptions of Ancient Plasters and Mortars From Cyprus (continued).

Sample No.	Matrix	Aggregates†	Miscellaneous
EPL01	v. fn. gr.; orange br. to red-br. to br.; mottled and patchy; most patches have diffuse boundaries and matrix appears iron-stained; dk. carbonate bf. (calcite? matrix)	1. limestone frag. subrounded, coarser gr. than matrix 2. few calcite crystals up to 0.82 mm 3. basalt frag., subrounded, weathered, contain feldspar, olivine, pyroxene and biotite crystals 4. siltstone iron stained, fractured quartz crystals	this sample is unusual in that it is characterized by extensive patchiness; this texture suggests repeated dehydration and subsequent hydration
EPL02	v. fn. gr.; clear to yel. in places mottled to gray yel.; diffuse red-orange patches; carbonate bf.; in general matrix has a v. uniform texture and appearance (calcite groundmass)	1. fractured quartz gr. up to 0.21 mm 2. calcite crystals up to 0.1 mm 3. few foraminifera	total agg. $\lesssim$10% of sample; this sample is unusual for a man-made material; it is probably a carbonate rock or was prepared from unhydrated starting materials; there are no chunks of uncrushed lime, etc.
EPL03	same as above	1. calcite crystals med. to coarse gr., $\lesssim$5%	same as above; this sample appears v. porous
EPL04	fn. gr.; gray yel. mottled to gray orange; carbonate bf. and extinction (calcite groundmass)	1. quartz gr.; angular to subrounded, $\gtrsim$30-40% 2. feldspar, olivine, biotite, and hornblende crystals 3. basaltic rock frag. containing abundant opaque minerals 4. foraminifera fossils $\lesssim$10%	rounded, somewhat diffuse areas show low bf. and may be gypsum-rich; this is a v. unusual sample and may be a rock instead of man-made or it may have been prepared from uncalcined starting materials
IDL01 (layers 1 and 2)	v. fn. gr.; yel. mottled to red br.; rounded to subrounded discrete patches up to 0.3 mm of coarse calcite (could be foraminifera frag.) (calcite matrix)	1. volcanic rock frag. containing quartz, feldspar, biotite and opaque crystals; others containing olivine crystals 2. carbonate rock frag., foraminifera-rich and iron-stained	chunks of uncrushed lime subsequently hydrated and recarbonated, characterized by v. fn. gr., distinct boundaries and sl. darker than bulk matrix; calcined carbonate rocks must have been v. foraminifera-rich (based on abundant fossils disseminated throughout the matrix)
IDL02	fn. gr.; lt. yel.; v. low bf.; tabular mosaic and checkerboard-like texture; radiating needle bundles are common (gypsum matrix)	1. gypsum frag. up to 2 mm 2. limestone frag. containing foraminifera	tabular-shaped "pluck-outs" are common (selenite crystal "ghosts"); texture and low bf. are indicative of a gypsum plaster/mortar
IDL03	same as above	same as above	same as above
KHL01	med. to coarse gr.; calcite bf. (calcite groundmass)	1. limestone frag. containing foraminifera	this sample appears to be a limestone breccia rather than a man-made material; the relative age of this breccia must be younger than the foraminifera-rich aggregates
KTL01	fn. gr.; v. lt. br. to lt. br. yel.; sl. mottled; low to med. bf.; red staining and webbing in portions of the sample (gypsum matrix)	less than 1%	matrix resembles gypsum in bf. and texture; typical carbonate bf. and extinction are absent; mottling results from variations in gr. size; abundant tabular shaped "pluck-outs" are common

Table C-2. Microscopic Descriptions of Ancient Plasters and Mortars From Cyprus (continued).

Sample No.	Matrix	Aggregate[†]	Miscellaneous
KTL03	fn. gr. carbonate cement	1. basalt gravel, rounded, up to 1 cm 2. variety of fossils (primarily formanifera) 3. quartz sand and crystals	cistern lining; appears relatively porous in thin section
KTL04	v. fn. gr.; lt. br. mottled to yel.; low bf. sl. mottled; relatively uniform in texture (gypsum groundmass)	less than 1%	texture and low bf. are indicative of fn. gr. gypsum; crystals are equant to tabular; in places there are larger laths of selenite up to 1 mm, and lath-shaped "pluck-outs"
KUL01	v. fn. gr.; yel.-br. mottled to br. and gray-br.; diffuse to discrete patches of coarser gr. calcite (generally rounded) (calcite + gypsum matrix)	1. carbonate rock frag. containing abundant foraminifera and other fossils, rounded 2. basic volcanic rock frag., fn. gr., rounded, dk. weathered selvages 3. olivine, pyroxene, and biotite crystals	portions of the matrix appear granular because of the abundance of small equant crystals; this material has the appearance of being a mixture of hydrated gypsum and lime. The hydrated lime has subsequently been recarbonated
KUL02 (layers 1 and 2)	v. fn. gr.; dk. br. mottled to yel.-br. or red-br.; diffuse patches of m. br. color display calcite bf. and extinction and are sl. coarser gr. than surrounding material (calcite matrix)	1. basic igneous rock frag., rounded, dk. weathered selvages 2. carbonate rock frag., fossiliferous ± foraminifera ± algal mats ± quartz gr. and coarse gr. calcite, dk. selvages 3. sandstone frag. 4. shale frag. altered or weathered, red, rounded 5. chunks of uncrushed lime subsequently uncarbonated	aggregates appear to be separated from matrix due to shrinkage of the matrix material; coarse gr. calcite commonly fills fractures in matrix and around agg. Dark selvages around agg. do not appear to be the result of typical matrix-agg. reactions; small fossils, primarily foraminifera are incorporated in the matrix
LML01	fn. gr.; lt. br. mottled to lt. yel., carbonate extinction and b.f. (calcite groundmass)	1. carbonate rock frag. 2. quartz sand, <2%	carbonate rock, fossiliferous foraminifera, algal mats and balls, plus other microfossils
LML02	fn. gr.; lt. br. mottled to lt. yel. br.; diffuse iron-stained patches; texture is v. uniform (calcite groundmass)	1. quartz and feldspar gr. 5%	coarse gr. calcite makes up 2% of sample (could be fracture filling or fossil replacement); this may be a v. fn. gr. carbonate rock or a homogeneous, carbonated lime plaster with a striking absence of agg.

*Abbreviations are standard for petrographic descriptions.

[†] Aggregates are listed in order of decreasing relative abundance.

APPENDIX D

Typical X-ray Powder Diffraction Data for Matrix Fractions of Ancient Cementitious Materials

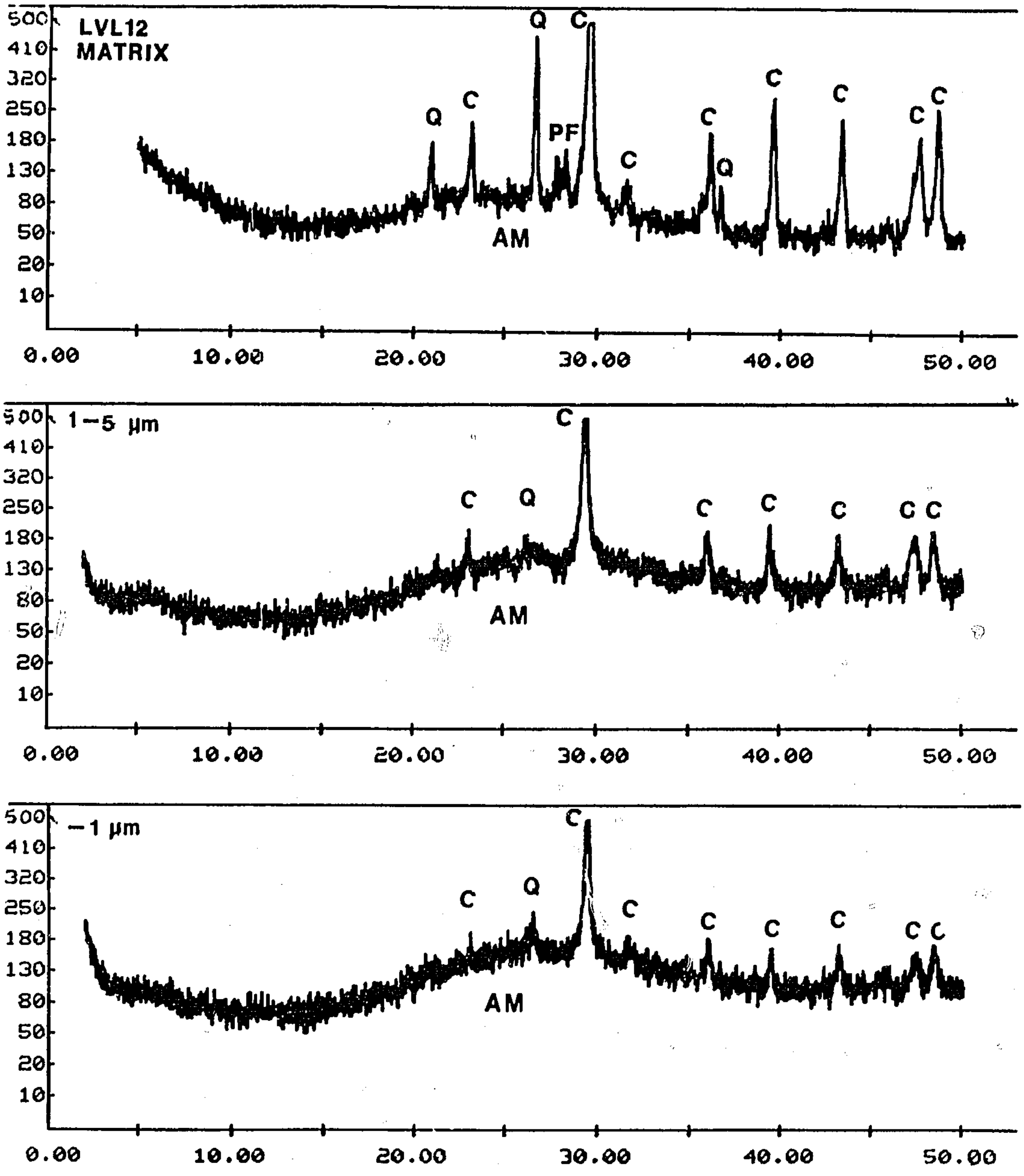

Figure D-1. X-Ray Diffraction Pattern of the Matrix Fraction of LVL12. [Top pattern was obtained by sieving and crushing (method A); middle pattern by settling 1-5 µm particles from suspension(method B); bottom pattern from -1 µm particles retained in suspension (method B).] AM = X-Ray Amorphous Material; C = Calcite; PF = Plagioclase Feldspar; Q = Quartz.

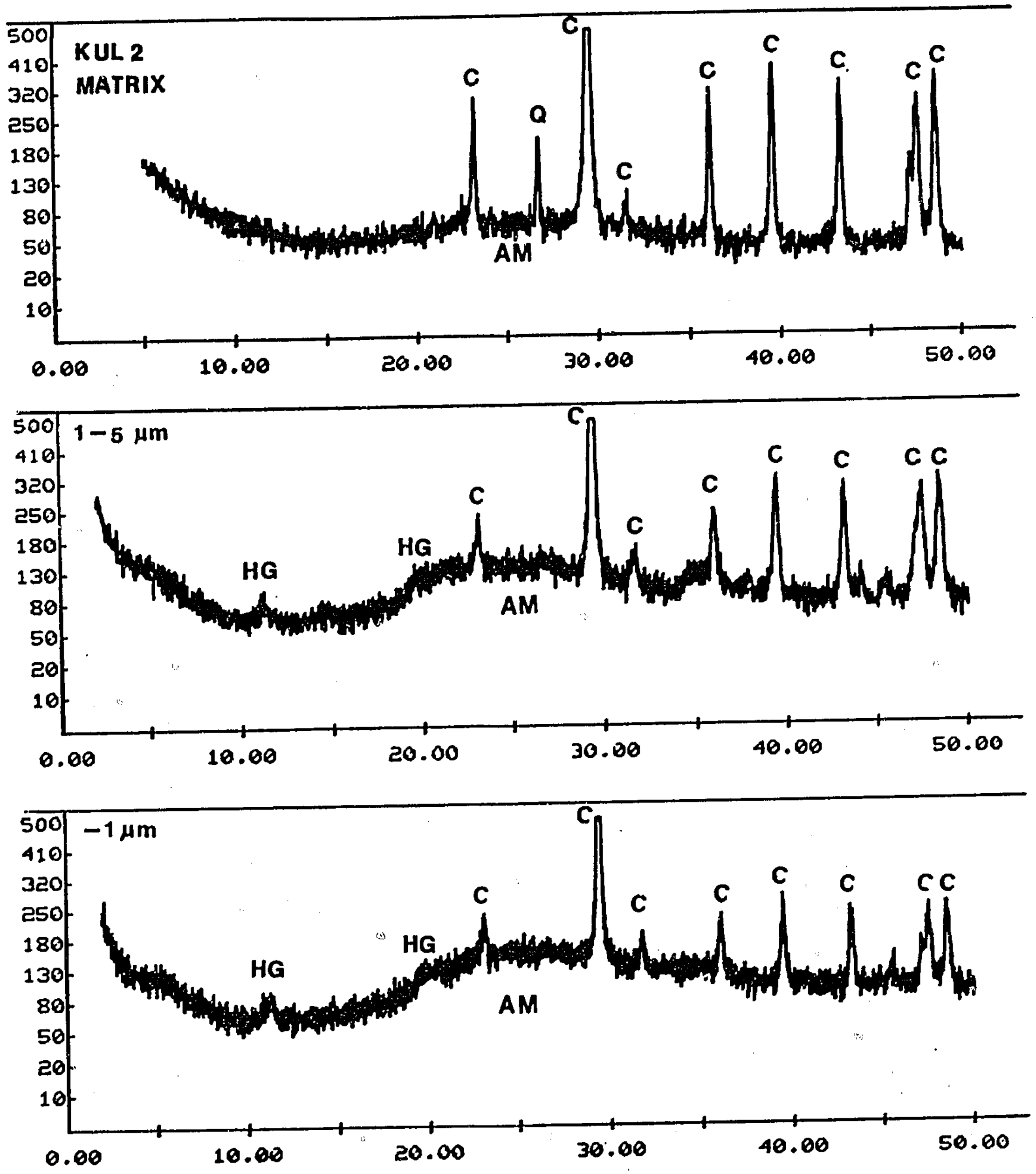

Figure D-2. X-Ray Diffraction Pattern of the Matrix Fraction of KUL2. [Top pattern was obtained by sieving and crushing (method A); middle pattern by settling 1-5 μm particles from suspension (method B); bottom pattern from -1 μm particles retained in suspension (method B).] AM = X-Ray Amorphous Material; C = Calcite; HG = Hydrogarnet; Q = Quartz.

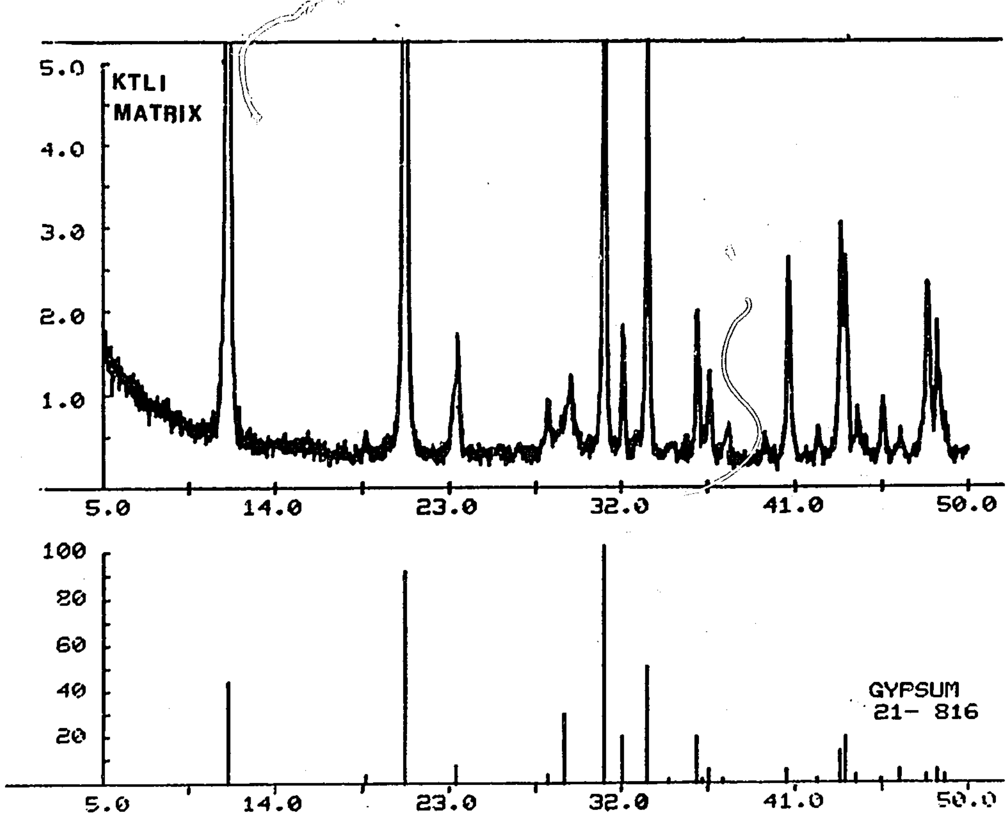

Figure D-3. X-Ray Diffraction Pattern of KTL1 Matrix. A Bar Diagram Illustrating the Position of the Gypsum Reflections is Shown (middle). C = Calcite.

APPENDIX E

Thermal Analysis Data

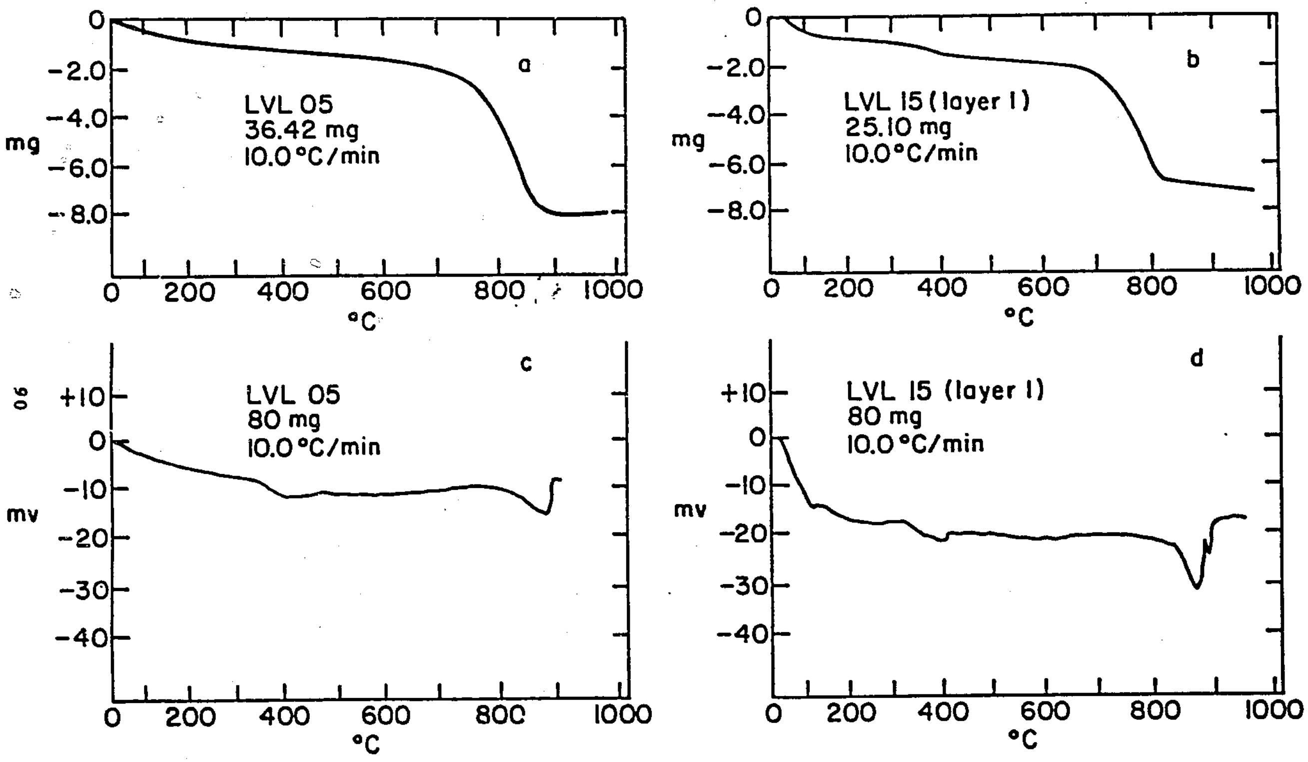

Figure E-1. TGA (a and b) and DTA (c and d) Data for LVL05 and LVL15, respectively.

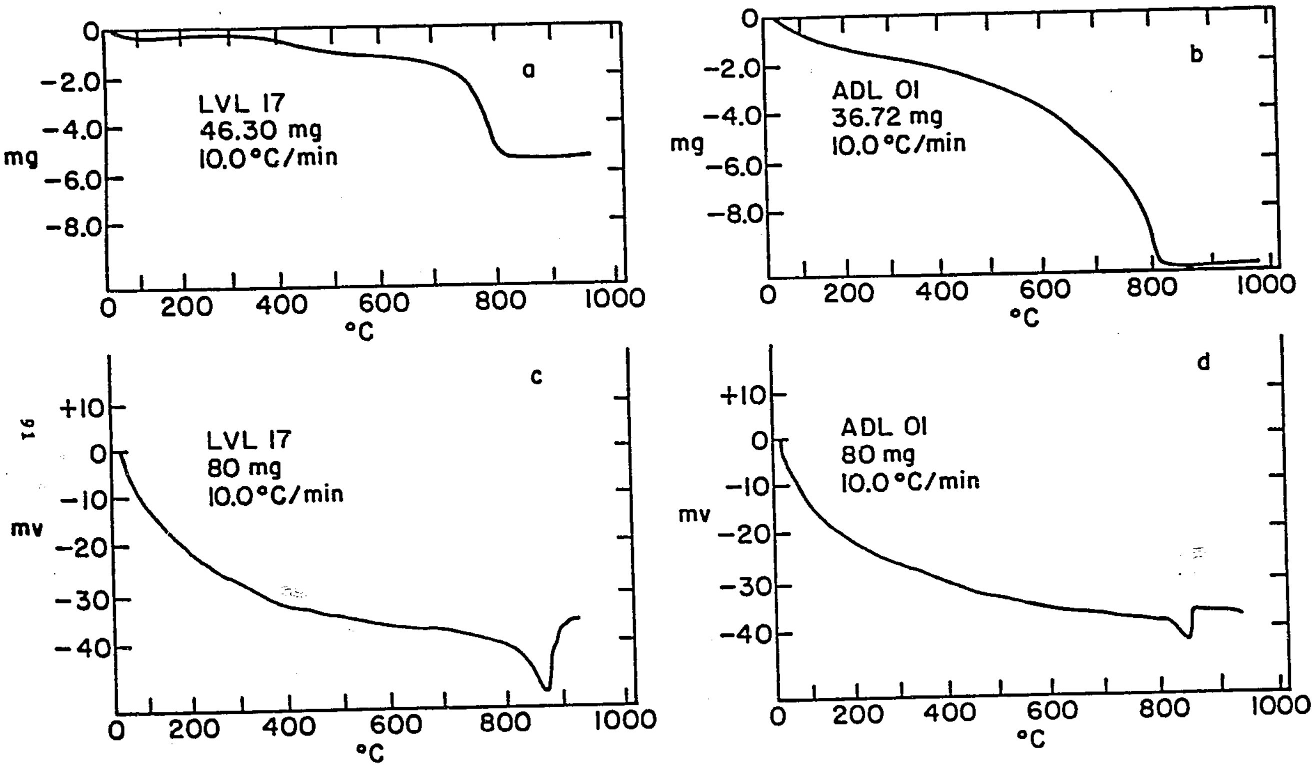

Figure E-2. **TGA (a and b) and DTA (c and d) Data for LVL17 and ADL01, respectively.**

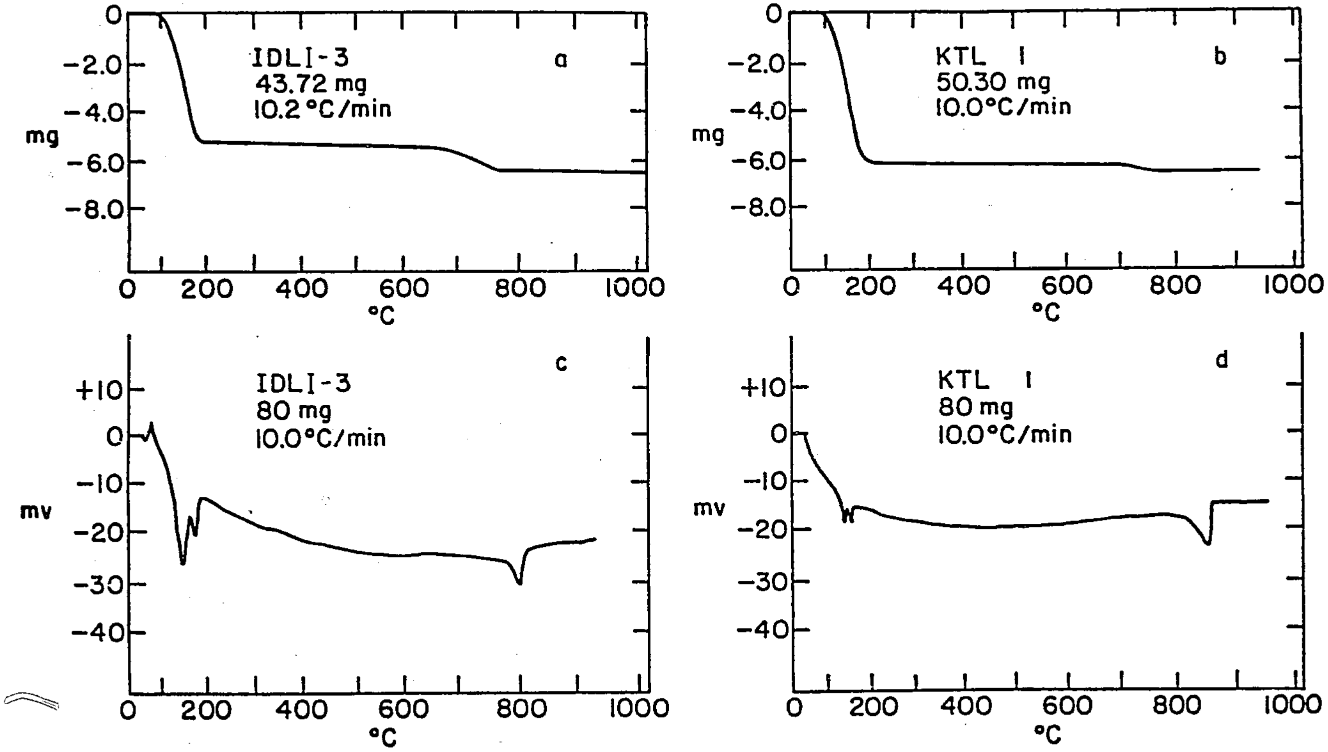

Figure E-3. **TGA (a and b) and DTA (c and d) Data for IDL1 (layer 3) and KTL1, respectively.**

LIST OF TABLES

DISTRIBUTION LIST

- **ACRES AMERICAN INC**
  - A. S. BURGESS
  - ROBERT H. CURTIS
  - R. STRUBLE
- **AGBABIAN ASSOCIATES**
  - CHRISTOPHER M. ST JOHN
- **AMARILLO PUBLIC LIBRARY**
- **AMERICAN EMBASSY - SWEDEN**
- **ANALYSIS AND TECHNOLOGY INC**
  - T. MAZOUR
- **APPLIED MECHANICS INC**
  - GRAHAM G. MUSTOE
- **ARGONNE NATIONAL LABORATORY**
  - DAVID F. FENSTER
  - WYMAN HARRISON
  - J. HOWARD KITTEL
  - MARTIN J. STEINDLER
- **ARINC RESEARCH CORP**
  - H. P. HIMPLER
- **ARKANSAS GEOLOGICAL COMMISSION**
  - NORMAN F. WILLIAMS
- **ARTHUR D. LITTLE INC**
  - AVIVA BRECHER
  - CHARLES R. HADLOCK
- **ATKINS RESEARCH & DEVELOPMENT - UNITED KINGDOM**
  - T. W. BROYD
- **ATOMIC ENERGY CONSULTANTS**
  - DONALD G. ANDERSON
- **ATOMIC ENERGY CONTROL BOARD - CANADA**
  - KEN SHULTZ
- **ATOMIC ENERGY OF CANADA LTD**
  - T. CHAN
  - ANN QUINN
  - F. P. SARGENT
- **BABCOCK & WILCOX**
  - INFORMATION SERVICES
- **BATTELLE COLUMBUS DIVISION**
  - JOHN T. MCGINNIS
  - STEPHEN NICOLOSI
- **BE INC**
  - K. J. ANDERSON
- **BECHTEL GROUP INC**
  - TOM S. BAER
  - DON B. CRANDALL
  - LESLIE J. JARDINE
  - R. C. LOVINGTON
  - N. A. NORMAN
  - RICHARD J. TOSETTI
- **BELGISCHE GEOLOGISCHE DIENST - BELGIUM**
  - NOEL VANDENBERGHE
- **BENDIX FIELD ENGINEERING CORP**
  - CHARLES A. JONES
  - DONALD LIVINGSTON
  - MICHAEL H. MOBLEY
  - JOHN C. PACER
- **BERKELEY GEOSCIENCES/HYDROTECHNIQUE ASSOCIATES**
  - BRIAN KANEHIRO
- **BILOXI PUBLIC LIBRARY**
- **BLACK & VEATCH**
  - M. JOHN ROBINSON
- **BRENK SYSTEMPLANUNG - W. GERMANY**
  - H. D. BRENK
- **BRIGHAM YOUNG UNIVERSITY**
  - HAROLD B. LEE LIBRARY
  - WILLIAM M. TIMMINS
- **BROOKHAVEN NATIONAL LABORATORY**
  - HELEN TODOSOW (2)
- **BUNDESANSTALT FUR GEOWISSENSCHAFTEN UND ROHSTOFFE - W. GERMANY**
  - MICHAEL LANGER
  - HELMUT VENZLAFF
- **BUNDESMINISTERIUM FUR FORSCHUNG UND TECHNOLOGIE - W. GERMANY**
  - ROLF-PETER RANDL
- **BUREAU DE RECHERCHES GEOLOGIQUES ET MINIERES - FRANCE**
  - BERNARD FEUGA
- **BUTTES GAS & OIL COMPANY**
  - ROBERT NORMAN
- **CALIFORNIA ASSEMBLY COMMITTEE ON NATURAL RESOURCES**
  - GENE VARANINI
- **CALIFORNIA DEPT OF CONSERVATION**
  - PERRY AMIMITO
- **CANYONLANDS NATIONAL PARK**
  - PETER L. PARRY
- **CAYUGA LAKE CONSERVATION ASSOCIATION INC**
  - D. S. KIEFER
- **CENTER FOR INTERDISCIPLINARY STUDIES**
  - DAVID M. ARMSTRONG
- **CENTRE D INFORMATIQUE GEOLOGIQUE - FRANCE**
  - GHISLAIN DEMARSILY
- **CITY OF MONTICELLO**
  - RICHARD TERRY
- **COLORADO OUTWARD BOUND SCHOOL**
  - DAVID L. BURGER
  - PETER ANTHONY ONEIL
- **COLORADO SCHOOL OF MINES**
  - W. HUSTRULID
- **COLUMBIA UNIVERSITY**
  - M. ASHRAF MAHTAB
- **CONROY ENGINEERING**
  - PETER CONROY
- **COPPE/UFRJ**
  - LUIZ OLIVEIRA
- **CORNELL UNIVERSITY**
  - ARTHUR L. BLOOM
  - FRED H. KULHAWY
- **CORTLAND COUNTY HEALTH DEPT**
  - J. V. FEUSS
- **DAMES & MOORE**
  - RON KEAR
  - JEFFREY KEATON
- **DAPPOLONIA CONSULTING ENGINEERS INC**
  - LISA K. DONOHUE
  - ABBY FORREST
  - AMINA HAMDY
  - PETER C. KELSALL
  - CARL E. SCHUBERT
- **DEAF SMITH COUNTY LIBRARY**
- **DELAWARE GEOLOGICAL SURVEY**
  - ROBERT R. JORDAN
- **DESERET NEWS**
  - GORDON WHITE
- **E.I. DU PONT DE NEMOURS & CO**
  - D. H. TURNO
- **E.L.H. PUBLICATIONS - THE RADIOACTIVE EXCHANGE**
  - HELMINSKI & WILKEN
- **E.R. JOHNSON ASSOCIATES INC**
  - E. R. JOHNSON
  - G. L. JOHNSON
- **EARTH SCIENCE AND ENGINEERING INC**
  - LOU BLANCK
- **EARTH SCIENCES CONSULTANTS INC**
  - HARRY L. CROUSE
- **EAST COMPANY INC**
  - RAYMOND PEREZ
- **EAST TENNESSEE STATE UNIVERSITY**
  - ALBERT F. IGLAR
  - VAY A. RODMAN
- **EBASCO SERVICES INC**
  - ZUBAIR SALEEM
  - RAYMOND H. SHUM
- **ECOLOGY & ENVIRONMENT INC**
  - MICHAEL BENNER
- **ECOLOGY CENTER OF LOUISIANA**
  - ROSS VINCENT
- **EDS NUCLEAR INC**
  - C. SUNDARARAJAN
- **EG & G IDAHO INC**
  - ROGER A. MAYES
  - ROBERT M. NEILSON, JR.
- **ELEKTRIZITAETS-GES. LAUFENBURG - SWITZERLAND**
  - H. N. PATAK
- **ELSAM - DENMARK**
  - A. V. JOSHI
  - ARNE PEDERSEN
- **ENERGY FUELS NUCLEAR**
  - GEORGE A. JONES
- **ENERGY FUELS NUCLEAR INC**
  - DON M. PILLMORE
- **ENERGY RESEARCH GROUP INC**
  - MARC GOLDSMITH
- **ENGINEERS INTERNATIONAL INC**
  - FRANCIS S. KENDORSKI
- **ENVIRONMENT CANADA**
  - CLAUDE BARRAUD
- **ENVIRONMENTAL POLICY INSTITUTE**
  - DAVID M. BERICK
- **ENVIROSPHERE COMPANY**
  - K. E. LIND-HOWE
- **EXXON NUCLEAR IDAHO COMPANY INC**
  - NATHAN A. CHIPMAN
  - ROGER N. HENRY
  - GARY WAYMIRE
- **FENIX & SCISSON INC**
  - JOSE A. MACHADO
  - CHARLENE U. SPARKMAN
- **FERRIS STATE COLLEGE**
  - MICHAEL E. ELLS
- **FLORIDA DEPT OF ENVIRONMENTAL REGULATION**
  - HAMILTON OVEN
- **FLORIDA INSTITUTE OF TECHNOLOGY**
  - JOSEPH A. ANGELO, JR.
- **FLORIDA POWER & LIGHT COMPANY**
  - JAMES R. TOMONTO
- **FLORIDA STATE UNIVERSITY**
  - JOSEPH F. DONOGHUE
- **FORD, BACON & DAVIS INC**
  - ROBERT D. BAIRD
  - DARRELL H. CARD
- **FOSTER-MILLER ASSOCIATES INC**
  - NORBERT PAAS
- **FOUNDATION SCIENCES INC**
  - LOU BATTAMS
- **FREIE UNIVERSITAET BERLIN**
  - HANSKARL BRUEHL
- **FRIENDS OF THE EARTH**
  - RENEE PARSONS
- **GABIE BETTS BURTON MEMORIAL LIBRARY**
- **GENERAL ATOMIC COMPANY**
  - MICHAEL STAMATELATOS
- **GENERAL COURT OF MASSACHUSETTS**
  - TIMOTHY J. BURKE
- **GEOLOGICAL SURVEY OF CANADA**
  - JEFFREY HUME

- **GEOLOGICAL SURVEY OF NORWAY**
  - SIGURD HUSEBY
- **GEORESULTS INC**
  - DAVID SNOW
- **GEORGIA INSTITUTE OF TECHNOLOGY**
  - ALFRED SCHNEIDER
  - CHARLES E. WEAVER
- **GEOSTOCK - FRANCE**
  - R. BARLIER
- **GEOTECHNICAL ENGINEERS INC**
  - RONALD C. HIRSCHFELD
- **GESELLSCHAFT F. STRAHLEN U. UMWELTFORSCHUNG M.B.H. - W. GERMANY**
  - WOLFGANG BODE
  - NORBERT FOCKWER
  - HANS W. LEVI
  - H. MOSER
- **GILBERT/COMMONWEALTH**
  - JERRY L. ELLIS
- **GOLDER ASSOCIATES**
  - MELISSA MATSON
  - J. W. VOSS
- **GOLDER ASSOCIATES - CANADA**
  - CLEMENT M. K. YUEN
- **GRAND COUNTY HIGH SCHOOL LIBRARY**
- **GRAND COUNTY PUBLIC LIBRARY**
- **GRIMCO**
  - DONALD H. KUPFER
- **GTC GEOLOGIC TESTING CONSULTANTS LTD - CANADA**
  - JOHN F. PICKENS
- **GULF INTERSTATE INC**
  - THOMAS J. HILL
- **H-TECH LABORATORIES INC**
  - BRUCE HARTENBAUM
- **HAHN-MEITNER-INSTITUT FUR KERNFORSCHUNG BERLIN**
  - KLAUS ECKART MAASS
- **HALEY AND ALDRICH INC**
  - JANICE HIGHT
- **HAMILTON COLLEGE**
  - DAVID K. SMITH
- **HANFORD ENGINEERING DEVELOPMENT LABORATORY**
  - ROBERT EINZIGER
  - W. E. ROAKE
- **HART-CROWSER AND ASSOCIATES**
  - MICHAEL BAILEY
- **HARVARD UNIVERSITY**
  - CHARLES W. BURNHAM
  - RAYMOND SIEVER
- **HATTIESBURG PUBLIC LIBRARY**
- **HIGH PLAINS UNDERGROUND WATER DISTRICT**
  - TROY SUBLETT
- **HIGH PLAINS WATER DISTRICT**
  - DON MCREYNOLDS
  - DON D. SMITH
- **HOUGH-NORWOOD HEALTH CARE CENTER**
  - GEORGE H. BROWN, M.D.
- **ILLINOIS STATE GEOLOGICAL SURVEY**
  - MORRIS W. LEIGHTON
- **IMPERIAL COLLEGE OF SCIENCE AND TECHNOLOGY - ENGLAND**
  - B. K. ATKINSON
- **INDIANA GEOLOGICAL SURVEY**
  - MAURICE BIGGS
- **INSTITUT FUR TIEFLAGERUNG - W. GERMANY**
  - WERNT BREWITZ
  - H. GIES
  - KLAUS KUHN
  - E. R. SOLTER
- **INSTITUTE OF GEOLOGICAL SCIENCES - ENGLAND**
  - STEPHEN THOMAS HORSEMAN
- **INTER/FACE ASSOCIATES INC**
  - RON GINGERICH
- **INTERA ENVIRONMENTAL CONSULTANTS INC**
  - F. J. PEARSON, JR.
  - LARRY RICKERTSEN
  - ROBERT WILEMS
- **INTERNATIONAL ENERGY ASSOCIATES LTD**
  - BLYTHE K. LYONS
- **INTERNATIONAL ENERGY SYSTEMS CORP**
  - JOHN A. BOWLES
- **INTERNATIONAL ENGINEERING COMPANY INC**
  - TERRY L. STEINBORN
  - MAX ZASLAWSKY
- **INTERNATIONAL RESEARCH AND EVALUATION**
  - R. DANFORD
- **INTERNATIONAL SALT COMPANY**
  - LEWIS P. BUSH
  - JOHN VOIGT
- **IOWA STATE UNIVERSITY**
  - BERNARD I. SPINRAD
- **IRAD-GAGE**
  - JAMES H. VEZINA
- **IRT CORP**
  - J. STOKES
- **ISMES - ITALY**
  - F. GERA
- **J.F.T. AGAPITO & ASSOCIATES INC**
  - MICHAEL P. HARDY
- **JACKSON STATE UNIVERSITY**
  - ESTUS SMITH
- **JACKSON-GEORGE REGIONAL LIBRARY**
- **JAY L. SMITH COMPANY INC**
  - JAY L. SMITH
- **JONES COUNTY JUNIOR COLLEGE LIBRARY**
- **KAISER ENGINEERS INC**
  - W. J. DODSON
  - H. L. JULIEN
- **KANSAS DEPT OF HEALTH AND ENVIRONMENT**
  - GERALD W. ALLEN
- **KARNBRANSLESAKERHET - SWEDEN**
  - LARS B. NILSSON
- **KELLER WREATH ASSOCIATES**
  - FRANK WREATH
- **KERNFORSCHUNGSZENTRUM KARLSRUHE GMBH - W. GERMANY**
  - K. D. CLOSS
  - R. KOESTER
- **KIHN ASSOCIATES**
  - HARRY KIHN
- **KLM ENGINEERING INC**
  - B. GEORGE KNIAZEWYCZ
- **KOREA INSTITUTE OF ENERGY AND RESOURCES (KIER)**
  - CHONG SU KIM
- **KUTA RADIO**
- **KYOTO UNIVERSITY - JAPAN**
  - YORITERU INOUE
- **LACHEL HANSEN & ASSOCIATES INC**
  - DOUGLAS E. HANSEN
- **LAKE SUPERIOR REGION RADIOACTIVE WASTE PROJECT**
  - C. DIXON
- **LAWRENCE BERKELEY LABORATORY**
  - JOHN A. APPS
  - EUGENE BINNALL
  - THOMAS DOE
  - M. S. KING
  - J. WANG
  - PAUL A. WITHERSPOON
- **LAWRENCE LIVERMORE NATIONAL LABORATORY**
  - DAE H. CHUNG
  - EDNA M. DIDWELL
  - HUGH HEARD
  - FRANCOIS E. HEUZE
  - LAWRENCE D. RAMSPOTT (2)
  - W. G. SUTCLIFFE
  - TECHNICAL INFORMATION DEPARTMENT L-53
  - JESSE L. YOW, JR.
- **LEHIGH UNIVERSITY**
  - D. R. SIMPSON
- **LOS ALAMOS NATIONAL LABORATORY**
  - P. L. BUSSOLINI
  - WAYNE R. HANSEN
  - W. C. MYERS
- **LOS ALAMOS TECHNICAL ASSOCIATES INC**
  - R. J. KINGSBURY
- **LOUISIANA DEPT OF NATURAL RESOURCES**
  - B. JIM PORTER
- **LOUISIANA DEPT OF TRANSPORTATION & DEVELOPMENT**
  - GEORGE H. CRAMER, II
- **LOUISIANA GEOLOGICAL SURVEY**
  - RENWICK DEVILLE
- **LOUISIANA NUCLEAR ENERGY DIVISION**
  - L. HALL BOHLINGER (3)
- **LOUISIANA TECH UNIVERSITY**
  - LIBRARY
- **LOUISIANA TECHNICAL UNIVERSITY**
  - R. H. THOMPSON
- **LUBBOCK COUNTY SOIL AND WATER CONSERVATION DISTRICT**
  - DON LANGSTON
- **M.J. OCONNOR & ASSOCIATES LTD**
  - M. J. OCONNOR
- **MARYLAND DEPT OF HEALTH & MENTAL HYGIENE**
  - MAX EISENBERG
- **MASSACHUSETTS DEPT OF ENVIRONMENTAL QUALITY ENGINEERING**
  - JOSEPH A. SINNOTT
- **MASSACHUSETTS INSTITUTE OF TECHNOLOGY**
  - RICHARD K. LESTER
  - MARSHA LEVINE
- **MATERIALS RESEARCH LABORATORY LTD - CANADA**
  - S. SINGH
- **MCDERMOTT INTERNATIONAL**
  - KAREN L. FURLOW
- **MCMASTER UNIVERSITY - CANADA**
  - L. W. SHEMILT
- **MELLEN GEOLOGICAL ASSOCIATES INC**
  - FREDERIC F. MELLEN
- **MEMBERS OF THE GENERAL PUBLIC**
  - L. ROBERT ANDERSON
  - KURT BALLING
  - BRET BLOSSER
  - JAMES BOYD
  - THOMAS G. BRADFORD
  - ROGER H. BROOKS
  - HAZEL CHAPMAN, PH.D.
  - LAWRENCE CHASE, PH.D.
  - TOM & SUSAN CLAWSON
  - STEVE CONEWAY
  - M. VAL DALTON
  - KENNETH & ALICE M. DROGIN
  - ROBERT DUDEK
  - CHARLES S. DUNN
  - JEAN EARDLEY
  - THAUMAS P. EHR

BOB GAMMELIN
CARL A. GIESE
SHIRLEY M. GIFFORD
MICHAEL J. GILBERT
STEVE & SUE GILSDORF
JUDY C. GOETTE
HARRY D. GOODE
OSWALD H. GREAGER
DOUGLAS H. GREENLEE
KENNETH GUSCOTT
ROBERT HIGGINS
DAVID W. JOHNSON
KENNETH S. JOHNSON
CRAIG W. JONES
JOSEPH KEYSER
SCOTT KRAMER
W. D. MCDOUGALD
MAX MCDOWELL
JEFF MEADOWS
A. ALAN MOGHISSI
BARBARA MORRA
THEA NORDLING
CAROLINE PETTI
SHAILER S. PHILBRICK
MARTIN RATHKE
TOM & MARY REES
BRUCE F. RUEGER
PETER J. SABATINI, JR.
JOANNE SAVOIE
OWEN SEVERANCE
PATRICIA SNYDER
P. E. STRALEY-GREGA
MARGUERITE SWEENEY
GARY WAGNER
BILL WALSH
MARTIN & ELAINE WALTER
JIMMY L. WHITE
LINDA WITTKOPF
MICHAEL BAKER, JR. INC
C. J. TOUHILL
MICHIGAN DEPT OF NATURAL RESOURCES
R. THOMAS SEGALL
MICHIGAN DEPT OF PUBLIC HEALTH
GEORGE W. BRUCHMANN
LEE E. JAGER
MICHIGAN ENVIRONMENTAL PROTECTION COMMITTEE
DAVE CHAPMAN
MICHIGAN STATE UNIVERSITY
WILLIAM C. TAYLOR
MICHIGAN TECHNICAL UNIVERSITY
DAE S. YOUNG
MINNESOTA ENVIRONMENTAL QUALITY BOARD
RICHARD PATON
MINNESOTA GEOLOGICAL SURVEY
LINDA L. LEHMAN
MATT S. WALTON
MINNESOTA STATE ENERGY AGENCY
MISSISSIPPI ATTORNEY GENERALS OFFICE
MACK CAMERON
MISSISSIPPI BUREAU OF GEOLOGY
MICHAEL B. E. BOGRAD
MISSISSIPPI CITIZENS AGAINST NUCLEAR DISPOSAL
STANLEY DEAN FLINT
MISSISSIPPI DEPT OF ENERGY AND TRANSPORTATION
RONALD J. FORSYTHE
MISSISSIPPI DEPT OF NATURAL RESOURCES
ALVIN R. BICKER, JR.
CHARLES L. BLALOCK
CURTIS W. STOVER
MISSISSIPPI EMERGENCY MANAGEMENT AGENCY
JAMES E. MAHER
MISSISSIPPI LIBRARY COMMISSION
SARA TUBB
MISSISSIPPI POWER & LIGHT
ROBERT SHADDIX
MISSISSIPPI STATE BOARD OF HEALTH
EDDIE S. FUENTE
GUY R. WILSON
MISSISSIPPI STATE UNIVERSITY
TROY J. LASWELL
VICTOR L. ZITTA
MITRE CORP
LESTER A. ETTLINGER
MITSUBISHI METAL CORP
TATSUO ARIMA
MOAB NUCLEAR WASTE INFORMATION OFFICE
MICHAELENE PENDLETON (2)
MONTANA BUREAU OF MINES AND GEOLOGY
EDWARD C. BINGLER
MONTICELLO HIGH SCHOOL LIBRARY
MEDIA CENTER
MONTICELLO NUCLEAR WASTE INFORMATION OFFICE
CARL EISEMANN (2)
MORRISON-KNUDSEN COMPANY INC
SERGI KAMINSKY
NATIONAL ACADEMY OF SCIENCES
JOHN T. HOLLOWAY
NATIONAL AERONAUTICS AND SPACE ADMINISTRATION
MICHAEL ZOLENSKY
NATIONAL BUREAU OF STANDARDS
RILEY M. CHUNG
NATIONAL HYDROLOGY RESEARCH INSTITUTE - CANADA
DENNIS J. BOTTOMLEY
NATIONAL PARK SERVICE
CECIL D. LEWIS, JR.
NATIONAL PARKS & CONSERVATION ASSOCIATION
T. DESTRY JARVIS
TERRI MARTIN
NATIONAL SCIENCE FOUNDATION
ROYAL E. ROSTENBACH
NAVAL WEAPONS STATION EARLE
GENNARO MELLIS
NEW ENGLAND NUCLEAR CORP
KERRY BENNERT
NEW JERSEY INSTITUTE OF TECHNOLOGY
BEN STEVENSON
NEW MEXICO BUREAU OF MINES AND MINERAL RESOURCES
FRANK E. KOTTLOWSKI
NEW MEXICO ENVIRONMENTAL EVALUATION GROUP
ROBERT H. NEILL
NEW YORK DEPT OF HEALTH
DAVID AXELROD, M.D.
NEW YORK ENERGY RESEARCH & DEVELOPMENT AUTHORITY
JOHN P. SPATH (8)
NEW YORK GEOLOGICAL SURVEY
ROBERT H. FAKUNDINY
NEW YORK LEGISLATIVE COMMISSION ON SCIENCE & TECHNOLOGY
JAMES T. MCFARLAND
NEW YORK STATE ENERGY RESEARCH AND DEVELOPMENT AUTHORITY
JOHN C. DEMPSEY
NEW YORK STATE PUBLIC SERVICE COMMISSION
FRED HAAG
NORTH CAROLINA STATE UNIVERSITY
M. KIMBERLEY
NORTHEAST UTILITIES SERVICE COMPANY
PATRICIA ANN OCONNELL
NORTHWESTERN UNIVERSITY
BERNARD J. WOOD
NTR GOVERNMENT SERVICES
THOMAS V. REYNOLDS
NUCLEAR ENERGY AGENCY/OECD - FRANCE
ANTHONY MULLER
NUCLEAR SAFETY RESEARCH ASSOCIATION
IZUMI KURIHARA
NUCLEAR WASTE WATCHERS
HELEN LETARTE
NUS CORP
W. G. BELTER
N. BARRIE MCLEOD
YONG M. PARK
NUTECH ENGINEERS INC
GARRISON KOST
OAK RIDGE NATIONAL LABORATORY
J. O. BLOMEKE
H. C. CLAIBORNE
ALLEN G. CROFF
LESLIE R. DOLE
CATHY S. FORE
DAVID C. KOCHER
ELLEN D. SMITH
ONTARIO HYDRO - CANADA
R. W. BARNES
K. A. CORNELL
C. F. LEE
ONTARIO MINISTRY OF THE ENVIRONMENT - CANADA
JAAK VIIRLAND
ONTARIO RESEARCH FOUNDATION - CANADA
LYDIA M. LUCKEVICH
OTHA INC
JOSEPH A. LIEBERMAN
P.O.W.E.R.
RALPH DILLER
TIM REVELL
PACIFIC GAS AND ELECTRIC COMPANY
ADRIAN C. SMITH, JR.
PACIFIC NORTHWEST LABORATORY
DON J. BRADLEY
L. L. CLARK
FLOYD N. HODGES
J. H. JARRETT
J. E. MENDEL
J. M. RUSIN
PARSONS BRINCKERHOFF QUADE & DOUGLAS INC
T. R. KUESEL
ROBERT PRIETO
MARK E. STEINER
PARSONS-REDPATH
BRUNO LORAN
GLEN A. STAFFORD
PB-KBB INC
JUDITH G. HACKNEY

PENBERTHY ELECTROMELT INTERNATIONAL INC
LARRY PENBERTHY
PENNSYLVANIA STATE UNIVERSITY
MICHAEL GRUTZECK
DELLA M. ROY
PERMIAN BASIN REGIONAL PLANNING COMMISSION
E. W. CRAWFORD
PERRY COUNTY CITIZENS AGAINST NUCLEAR WASTE DISPOSAL
MRS. DURLEY HANSON
WARREN STRICKLAND
PETTIS WALLEY
PHILADELPHIA ELECTRIC COMPANY
JOHN J. TUCKER
PHYSIKALISCH-TECHNISCHE BUNDESANSTALT - W. GERMANY
PETER BRENNECKE
HORST SCHNEIDER
PINE FOREST REGIONAL LIBRARY
POINT BEACH NUCLEAR PLANT
JAMES J. ZACH
POTASH CORP OF SASKATCHEWAN MINING LTD - CANADA
PARVIZ MOTTAHED
PRESQUE ISLE COURTHOUSE
PSE & G
JOHN J. MOLNER
PUBLIC SERVICE INDIANA
ROBERT S. WEGENG
PURDUE UNIVERSITY
PAUL S. LYKOUDIS
RALPH M. PARSONS COMPANY
JERROLD A. HAGEL
RANDALL COUNTY LIBRARY
RE/SPEC INC
GARY D. CALLAHAN
PAUL F. GNIRK
WILLIAM C. MCCLAIN
RED ROCK 4-WHEELERS
GEORGE SCHULTZ
RENSSELAER POLYTECHNIC INSTITUTE
BRIAN BAYLY
RHOADS MEMORIAL LIBRARY
RHODE ISLAND GOVERNORS ENERGY OFFICE
BRUCE VILD
RHODE ISLAND GOVERNORS OFFICE
JOHN A. IVEY
RIO ALGOM CORP
DUANE MATLOCK
ROCKWELL HANFORD OPERATIONS
JAMES L. ASH
HARRY BABAD
R. J. GIMERA
KUNSOO KIM
KARL M. LA RUE
MICHAEL J. SMITH
DAVID L. SOUTH
RICHARD T. WILDE
ROCKWELL INTERNATIONAL ENERGY SYSTEMS GROUP
ROGERS & ASSOCIATES ENGINEERING CORP
ARTHUR SUTHERLAND
ROGERS, GOLDEN & HALPERN
JACK A. HALPERN
ROY F. WESTON INC
WILLIAM IVES
RONALD MACDONALD
JILL RUSPI
ROBERT SCHULER
HARRY W. SMEDES
DOUGLAS W. TONKAY
LAWRENCE A. WHITE
RPC INC
JAMES VANCE
S.E. LOGAN & ASSOCIATES INC
STANLEY E. LOGAN
SALT LAKE CITY PUBLIC LIBRARY
SALT LAKE CITY TRIBUNE
JIM WOOLF
SALT LAKE COUNTY LIBRARY SYSTEM
WHITMORE LIBRARY
SAN DIEGO GAS & ELECTRIC COMPANY
LOUIS BERNATH
SAN JOSE STATE UNIVERSITY SCHOOL OF ENGINEERING
R. N. ANDERSON
SAN JUAN COUNTY COMMISSIONER
ROBERT LOW
SAN JUAN RECORD
DEBORAH A. MARCUS
JOYCE MARTIN
SANDIA NATIONAL LABORATORIES
KEN BEALL
MARGARET S. CHU
JOE A. FERNANDEZ
NANCY C. FINLEY
THOMAS O. HUNTER
A. R. LAPPIN
R. W. LYNCH
RUDOLPH V. MATALUCCI
MARTIN A. MOLECKE
E. J. NOWAK
WOLFGANG WAWERSIK
WENDELL D. WEART
WIPP CENTRAL FILES
SANTA FE SHAFT DRILLING CO
ROBERT J. PLISKA
SAVANNAH RIVER LABORATORY
I. WENDELL MARINE
WILLIAM R. MCDONELL
SCIAKY BROTHERS
JOHN C. JASPER
SCIENCE APPLICATIONS INC
JEFFREY ARBITAL
NADIA DAYEM
BARRY DIAL
MICHAEL B. GROSS
JAMES E. HAMMELMAN
DAVID H. LESTER
JOHN E. MOSIER
HOWARD PRATT
MICHAEL E. SPAETH
M. D. VOEGELE
ROBERT A. YODER
SENECA COUNTY DEPT OF PLANNING & DEVELOPMENT
SERATA GEOMECHANICS INC
FRANK TSAI
SERIOUS TEXANS AGAINST NUCLEAR DISPOSAL (S.T.A.N.D)
DELBERT DEVIN
SHANNON & WILSON INC
HARVEY W. PARKER
SHIMIZU CONSTRUCTION COMPANY LTD
JUNJI TAKAGI
SHIMIZU CONSTRUCTION COMPANY LTD - JAPAN
TAKASHI ISHII
SIERRA CLUB
MARVIN RESNIKOFF
BROOKS YEAGER
SIERRA CLUB - COLORADO OPEN SPACE COUNCIL
ROY YOUNG
SIERRA CLUB - MISSISSIPPI CHAPTER
SIMECSOL CONSULTING ENGINEERS - FRANCE
MATTHEW LEONARD
SLICKROCK COUNTRY COUNCIL
BRUCE HUCKO
LUCY K. WALLINGFORD
SNAKE RIVER ALLIANCE
TIM MCNEIL
SOCIETY OF PROFESSIONAL ARCHEOLOGISTS
L. M. PIERSON
SOGO TECHNOLOGY INC
TIO C. CHEN
SOUTH DAKOTA GEOLOGICAL SURVEY
RICHARD BRETZ
SOUTH DAKOTA SCHOOL OF MINES AND TECHNOLOGY
CANER ZANBAK
SOUTH SALT LAKE LIBRARY
SOUTHEAST UTAH ASSOCIATION OF GOVERNMENTS
WILLIAM D. HOWELL
SOUTHERN METHODIST UNIVERSITY
GEORGE W. CRAWFORD
SOUTHERN STATES ENERGY BOARD
J. F. CLARK
SOUTHERN UTAH STATE COLLEGE LIBRARY
SOUTHWEST RESEARCH AND INFORMATION CENTER
DON HANCOCK
ALISON P. MONROE
SPRINGVILLE CITY LIBRARY
STANFORD UNIVERSITY
KONRAD B. KRAUSKOPF
IRWIN REMSON
STEARNS-ROGER SERVICES INC
VERYL ESCHEN
STONE & WEBSTER ENGINEERING CORP
SUE NEWHAMS
JOHN H. PECK
ARLENE C. PORT
EVERETT M. WASHER
SWISHER COUNTY LIBRARY
SYRACUSE UNIVERSITY
WALTER MEYER
SYSTEMS SCIENCE AND SOFTWARE
PETER LAGUS
T.M. GATES INC
TODD M. GATES
TECHNICAL INFORMATION PROJECT
DONALD PAY
TECHNICAL SERVICES AND INSTRUMENTATION INC
BURTON ANDREPONT
TELEDYNE PIPE
TOBY A. MAPLES
TERRA TEK INC
KHOSROW BAKHTAR
NICK BARTON
DANIEL D. BUSH
TERRAMETRICS INC
HOWARD B. DUTRO
TEXAS A & M UNIVERSITY
JOHN HANDIN
EARL HOSKINS
STEVE MURDOCK
JAMES E. RUSSELL

- **TEXAS ATTORNEY GENERALS OFFICE**
  - MICHAEL PLASTER
- **TEXAS DEPT OF HEALTH**
  - DAVID K. LACKER
- **TEXAS DEPT OF WATER RESOURCES**
  - C. R. BASKIN
- **TEXAS ENERGY COORDINATORS OFFICE**
  - ARNULFO ORTIZ
- **TEXAS GOVERNORS OFFICE**
  - STEVE FRISHMAN
- **TEXAS GOVERNORS OFFICE OF GENERAL COUNSEL**
  - R. DANIEL SMITH
- **TEXAS HOUSE OF REPRESENTATIVES**
  - ELLEN SALYERS
- **TEXAS STATE HOUSE OF REPRESENTATIVES**
  - PETE LANEY
- **THE ANALYTIC SCIENCES CORP**
  - CHARLES M. KOPLIK
- **THE EARTH TECHNOLOGY CORP**
  - JOSEPH G. GIBSON
  - FIA VITAR
  - MATT WERNER
  - KENNETH L. WILSON
- **THE JACKSON CLARION-LEDGER**
  - MARK SCHLEIFSTEIN
- **THOMSEN ASSOCIATES**
  - C. T. GAYNOR, II
- **TRANSNUCLEAR INC**
  - BILL R. TEER
- **U.H.D.E. - W. GERMANY**
  - FRANK STEINBRUNN
- **U.S. ARMY CORPS OF ENGINEERS**
  - ALAN BUCK
- **U.S. BUREAU OF LAND MANAGEMENT**
  - JIM BIGGINS
  - LYNN JACKSON
  - GENE NODINE
  - MARY PLUMB
  - EDWARD R. SCHERICK
- **U.S. BUREAU OF MINES**
  - ANTHONY IANNACCHIONE
- **U.S. BUREAU OF RECLAMATION**
  - JOHN BROWN
  - REGE LEACH
- **U.S. DEPT OF ENERGY**
  - CHED BRADLEY
  - R. COOPERSTEIN
  - LAWRENCE H. HARMON
  - CARL NEWTON
- **U.S. DEPT OF ENERGY - ALBUQUERQUE OPERATIONS OFFICE**
  - PHILIP LARRAGOITE
  - JOSEPH M. MCGOUGH
  - DORNER T. SCHUELER
- **U.S. DEPT OF ENERGY - CHICAGO OPERATIONS OFFICE**
  - NURI BULUT
  - GARY C. MARSHALL
  - C. MORRISON
  - PUBLIC READING ROOM
  - R. SELBY
- **U.S. DEPT OF ENERGY - CRYSTALLINE ROCK PROJECT OFFICE**
  - SALLY A. MANN
- **U.S. DEPT OF ENERGY - DIVISION OF WASTE REPOSITORY DEPLOYMENT**
  - JEFF SMILEY
- **U.S. DEPT OF ENERGY - GEOLOGIC REPOSITORY DIVISION**
  - J. W. BENNETT
  - C. R. COOLEY (2)
  - JIM FIORE
  - MARK W. FREI
  - RALPH STEIN
- **U.S. DEPT OF ENERGY - GRAND JUNCTION OFFICE**
  - WAYNE ROBERTS
- **U.S. DEPT OF ENERGY - HEADQUARTERS**
  - PUBLIC READING ROOM
- **U.S. DEPT OF ENERGY - IDAHO OPERATIONS OFFICE**
  - M. BARAINCA
  - JAMES F. LEONARD
  - PUBLIC READING ROOM
- **U.S. DEPT OF ENERGY - NEVADA OPERATIONS OFFICE**
  - PUBLIC READING ROOM
  - DONALD L. VIETH
- **U.S. DEPT OF ENERGY - NWTS PROGRAM OFFICE**
  - J. O. NEFF
- **U.S. DEPT OF ENERGY - OAK RIDGE OPERATIONS OFFICE**
  - PUBLIC READING ROOM
- **U.S. DEPT OF ENERGY - OFFICE OF PROJECT AND FACILITIES MANAGEMENT**
  - D. L. HARTMAN
- **U.S. DEPT OF ENERGY - SAN FRANCISCO OPERATIONS OFFICE**
  - ENERGY RESOURCES CENTER
  - PUBLIC READING ROOM
- **U.S. DEPT OF ENERGY - SAVANNAH RIVER OPERATIONS OFFICE**
  - T. B. HINDMAN
- **U.S. DEPT OF ENERGY - TECHNICAL INFORMATION CENTER (317)**
- **U.S. DEPT OF LABOR**
  - ALEX G. SCIULLI
  - KELVIN K. WU
- **U.S. DEPT OF THE INTERIOR**
  - PAUL A. HSIEH
- **U.S. ENVIRONMENTAL PROTECTION AGENCY**
  - JAMES NEIHEISEL
- **U.S. GENERAL ACCOUNTING OFFICE**
  - WILLIAM DAVID BROOKS
- **U.S. GEOLOGICAL SURVEY - ALEXANDRIA**
  - G. N. RYALS
- **U.S. GEOLOGICAL SURVEY - COLUMBUS**
  - A. M. LA SALA, JR.
- **U.S. GEOLOGICAL SURVEY - DENVER**
  - JESS M. CLEVELAND
  - ROBERT J. HITE
- **U.S. GEOLOGICAL SURVEY - JACKSON**
  - GARALD G. PARKER, JR.
- **U.S. GEOLOGICAL SURVEY - RESTON**
  - JOHN ROBERTSON
  - EDWIN ROEDDER
  - EUGENE H. ROSEBOOM, JR.
  - DAVID B. STEWART
- **U.S. HOUSE OF REPRESENTATIVES**
  - B. JEANINE HULL
- **U.S. HOUSE SUBCOMMITTEE ON ENERGY AND THE ENVIRONMENT**
  - MORRIS K. UDALL
- **U.S. NATIONAL PARK SERVICE**
  - THOMAS C. WYLIE
- **U.S. NUCLEAR REGULATORY COMMISSION**
  - LEON BERATAN
  - GEORGE BIRCHARD
  - EILEEN CHEN
  - ENRICO F. CONTI
  - DOCKET CONTROL CENTER
  - PAUL F. GOLDBERG
  - KYO KIM
  - MALCOLM R. KNAPP
  - JOHN C. MCKINLEY
  - THOMAS J. NICHOLSON
  - JAY E. RHODERICK
  - KRISTIN B. WESTBROOK
  - ROBERT J. WRIGHT
- **UHDE GMBH - W. GERMANY**
  - OLINGER
- **UNION CARBIDE CORP**
  - JOHN D. SHERMAN
- **UNION OF CONCERNED SCIENTISTS**
  - MICHAEL FADEN
- **UNION OIL COMPANY OF CALIFORNIA**
  - BRAD GOVREAU
- **UNITED KINGDOM DEPT OF THE ENVIRONMENT**
  - F. S. FEATES
- **UNIVERSITY OF AKRON**
  - LORETTA J. COLE
- **UNIVERSITY OF ARIZONA**
  - JAAK DAEMEN
  - JAMES G. MCCRAY
  - WILLIS D. SAWYER, JR.
- **UNIVERSITY OF BRITISH COLUMBIA - CANADA**
  - CRAIG FORSTER
- **UNIVERSITY OF CALIFORNIA AT BERKELEY**
  - NEVILLE G. W. COOK
  - RICHARD E. GOODMAN
  - TODD LAPORTE
  - BJORN PAULSSON
  - THOMAS H. PIGFORD
- **UNIVERSITY OF CALIFORNIA AT LOS ANGELES**
  - KRIS PRESTON
- **UNIVERSITY OF CALIFORNIA AT RIVERSIDE**
  - LEWIS COHEN
  - DON STIERMAN
- **UNIVERSITY OF DELAWARE**
  - FRANK A. KULACKI
- **UNIVERSITY OF FLORIDA**
  - DAVID E. CLARK
  - DOLORES C. JENKINS
- **UNIVERSITY OF HAWAII AT MANOA**
  - DAVID EPP
- **UNIVERSITY OF ILLINOIS AT URBANA - CHAMPAIGN**
  - MAGDI RAGHE
- **UNIVERSITY OF LULEA - SWEDEN**
  - SVEN KNUTSSON
- **UNIVERSITY OF MINNESOTA**
  - CHARLES FAIRHURST
  - DONALD GILLIS
- **UNIVERSITY OF MISSISSIPPI**
  - GEORGE D. BRUNTON
- **UNIVERSITY OF MISSOURI AT KANSAS CITY**
  - EDWIN D. GOEBEL
  - SYED E. HASAN
- **UNIVERSITY OF NEWCASTLE UPON TYNE - ENGLAND**
  - I. W. FARMER
- **UNIVERSITY OF OKLAHOMA**
  - DANIEL T. BOATRIGHT
- **UNIVERSITY OF PITTSBURGH**
  - B. L. COHEN

- **UNIVERSITY OF SOUTHERN MISSISSIPPI**
  - CHARLES R. BRENT
  - JAMES W. PINSON
  - DANIEL A. SUNDEEN
  - GARY C. WILDMAN
- **UNIVERSITY OF SOUTHWESTERN LOUISIANA**
  - RICHARD U. BIRDSEYE
- **UNIVERSITY OF TEXAS AT AUSTIN**
  - BUREAU OF ECONOMIC GEOLOGY
  - EARNEST F. GLOYNA
  - THOMAS C. GUSTAVSON
  - DALE KLEIN
  - JOE O. LEDBETTER
  - DOUGLAS C. RATCLIFF
  - E. G. WERMUND
- **UNIVERSITY OF TOKYO - JAPAN**
  - RYOHEI KIYOSE
- **UNIVERSITY OF TORONTO - CANADA**
  - N. S. BRAR
- **UNIVERSITY OF UTAH**
  - JAMES W. BUNGER
  - MARRIOTT LIBRARY
  - GARY M. SANDQUIST
- **UNIVERSITY OF WISCONSIN**
  - B. C. HAIMSON
- **UNIVERSITY OF WISCONSIN AT MILWAUKEE**
  - HOWARD PINCUS
- **UPPER PEASE SOIL AND WATER CONSERVATION DISTRICT**
  - W.H. MARSHALL
- **URS-BERGER**
  - TONY MORGAN
- **URS/JOHN A. BLUME & ASSOCIATES, ENGINEERS**
  - ANDREW B. CUNNINGHAM
- **UTAH DEPT OF NATURAL RESOURCES & ENERGY**
  - MARK A. PAGE
- **UTAH DEPT OF TRANSPORTATION**
  - DAVID LLOYD
- **UTAH DIVISION OF ENVIRONMENTAL HEALTH**
  - DENNIS R. DALLEY
  - MARV H. MAXELL
- **UTAH DIVISION OF OIL, GAS & MINING**
  - SALLY J. KEFER
- **UTAH DIVISION OF PARKS & RECREATION**
  - JOHN KNUDSON
  - GORDON W. TOPHAM
- **UTAH ENERGY OFFICE**
  - ROD MILLAR
- **UTAH ENVIRONMENT CENTER**
  - JUNE WICKHAM
- **UTAH GEOLOGICAL AND MINERAL SURVEY**
  - GENEVIEVE ATWOOD
  - BILL LUND
  - MAGE YONETANI
- **UTAH SOUTHEASTERN DISTRICT HEALTH DEPARTMENT**
  - ROBERT L. FURLOW
- **UTAH STATE GEOLOGIC TASK FORCE**
  - DAVID D. TILLSON
- **UTAH STATE UNIVERSITY**
  - JOEL E. FLETCHER
  - MERRILL LIBRARY AND LEARNING
  - JACK T. SPENCE
- **UTAHNS AGAINST THE DUMP COALITION**
- **VANDERBILT UNIVERSITY**
  - FRANK L. PARKER
- **VERMONT DEPT OF WATER RESOURCES AND ENVIRONMENTAL ENGINEERING**
  - CHARLES A. RATTE
- **VERMONT STATE NUCLEAR ADVISORY PANEL**
  - VIRGINIA CALLAN
- **VIRGINIA DEPT OF HEALTH**
  - WILLIAM F. GILLEY
  - ROBERT G. WICKLINE
- **VIRGINIA DIVISION OF MINERAL RESOURCES**
  - ROBERT C. MILICI
- **VIRGINIA HOUSE OF DELEGATES**
  - A. VICTOR THOMAS
- **VIRGINIA POLYTECHNICAL INSTITUTE AND STATE UNIVERSITY**
  - GARY L. DOWNEY
- **WA STATE DEPARTMENT OF ECOLOGY**
  - DAVID W. STEVENS
- **WASHINGTON HOUSE OF REPRESENTATIVES**
  - RAY ISAACSON
- **WATTLAB**
  - BOB E. WATT
- **WEBSTER PARISH LIBRARY**
- **WESTERN STATE COLLEGE**
  - FRED R. PECK
- **WESTINGHOUSE ELECTRIC CORP**
  - JAMES H. SALING
- **WIPP PROJECT**
  - WESTINGHOUSE ELECTRIC CORPORATION
- **WISCONSIN GEOLOGICAL AND NATURAL HISTORY SURVEY**
  - MEREDITH E. OSTROM
- **WOODWARD-CLYDE CONSULTANTS**
  - F. R. CONWELL (2)
  - TERRY A. GRANT
  - ASHOK PATWARDHAN
  - WESTERN REGION LIBRARY
- **WRIGHT STATE UNIVERSITY**
  - MICHAEL FARRELL
- **YALE UNIVERSITY**
  - BRIAN SKINNER

END

DATE FILMED

05/02/84